UNIVERSIDADE FEDERAL DO RIO GRANDE DO NORTE
CENTRO DE CIÊNCIAS EXATAS E DA TERRA
INSTITUTO DE QUÍMICA
PROGRAMA DE PÓS-GRADUAÇÃO EM QUÍMICA

Programa de Pós-Graduação em Química

Development of chemosensors for ions based on quinoxaline and quercetine derivatives

Lilian Cavalcante da Silva

Tese de Doutorado

Natal/RN, fevereiro de 2020

LILIAN CAVALCANTE DA SILVA

DEVELOPMENT OF CHEMOSENSORS FOR IONS BASED ON QUINOXALINE AND QUERCETINE DERIVATIVES

Thesis submitted to Chemistry Postgraduate Program of Federal University of Rio Grande do Norte (PPGQ/UFRN) in partial fulfillment of the requirements for the degree of Doctor of Philosophy in Chemistry.

Advisors: Prof. Dr. Fabrício Gava Menezes
Prof.ª Dra. Renata Mendonça Araújo

NATAL, RN
2020

Universidade Federal do Rio Grande do Norte - UFRN
Sistema de Bibliotecas - SISBI
Catalogação de Publicação na Fonte. UFRN - Biblioteca Setorial Prof. Francisco Gurgel De Azevedo - Instituto Química – IQ

Silva, Lilian Cavalcante da.
Development of chemosensors for ions based on quinoxaline and quercetine derivatives / Lilian Cavalcante da Silva. - Natal: UFRN, 2020.
111f.: il.

Tese (Doutorado) - Universidade Federal do Rio Grande do Norte. Centro de Ciências Exatas e da Terra - CCET, Instituto de Química. Programa de Pós-Graduação em Química (PPGQ).
Orientador: Dr. Fabrício Gava Menezes.
Coorientador: Dra. Renata Mendonça Araújo.

1. Quimiossensores - Tese. 2. Cátions - Tese. 3. Ânions - Tese. 4. Quinoxalina - Tese. 5. Quercetina - Tesse. I. Menezes, Fabrício Gava. II. Araújo, Renata Mendonça. III. Título.

RN/UF/BSQ CDU 54(043.2)

Elaborado por FERNANDO CARDOSO DA SILVA - CRB-759/15

Lilian Cavalcante da Silva

DEVELOPMENT OF CHEMOSENSORS FOR IONS BASED ON QUINOXALINE AND QUERCETINE DERIVATIVES.

Tese apresentada ao Programa de Pós-graduação em Química da Universidade Federal do Rio Grande do Norte, em cumprimento às exigências para obtenção do título de Doutora em Química.

Aprovada em: 10 de fevereiro de 2020

Comissão Examinadora:

Dr. Fabrício Gava Menezes – UFRN (orientador)

Dr. Rodrigo Cristiano – UFPB

Dr. Savio Moita Pinheiro – UFPB

Dra. Luciene da Silva Santos – UFRN

Dr. Júlio Cezar de Oliveira Freitas – UFRN

To my parents, Humberto Freitas e Lídia Cavalcante

ACKNOWLEDGMENTS

To God for giving me strength, health, and patience on this journey.

To my parents for all their support, patience, affection, love and for always being by my side in my decisions.

To my advisor Fabrício Gava Menezes for all support, for his great patience, guidance, and teachings. Thank you for guiding me from the undergraduate monitoring, to the master's degree, until the present moment.

I thank my lab friends, I'm sure that life in research would be a lot harder without your support. I will surely cherish all the good times we have spent together, even the bad ones when the reactions do not work out or scare us. I thank especially to my friends Gizely, Rusceli, Marcela and Taiza for all the laughs, snacks, lunches and moments that we spent together (which surely would have snacks). To my friend Luan, who always supports me in good and bad times, for his advice, companionship, for always saving me with English tasks and for helping to complete this work.

To the friends that the synthesis brought me, since the master's degree at the Laboratory of Synthesis of Heterocycles and Applied Methodologies.

To the teacher Renata Mendonça Araújo who since graduation has been following and contributing to my academic background. Thank you for so many hours that you spent at NMR getting my spectra and for all the contributions in this work.

To the Analytical Center and the technicians of the Institute of Chemistry of UFRN for the analyzes.

To Professor Vanderlei G. Machado of UFSC for their contributions and collaboration.

To Professor Miguel for his collaboration with our research group and especially with this work.

The Group of Biological Chemistry and Chemometrics for their support and contributions to the work.

To the Postgraduate Program in Chemistry.

RESUMO

O desenvolvimento de sensores artificiais para detecção de analitos iônicos em solução tem atraído grande atenção, principalmente, para as áreas biológica e ambiental, em função da possibilidade de análises rápidas e de alta sensibilidade, por meio de procedimentos simples e de baixo custo. No presente trabalho foram realizadas sínteses de novos derivados de quinoxalina com o objetivo de aplicá-los na detecção de íons em solução aquosa. Um total de nove compostos derivados foram obtidos com bons rendimentos (65-84%) por um procedimento do tipo *one-pot*. O processo tem início com a oxidação do ácido *L*-ascórbico, seguido da reação com dois equivalentes de *o*-fenilenodiamina para gerar o composto AAQX que é convertido nos produtos finais via formação de uma base de Schiff a partir da reação com aldeídos aromáticos. Entre os nove compostos sintetizados, dois foram testados como quimiossensores. Foi verificado que o produto final obtido a partir do benzaldeído (*N*-[(E)-2-(fenilmetilideno)amino)fenil]-3-(1,2,3-trihidroxipropil)naftaleno-2-carboxamida) mostrou-se um quimiossensor cromogênico seletivo para o íon Cu^{2+} frente a outros cátions em solução de metanol-água 20%. O composto obtido a partir do *p*-nitrobenzaldeído (*N*-[(E)-2-(4-nitrobenzilideno)amino)fenil]-3-((1S,2S)-1,2,3-trihidroxipropil)quinoxalina-2-carboxamida), foi eficaz na detecção de íons F^- em DMSO e em solução DMSO-água (2,5%). Os mecanismos de ação desses quimiossensores foram propostos com base em dados espectroscópicos e teóricos. Por fim, uma proposta multidisciplinar para aulas de Química com base na capacidade de um complexo formado por Al^{3+} e o produto natural quercetina (QCT) para detecção de ânions F^- em meio aquoso é apresentada. A proposta se inicia com o fácil isolamento de Rutina a partir da raiz da planta *Bredemeyera floribunda* Willd, seguido de uma proposta sintética de hidrólise da substância isolada, obtendo-se a quercetina. A partir da quercetina obteve-se um complexo com Al^{3+} em uma estequiometria 2:1 (QCT:Al^{3+}) que foi caracterizado e aplicado como quimiossensor para F^- por meio de testes colorimétricos, UV-visível e fluorescência. O caráter multidisciplinar desse projeto envolve as áreas de produtos naturais, síntese, Química dos complexos e cálculos teóricos, sendo, portanto, capaz de fornecer estímulos relevantes para o estudante de Química em seus cursos de formação.

Palavras-chaves: Quimiossensores; cátions; ânions; quinoxalina; quercetina.

ABSTRACT

The development of artificial sensors for detecting ionic analytes in solution has attracted much attention, mainly to the biological and environmental areas, due to the possibility of rapid and high sensitivity analysis through simple and low-cost procedures. In the present work, syntheses of new quinoxaline derivatives were performed aiming to the detection of ions in aqueous solution. A total of nine derivatives compounds were obtained in good yields (65-84%) by a one-pot type procedure. The process begins with the oxidation of L-ascorbic acid, followed by reaction with two equivalents of o-phenylenediamine, to generate the AAQX compound which is converted to the final products via formation of a Schiff base from reaction with aromatic aldehydes. Nine compounds were synthesized and two were tested as chemosensors. It has been found that the final product obtained from benzaldehyde (*N*-(2-((Z)-benzylidene)amino)phenyl)-3-((1S,2S)-1,2,3-trihydroxypropyl)quinoxaline-2-carboxiamide) proved to be a selective chromogenic chemosensor for Cu^{2+} over the other cations in methanol-water solution 20%. The compound obtained from *p*-nitrobenzaldehyde (*N*-(2-((Z)-(4-nitrobenzylidene)amino)phenyl)-3-((1S,2S)-1,2,3-trihydroxypropyl)quinoxaline-2-carboxamide), was effective in detecting F^- ions in DMSO and DMSO-water solution (2.5%). The mechanism of action for these chemosensors has been proposed based on theoretical and spectroscopic data. Finally, a multidisciplinary proposal for chemistry lectures based on the capacity of a complex formed by Al^{3+} and quercetin natural product (QCT) for the detection of F^- anions in an aqueous medium is presented. The proposal begins with the easy isolation of Rutin from the root of the *Bredemeyera floribunda* Willd plant, followed by a synthetic proposal for hydrolysis of the isolated substance, obtaining then quercetin. From quercetin was obtained a complex with Al^{3+} in a 2:1 stoichiometry (QCT: Al^{3+}) that was characterized and applied as a chemosensor for F^- by colorimetric, UV-visible and fluorescence tests. The multidisciplinary character of this project involves the areas of natural products, synthesis, complex chemistry, and theoretical calculations, and is, therefore, able to provide relevant stimuli for the chemistry student in their undergraduate courses.

Keywords: Chemosensors; cations; anions; quinoxaline; quercetin.

ABBREVIATIONS

QCT: Quercetin

RT: Rutin

DSSC: Dye-Sensitized Solar Cell

NMR: Nuclear Resonance Magnetic

IR: Infrared

UV: Ultraviolet

PET: Photoinduced Electron Transfer

PCT: Photoinduced Charge Transfer

FRET: Förster Resonance Energy Transfer

LMCT: Ligand to Metal Charge Transfer

AA: Ascorbic Acid

COSY: Correlation Spectroscopy

HSQC: Heteronuclear Single-Quantum Correlation

HMBC: Heteronuclear Multiple-Bond Correlation

FIGURES

TABLES

CONTENTS

CHAPTER 1 INTRODUCTION AND OBJECTIVES

Over the years, research in the field of chemosensors has been very relevant and has shown significant growth. This field of research involves several areas and receives important contribution from the works in organic synthesis, mainly through the synthesis of sensors derived from aromatic heterocycle compounds, which present favorable structures for this application[1-5].

Chemosensors are species capable of detecting an analyte through covalent or non-covalent interactions, such as hydrogen bonds, electrostatic attractions, metal coordination, among others[6]. These compounds need to have a receptor site, which enables interaction with the analyte of interest, and a signaling site at which a detectable signal occurs, such as changes in solution coloration or fluorescence following sensor-analyte interaction[7]. The literature reports several fields of application for chemosensors, such as medical diagnosis[8], environmental monitoring[9], toxicological analyzes[10], biomarkers[11].

An important point in planning the construction of a new sensor is the use of reagents that are low cost, low toxicity and structures favorable to the sensitivity and selectivity of relevant target molecules. Besides, syntheses that occur under mild conditions and good yields have been the main target of research. In this context, synthesis performed in a single reaction medium (known as ‘one-pot’) is an efficient strategy in synthetic Organic Chemistry, in which a reagent can be subjected to successive chemical reactions. Thus, it is possible to save time, avoid purification steps and waste reagents in multi-step reactions, for example[12].

Ascorbic acid, known as Vitamin C, is very useful as a starting reagent, as this molecule has a polyfunctional structure and can be found as *L*-ascorbic acid or *D*-ascorbic acid, so it is possible to perform many modifications in this compound, for example, oxidation reactions followed by hydrolysis[13], as shown in Fig. 1.

Figure 1 – Oxidation reaction of *L*-ascorbic acid followed by hydrolyses.

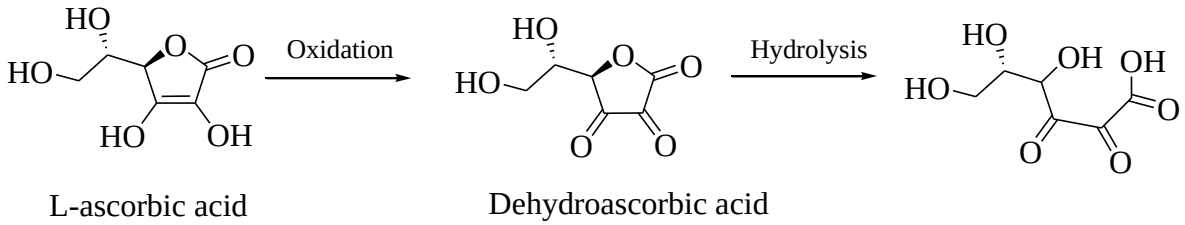

author, 2020.

In a paper previously published by our research group[14], a chromogenic chemosensor, AAQX, synthesized from Cu^{2+} ion-selective ascorbic acid (AAQX) has been reported against several ionic species (Sr^{2+}, Fe^{2+}, Pb^{2+}, Mn^{2+}, Mg^{2+}, Ni^{2+}, Zn^{2+}, Sn^{2+}, Hg^{2+}, Ca^{2+}, Ba^{2+}, Co^{2+}, Cr^{3+}, Al^{3+}, and Fe^{3+}). This compound already had reported in the literature[15,16], however, it had not been applied in this area. Figure 2 shows some results present in the work, which brought a significant contribution in chemosensors area, through a synthesis of easy accomplishment and good performance, with the precursor reagent a cheap and easily found.

Figure 2 – Results AAQX sensor. (a) synthesis; (b) Colorimetric test[14].

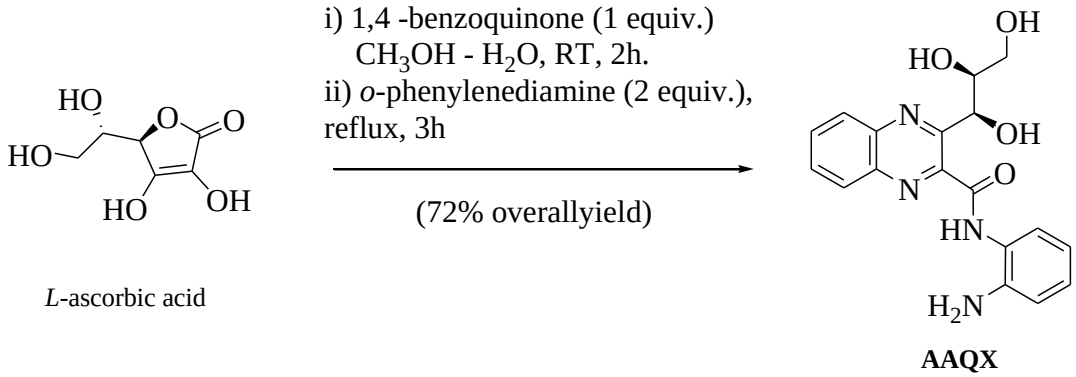

-

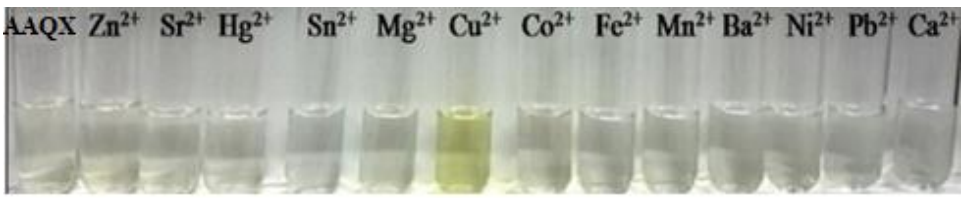

author, 2020.

In this context, a search for new sensors started from the AAQX structure, giving rise to the first work described in this thesis, in which nine new compounds were synthesized from the condensation reaction of AAQX with different aromatic aldehydes, aiming to synthesize new sensors from AAQX. Among the synthesized compounds, two were tested as chemosensors in solution for ionic species, resulting in a new chemosensor for Cu^{2+} and F^- ions. The reported sensors can be applied to detect these ions in real samples, once it allows the use of a percentage of water in the analysis.

Following this same line of research with chemosensors, the second work of this thesis reports the preparation of a Quercetin-Al^{3+} complex and its application in the detection of F^- ions in solution. Intending to contribute to the teaching area, this second work has a multidisciplinary project structure applied to undergraduate students, involving the following lines of research: natural product chemistry, synthesis, supramolecular chemistry, and computational chemistry.

Based on reports in the literature about quinoxaline derivative chemosensors, a review was developed only with these derivatives for the detection of metal cations, since recently a survey on quinoxaline derived chemosensors have been found[17].

CHAPTER 2 LITERATURE REVIEW

2.1 Quinoxaline

Heterocyclic aromatic compounds are the basis for derivatives applied in various fields such as medical, biological, and industrial, which makes these compounds subject to many researches in various areas[18-21]. Among the present classes of these compounds it is possible to highlight the quinoxaline, which, its derivatives have a multitude of properties and applications explored throughout the development of many researches.

The quinoxaline nucleus, also known as benzopyrazine, benzoparadiazines, 1,4-benzodiazine, 1,4-diazanaphthalene, phenopyrazine or benzo(α)pyrazines, has a molecular formula $C_8H_6N_2$, with a pyrazine unit coupled to a benzene ring in its structure. The literature reports considerable methods for obtaining the quinoxaline nucleus[22-24], with an easy synthesis procedure. A classic synthesis method is carried out through condensation, where *o*-phenylenediamine reacts with α-dicarbonyls, depending on the substituents of interest to be obtained in the nucleus, in the presence of a catalyst, such as the reaction of *o*-phenylenediamine with glyoxal (Fig. 3)[25].

Figure 3 – Condensation of *o*-phenylenediamine with an α-dicarbonyl compound.

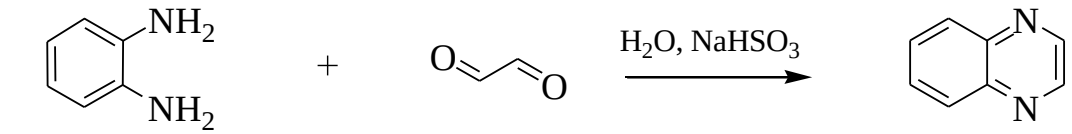

o-phenylenediamine glyoxal quinoxaline

author, 2020

Many reports found in the literature regarding quinoxalines point out the o-phenylenediamine as the main reagent, but it is possible to perform the synthesis from other precursors, as can be observed through some examples in figure 4.

Figure 4 – Examples of synthetic routes to obtain quinoxalines[26-32].

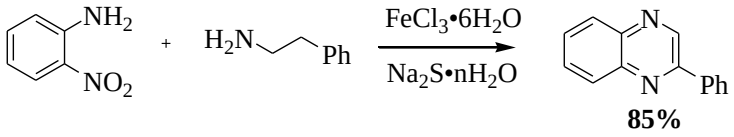

Nguyen, Al-mourabit, Ermolenko, 2015.

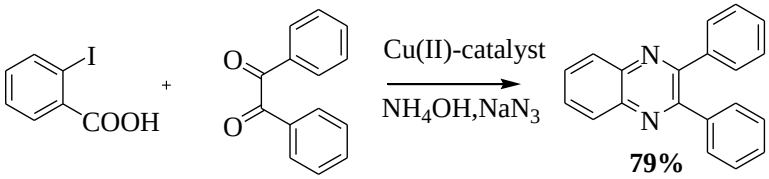

Saha et al., 2018.

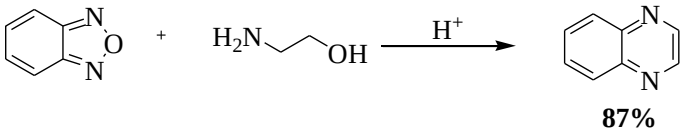

Samsonov, V. A., 2007.

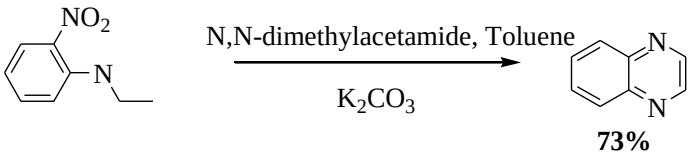

Walczak et al., 2014.

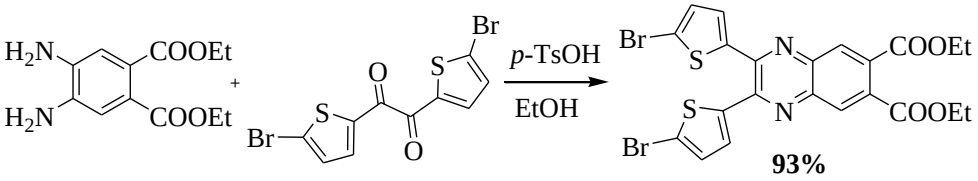

Park et al., 2019.

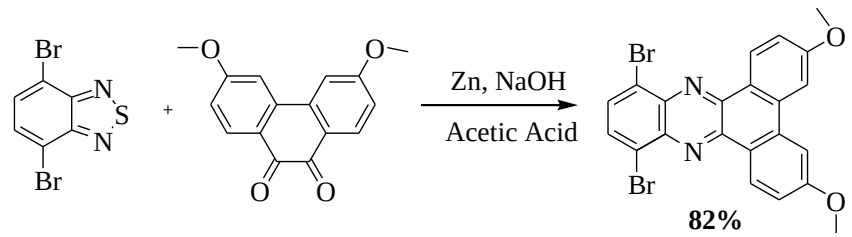

Kim, Han e Moon, 2019.

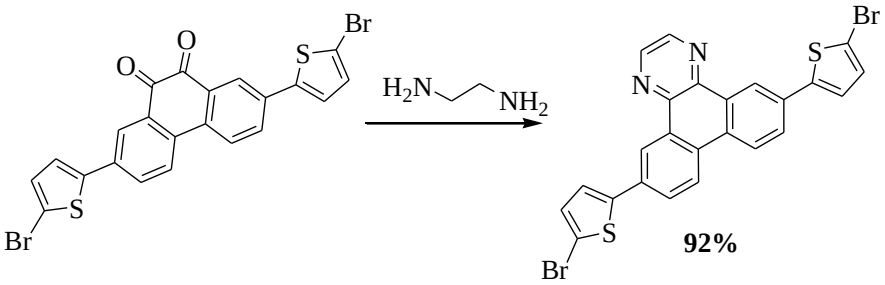

Alameddine et al., 2019

In addition to currently known methods, research in synthesis of these compounds has been devoted to finding less environmentally harmful methods, as reported by Bhargava, Soni, and Rathore (2019)[33], who describe the synthesis of various quinoxaline derivatives using ionic liquid (Fig. 5), those which act as the reaction solvents and catalysts, discarding thus the use of organic solvents. Moreover, the results showed shorter reaction times when using this methodology compared to other reported methods.

Figure 5 – Chemical structures of ionic liquids used in the synthesis of quinoxalines.

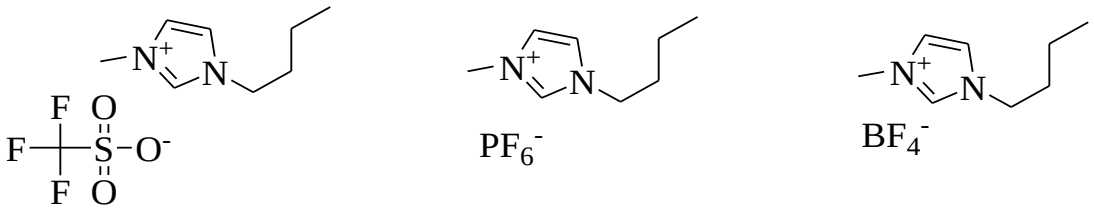

author, 2020.

Another environmentally favorable proposal was reported by Bachhav, Bhagat and Telvekar (2011)[34] who describe the synthesis of quinoxaline using glycerol: H_2O at 90 °C. By observing one of the reported reactions (Fig. 6), it is possible to verify that this is an efficient methodology when compared to other reports found in the literature, which make use of organic solvents such as tetrahydrofuran (THF)[35] and catalysts such as zirconium (IV) chloride ($ZrCl_4$)[36] and gallium (III) triflate ($C_3F_9GaO_9S_3$)[37].

Figure 6 – Preparation of 2,3-diarylquinoxaline[34].

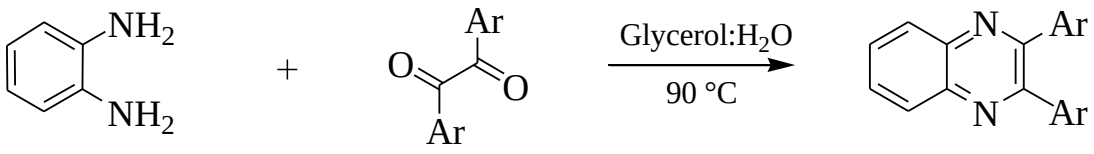

Furthermore, taking as a starting material the quinoxaline nucleus or derivatives thereof, numerous synthetic modifications are possible even under severe conditions, for example, nitration using H_2SO_4/HNO_3 (Fig. 7i)[14] and sulfonation using H_2SO_4 (Fig. 7ii)[38]. However, other reactions occur easily and under mild conditions, such as nucleophilic

substitutions using Grignard Reagent (Fig. 7 iii)[39], oxidation reactions (Fig. 7iv)[40], among others.

Figure 7 – Reactions of quinoxalines.

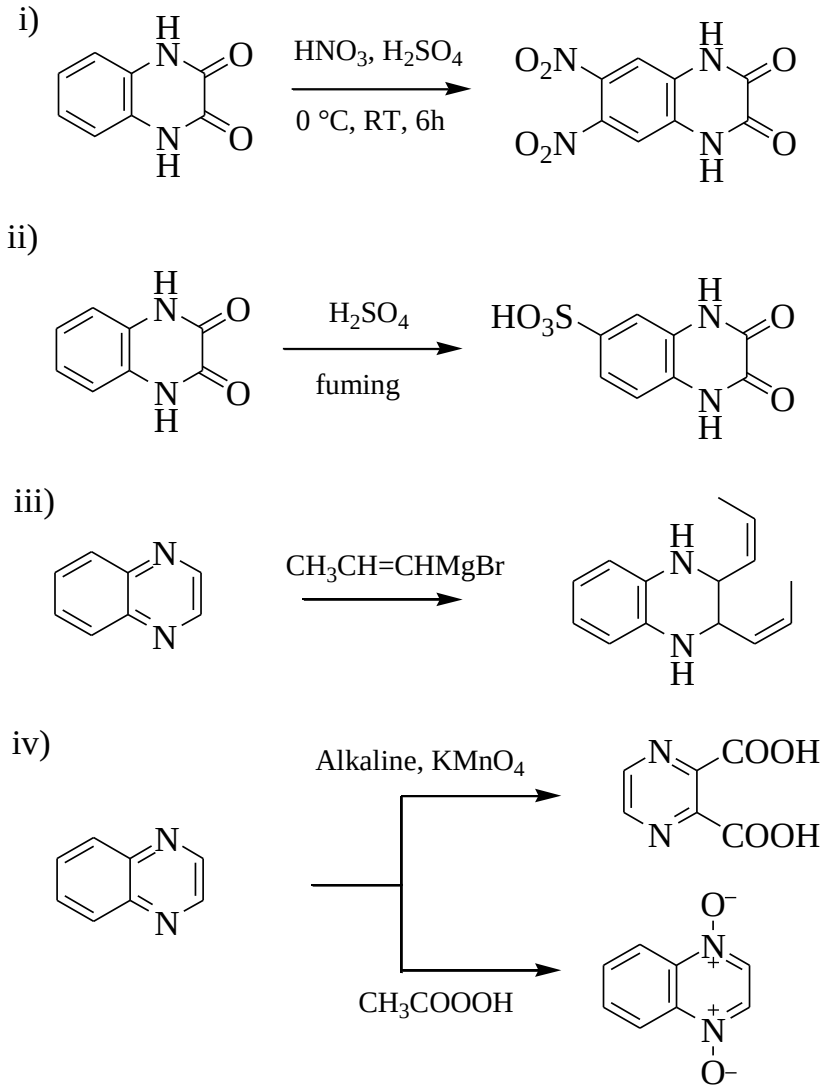

author, 2020.

The diverse possibilities of obtaining these compounds and the versatility to incorporate other structures into this nucleus make the quinoxaline nucleus very interesting for organic synthesis. The literature reports that quinoxaline-derived compounds researches have taken research groups in different areas, especially when it comes to their pharmacological potential (Fig. 8), in which several studies in this field are devoted[41-43].

Figure 8 – Structures of compounds derived from the quinoxaline nucleus[44-49].

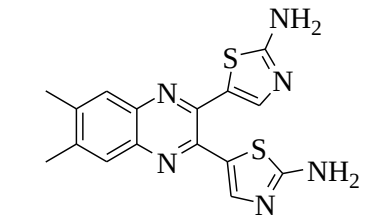

Alzheimer's Disease Treatment
Sagar et al.,2019

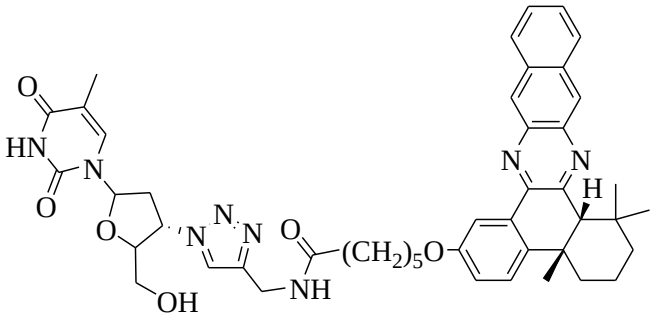

Anticancer
Yuan et al., 2019

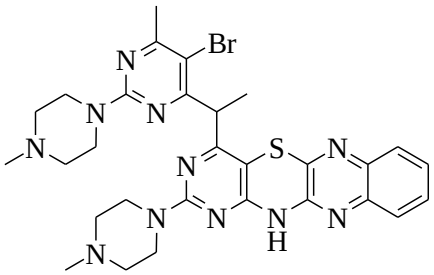

Antibacterial
Afrough et al., 2019

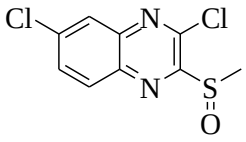

Anti-leishmania
Cogo et al.,2018

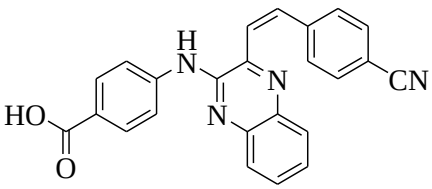

Antimicrobial
Patel et al., 2019

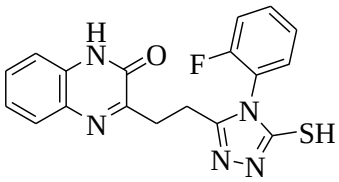

Anti-inflammatory
Tariq, Alam e Amir, 2018

author, 2020.

Quinoxaline nucleus derivatives are used as building blocks of luminescent compounds due to their π-extended conjugation that allows electron transport via conjugation, making them interesting candidates for application as materials in various electroluminescent devices[50], in molecular probes used in biochemistry[51], in dye-sensitized solar cells (DSSCs)[52], as well as fluorescent dyes[53]. The fluorescent properties of the quinoxalines can also be exploited even from the formation reaction of these derivatives, as reported by Lai et al., 2020 having a fluorescent probe 2-(naphthalen-6-yl)quinoxaline formed from the compound 2-bromo-1-(naphthalen-2-yl)ethenone with *o*-phenylenediamine[54]. The presence of this probe is used as a result of o-phenylenediamine detection in the solution (Fig. 9).

Figure 9 – Fluorescent probe formation reaction 2-(naphthalen-6-yl)quinoxaline.

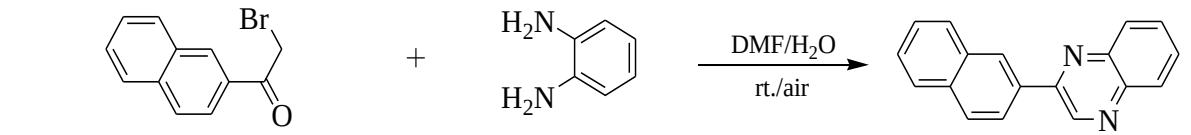

2-bromo-1- (naphthalen-2-yl)ethanone o-phenylenediamine 2-(naphthalen-6-yl)quinoxaline

In industry, quinoxaline derivatives have also been applied as corrosion inhibitors. The literature reports this potential for corrosion inhibition of copper in nitric acid[55] and mild steel in hydrochloric acid[56], and in sulfuric acid[57], for example. This is possible due to the compounds with π electrons, heteroatoms, and functional groups such as – N = N -, - C = N -, - C = O, - C = S, - S = O, - OH, > NH generally exhibit corrosion inhibiting properties in which they form a film on the metal surface and may slow the metal dissolution process (an anodic reaction) as well as the evolution of hydrogen (a cathodic reaction), but the mechanism and efficiency of the inhibitor will depend on variables such as the nature of the corrosive environment and the metal it was intended to protect[56,58].

2.2 Chemosensors

Chemosensors can be defined as a compound capable of interacting with an analyte, generating a detectable signal[59], targeting ionic species, pesticides, explosives, small neutral molecules or biomacromolecules[60]. The signal produced by the interaction, which can occur by non-covalent interactions, such as coordination with metals, for example, can be identified with the naked eye through colorimetric change, for example, as well as by various spectroscopic techniques (e.g. NMR, UV, IR, fluorescence) or producing electrochemical responses.

Organic synthesis has a great contribution in this area, with the planning of new methodologies and the emergence of new compounds capable of being used for such purposes. Studies of fluorescent chemosensors, for example, are already known for the past 150 years[60] and currently, focused on the area of supramolecular chemistry that has emerged a few decades ago, and has developed rapidly. The first works were developed by Charles J. Pedersen, Jean-Marie Lehn, Donald J.Cram who, in 1987, received the Nobel Prize in Chemistry for their research in this area[61].

In planning the synthesis of a chemosensor, the compound must have in its structure (i) a receiver part responsible for signal induction, (ii) a signaling unit whose properties must change with interaction with the analyte. Also, if the unit the signaling device contains chromophores, the receiver is known as a chromogenic or colorimetric sensor, and (iii) in some cases a spacer, which may modify the sensor geometry by adjusting its selectivity[62]. Figure 10 shows schematically the process to obtain the sensor and the most prospected changes, such as color changes, fluorescence or redox potential.

Figure 10 – Illustrative scheme of synthesis, interaction with analyte and property changes in a chemosensor.

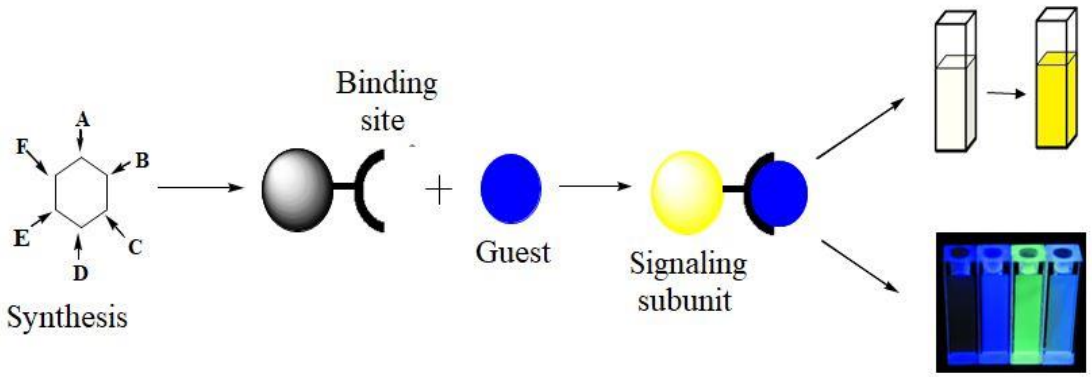

author, 2020.

The sensor-analyte interaction occurs through a specific mechanism that may cause, for example, an increase or decrease in fluorescence intensity, appearance or shift of UV-visible absorption band, among others. The following briefly describes some interaction mechanisms.

Photoinduced Electron Transfer (PET): The PET system works through the redox mechanism, in which two situations may occur (Fig. 11): i) ahead to the interaction with the analyte, occurs an electron transfer with absence of fluorescence, and from the moment the interaction with the analyte occurs, the electron transfer is interrupted, the moment when the sensor shows itself fluorescent (type OFF-ON); ii) fluorescence suppression occurs when the analyte interacts with and the sensor due to electron transfer occurring after the sensor-analyte interaction. PET-type sensors have a receptor part, a spacer, a fluorophore group and an internal device capable of supplying electrons, for example, nitrogen with free electrons. When it comes to the detection of transition metals, the electron supplier may be dispensed due to the various oxidation states possible for these metals, which transfer electrons to a fluorophore[63-65].

Figure 11 – Representation PET fluorescent sensors.

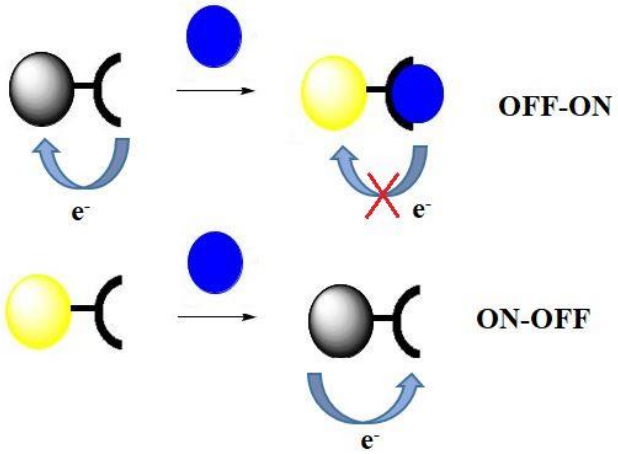

author, 2020.

Photoinduced Charge Transfer (PCT): This occurs by transferring charge between a donor group and an electron receptor group present in the sensor frame. Thus, when the analyte interacts with the sensor, there is a change in electron transfer between the sensor components, changing the photo-physical properties that can be detected. Sensors that work through this mechanism do not have the spacer portion between the receptor and fluorophore[64,65].

Förster Resonance Energy Transfer (FRET): occurs when there is a photon transfer between two portions of fluorophore in the molecule donor and recipient, because of the change in conformation of the molecule to interact with the analyte. Structurally, donor and recipient must be close[64,65] (Fig. 12).

Figure 12 – Fluorescence resonance energy transfer (FRET).

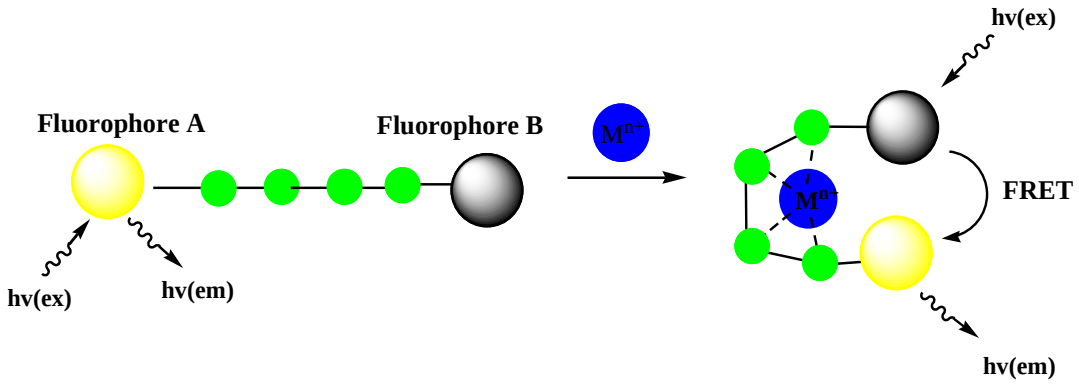

author, 2020.

Regardless of the mechanism of interaction, it is possible to relate the efficiency of a sensor to the ease of synthesis, selectivity and simplicity in measuring the detectable signal[63].

2.1.1 Chemosensors for Cations Detection.

Metal ions play key roles in the biological mechanisms of the human body, such as Na^{+} that regulates blood pressure and Mg^{2+} that is related to muscle contractility and nerve cell function[66]. However, the excess or deficiency of these ions in the human organism can lead to the emergence of several pathologies. Also, some are toxic not only to humans but also to the environment through contamination of soil and aquatic environments, causing serious public health and environmental problems such as Hg^{2+}, Cr^{6+}, Cd^{2+} and As^{3+} [67].

Among the pathologies related to metal ion deregulation, Alzheimer's disease, a neurodegenerative disease, has caused great concern due to the high number of reported cases worldwide. Research shows that Alzheimer's disease is caused by a complex set of factors such as neuroinflammation, metabolic deficiencies, oxidative stress, as well as the dysregulation of Cu^{2+} and Zn^{2+} ions[68]. In addition to Alzheimer's disease, other neurological diseases are associated with Cu^{2+} dysregulation, such as Menkes disease and Wilson's disease[69]. Therefore, one of the chemosensor target molecules for detection and quantification has been the Cu^{2+} ion.

In the search for new sensors for metal cations, Schiff bases have been showing good results and have been the target of many research[5] due to the presence of C=N group π electrons that offer a good possibility of chelation with ions, which increases intramolecular charge transfer or the possibility of LMCT (Ligant to Metal Charge Transfer) transition, as reported by Jung, Lee and Kim (2017) which presents a new sensor capable of detecting Cu^{2+}, Co^{2+} and Fe^{2+}, in an aqueous medium using colorimetric change and Cu^{2+} and Co^{2+} differentiation also by spectral differences in the UV- visible spectroscopy[70] (Fig. 13).

Figure 13 – (a) Selective chemosensor for Cu^{2+}, Co^{2+} and Fe^{2+}, (b) UV-visible spectrum of sensor interaction with cations.[70]

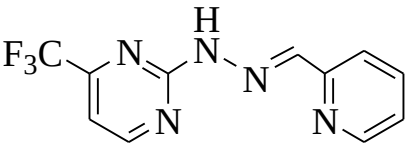

(a)

(b)

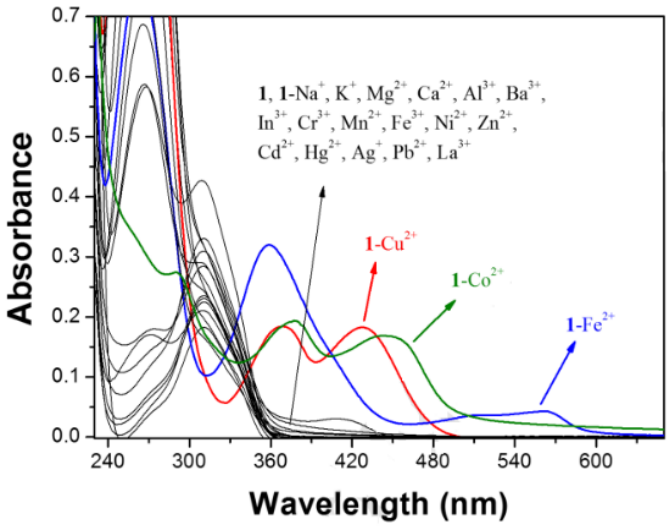

Another sensor capable of detecting various cations is reported by Kim et al. (2013) that shows the turn-on colorimetric and fluorescent sensor capable of detecting Zn^{2+}, including applications to intracellular environment, and colorimetric for Cu^{2+} and Fe^{2+}. The reported sensor is also able to differentiate Fe^{2+} from Fe^{3+} which is important in understanding the biological functions of these two cations in the body[71] (Fig. 14).

Figure 14 – Chemosensor structure for Zn^{2+}, Fe^{2+} and Cu^{2+} in aqueous medium.

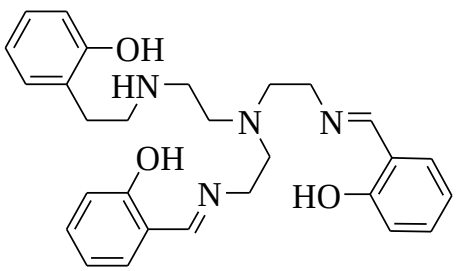

author, 2020.

2.2.2 Chemosensors for Anions Detection.

Studies on anion chemosensors have been growing throughout anions because they play an important role in industrial processes, the human body and the environment[72]. In addition to their importance, like the cations, anions can also have toxicity depending on the amount, for example, the CN^- anion, which is widely used in industrial processes, has high toxicity to the environment and human health and can be inhaled or absorbed through the skin[73]. Another important anion for humans is F^-, which in small amounts, helps strengthen tooth enamel. However, when in larger quantities it may bring problems to teeth as well as bones, a condition known as dental and skeletal fluorosis, which makes bones denser, harder and brittle[74].

In this context, several classes are studied in the search for anionic selectivity, such as derivatives containing groups urea, thiourea, amides, pyrroles, indoles, among others[75]. Besides, coupled with the presence of acidic hydrogens, is required a favorable geometry of sensor-analyte interaction, such as the presence of multiple groups, as is achieved with polycyclic structures.

One of the factors that make anion detection difficult and must be considered in sensor design is the fact that there is competition between the receptor and hydroxyl solvents such as water due to the strong interaction of hydrogen between the anion and the solvent, thus hindering detection by the sensor[76].

The quinoxaline nucleus has been used in the synthesis of various anionic sensors. Figure 15 shows some examples of such sensors, also showing which anions can be possible to detect by them.

Figure 15 – Examples of quinoxaline-derived chemosensors for anions[77-83].

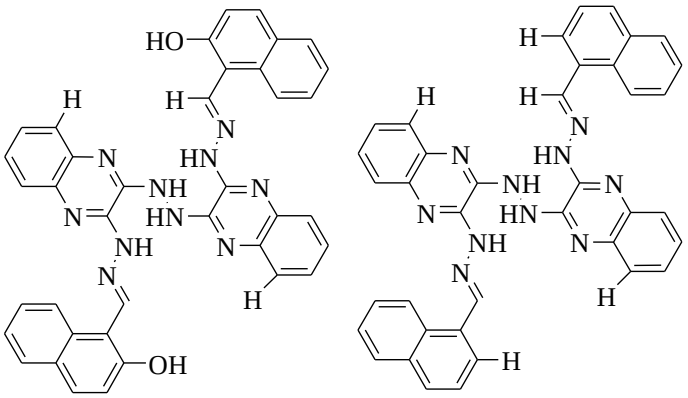

Seletctive to F^-, OAc^- e $H_2PO_4^-$
Chen et al, 2008.

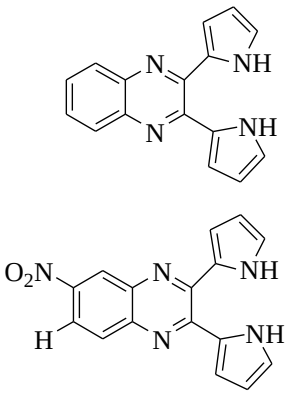

Seletctive to F^-
Black et al., 1999.

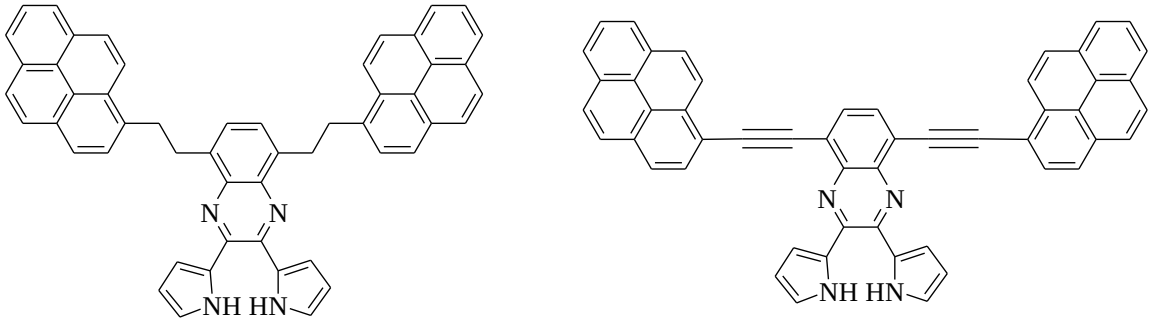

Selective to F^- e $HP_2O_7^{3-}$
POHL et al., 2004.

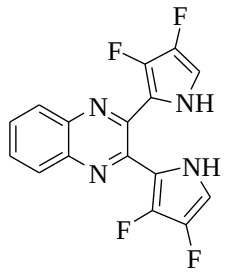

Selective to F^- e $H_2PO_4^-$
Anzenbacher et al.,2000.

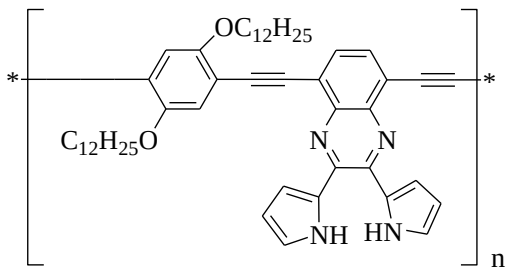

Seletive to F^-
Wu et al.,2006.

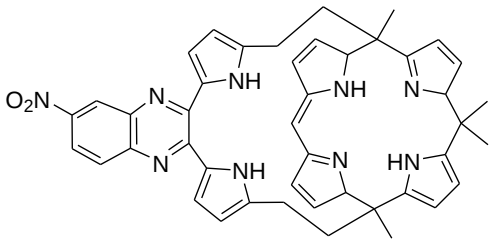

Selective to F^-, $H_2PO_4^-$ e AcO^-
YOO et al., 2009

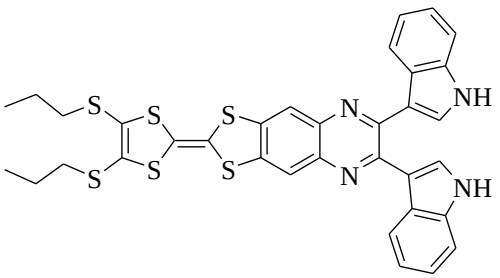

Selective to $H_2PO_4^-$
BEJGER et al., 2010

author, 2020.

2.2.3 Metal complexes as chemosensors

The synthesis of metal complexes has been used as a tool to obtain new sensors, even in smaller numbers when compared to sensors by organic molecules, which has shown good results in this field. Some reported metal complexes have the advantage of enabling the receptor molecule to have better water solubility, which makes possible analysis in biological media and real water samples[84].

Another strategy aimed at complex formation is to increase the H-donor property of the receptor unit for anion receptors, as reported in the work of Madhupriya and Elango (2012)[85], which synthesized Co^{2+} and Ni^{2+} complexes applied in the detection of F^- ions from naphthoquinone derivatives, which the interaction with F^- occurs with aliphatic amine (Fig. 16).

Figure 16 – Complexes of Co^{2+} e Ni^{2+} from the compound 2-((29yridine-2-yl)methylamino)-3-chloronaphthalene-1,4-dione.

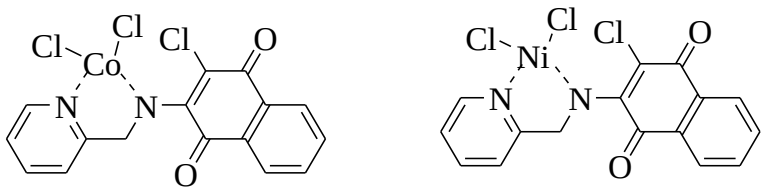

author, 2020.

In addition to Co^{2+} and Ni^{2+}, other transition metals have also been used in the synthesis of anion-selective complexes. This is because these metal complexes have advantages such as i) generally have a positive charge; ii) have defined geometry; iii) have certain characteristics such as redox activity, magnetism, luminescence and catalytic capacity[76].

Besides of other stable complexes from flavonoids is also reported using metals such as Al^{3+} [86], Fe^{3+} [87], Pb^{2+} [88] and Zn^{2+} [89], thus showing the various possibilities in the search for new sensors. Another example of the effectiveness of the formation of these complexes is reported by Roy et al. (2016) which presents a complex formed by rutin, a flavonoid well known for its antioxidant activity, and Cu^{2+} in a stoichiometry 2:1 (Rutin Cu^{2+})[90], as shown in figure 17.

Figure 17 – Rutin-Cu^{2+} complex representation in a 2:1 stoichiometry (Rutin: Cu^{2+}).

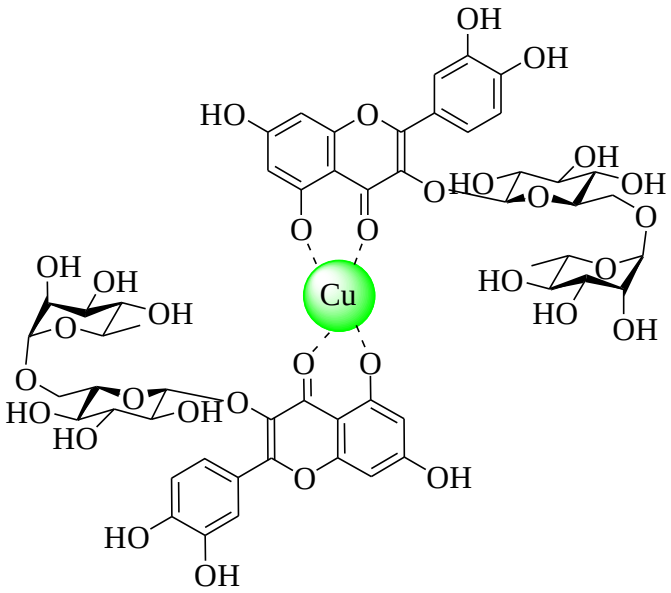

author, 2020.

Cornard and Merlin (2002) also report quercetin complexes (QCT), a flavonoid with various pharmacological activities, with Al^{3+}, showing two possibilities of complexes, the first with 2:1 stoichiometry (QCT: Al^{3+}) and the second 1:2 (QCT: Al^{3+})[91] (Fig. 18).

Figure 18 – Representation of quercetin (QCT)-Al^{3+} complexes in stoichiometry 2:1 (QCT:Al^{3+}) and 1:2 (QCT:Al^{3+}).

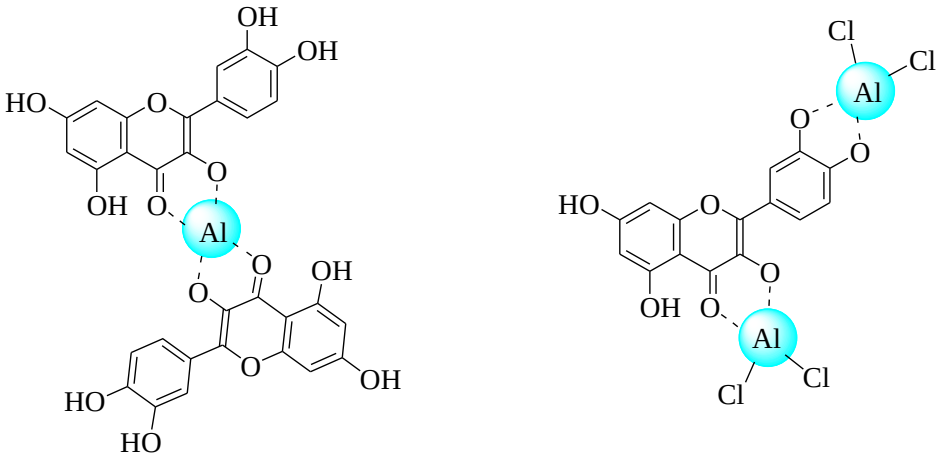

2:1 (QCT:Al^{3+}) 1:2 (QCT:Al^{3+})

author, 2020.

CHAPTER 3 CHROMOGENIC AND FLUOROGENIC OPTICAL DEVICES BASED ON QUINOXALINE DERIVATIVES FOR THE DETECTION OF METAL CATIONS

Lilian C. da Silva[1], Vanderlei G. Machado[2] and Fabrício G. Menezes[1]

[1] *Federal University of Rio Grande do Norte, Institute of Chemistry, PPGQ, Biological Chemistry and Chemometrics,59072-970 Natal, RN, Brazil*

[2] *Departamento de Química, Universidade Federal de Santa Catarina, Florianópolis, SC, 88040-900, Brazil*

Manuscript in finalization

1 INTRODUCTION

Metal cations play essential role in nature due their presence in many biological process[3]. For example, Cu^{2+} is essential to many enzymes and intracellular balance[92], however, when in abnormal levels, it is directly associated to several pathologies such as Menkes syndrome, Wilson's disease, Alzheimer's disease, among others[93-95]. Zn^{2+} consists in another key-cation in biological process, but in elevated levels is associated with a number of serious diseases, such as Alzheimer's disease, Parkinson's disease, diabetes, depression and dysplasia[96,97]. Ag^{+} ions are widely used in industry and pharmaceuticals, but their bioaccumulation and toxicity become a problem for the environment[98].

Hg^{2+} is considered one of the most toxic metals to humans and the environment, mainly because it is related to neurological diseases, and is absorbed by aquatic animals that are part of the human diet[99]. Therefore, the periodic control of metal levels becomes essential to health and environmental issues[1].

Rare-earth elements have great applications in many fields, notably medicinal, electronics and catalysis, and therefore, development of chemosensors for intern transition metals is also an interesting field[100].

The standard methods for quantitative analysis of metal cations include atomic absorption spectrometry[101], inductively coupled plasma techniques[102], and electrochemical measurements[103], among others. However, these techniques have considerable drawbacks, including need for sophisticated instrumentation as well as laborious and time-consuming procedures. To overcome this limitation, the development of artificial chromogenic and fluorogenic chemosensors has attracted great attention to many fields due the possibility of fast, low cost and accurate analysis in complex systems.

The supramolecular strategies for metal cation sensing usually considers the design of a device presenting in its framework two components, a receptor unit, which is responsible for the recognition of the analyte, and a signalizing unit, which is a chromophore or fluorophore (Fig. 19). These two components are connected by a covalent or noncovalent approach, being verified that the recognition of a particular analyte by the receptor unit causes a change in the optical signal of the signalizing unit. In other words, a change in the color and/or fluorescence emission occurs if a particular analyte is present in the medium, which enables the device to indicate the presence of the analyte in the medium qualitatively (naked-eye detection) and quantitatively, with the proper use of spectrophotometric techniques.

Figure 19 Operating mechanism in most chromogenic and fluorogenic optical devices for the detection of analytes.

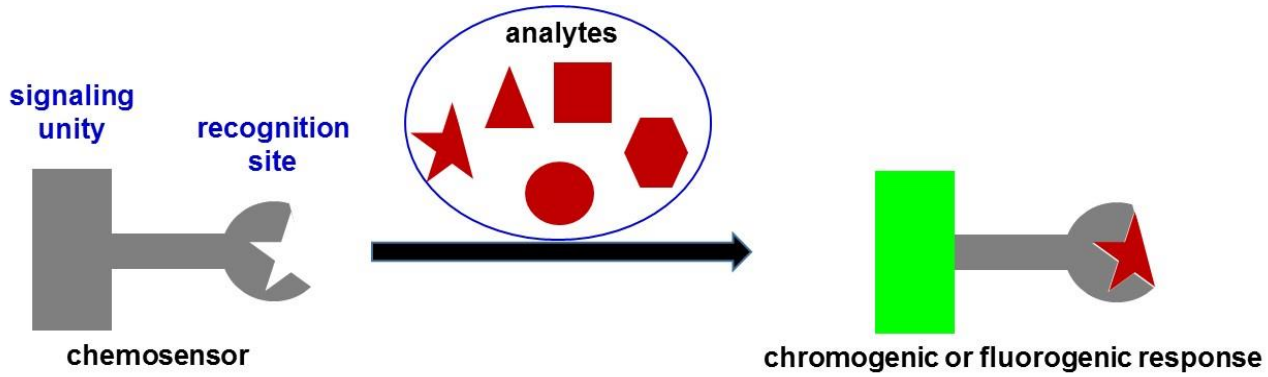

author, 2020.

The recognition of cationic species in these supramolecular optical devices occurs via a receptor-substrate type model, in which Lewis-base donor ability of the receptor induces the formation of a coordination complex with a specific metal analyte. Some considerations may be taken into account in the choice of the receptor unit, such as the nature of chelating sites, geometric parameters, compatible binding affinity with the target analyte, solubility, pH dependence on the recognition, charge and ionic radius of the analyte[104].

The signalizing unit provides a photophysical response (change of color and/or enhancement or quenching of fluorescence emission) related with the recognition of the analyte. The detectable response to an external input may proceed via different mechanisms[104,105], such as: i) photoinduced electron transfer (PET), in which an electron is relocated directly from donor to the acceptor, resulting in a donor-acceptor complex; ii) Förster resonance energy transfer (FRET), which proceeds when the acceptor absorbs photons emitted by the donor; iii) electron exchange (EE), associated to the proximity of donor and acceptor sites, proceeds via transfer of an electron from the LUMO of the excited donor to the LUMO of the acceptor; iv) other mechanisms, such as metal-ligand charge transfer (MLCT).

A considerable number of relevant reviews have been reported in the recent years focusing on the constant progress associated to the development of optical devices for cation sensing and their applications[60,104-121]. Those reviews clearly demonstrate the relevance of the design of a variety of coordinating sites (heteroatoms) for the recognition of the desired species allied with the choice of signaling unities based on aromatic heterocycles for the detection of cations. In fact, the relevance of the chemistry of heterocyclic compounds has also stimulated the publication of some relevant reviews associated to a specific class of heterocycles applied

in sensor fields, such as coumarins[109], crown ethers and other macrocycles[110,121], porphyrins[111,112], cyanines[113], pyridinium *N*-phenolate betaines[118], xanthenes and related compounds[120].

The quinoxaline group is well stablished as a pharmacophore heterocyclic unity due their biological activities for many pathologies, notably their anticancer activity[42,43,122-125], as well as other biological applications[126]. On the other hand, their derivatives are also relevant in material chemistry[14,127,128]. Related to the development of chemosensors, a recent comprehensive review from Dey et al. reported the ability of several quinoxaline derivatives in chromogenic and fluorogenic anion sensing, which is very relevant for both biological and environmental fields[17]. Quinoxaline derivatives have also attracted attention due to their luminescent properties[129] and as ligands in coordination chemistry[17], and based in these latter applications, it becomes evident the potentiality of quinoxaline moiety as signaling unity to the development of artificial receptors for metal cation sensing.

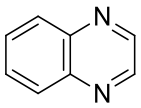

quinoxaline

In this review, we present a survey of the recent literature associated to the use of quinoxaline derivatives as molecular block for the construction of supramolecular strategies for the detection of metal cations. Several examples of quinoxaline derivatives able to detect different cations in solution are presented herein. In addition, the mechanisms involved in the optical device-analyte interactions, as well as the limits of detection and solvent effects, are discussed.

2 Quinoxaline derivatives in metal cation sensing

2.3 Detection of Cu^{2+}

Due the relevant role of Cu^{2+} ions in many biological processes, and, consequently to health, several optical strategies for detection of this metal ion have been presented in literature. Guo et al. reported a series of four dipyrrolylquinoxaline-bridged hydrazones (**1a**-**1d**) as chemosensor for Cu^{2+} in acetonitrile solution (Fig. 20)[130]. Interestingly, small structural changes in the structure of molecules as well as amount of the analytes were found to affect the selectivity in Cu^{2+} sensing. For example, naked eye analysis clearly demonstrated a change from yellow to orange in color of solutions of compound **1b** only in the presence of Cu^{2+} (5 equiv), and this behavior is consistent with spectroscopic data. On the other hand, there is a clear change in the color of solution containing **1d** (from yellow to green) in the presence of 1 equiv of Ni^{2+}, and to red in the presence of 5 equiv of Cu^{2+}. The general binding mechanism involves 1:1 ligand-metal coordination, with association constants from 1.3×10^5 L mol^{-1} to 7.2×10^6 L mol^{-1}, depending on the structure of the chemosensor.

Figure 20 – (a) Binding model for reactions of compounds **1a-1d** and Cu^{2+} in acetonitrile. Naked eye analysis of compound **1b** (b) and **1d** (c) in the presence of different cations (from left to right: Co^{2+}, 1 equiv; Co^{2+}, 5 equiv; Ni^{2+}, 1 equiv; Ni^{2+}, 5 equiv; Cu^{2+}, 1 equiv; Cu^{2+}, 5 equiv; Zn^{2+}, 1 equiv; Zn^{2+}, 5 equiv)[130]

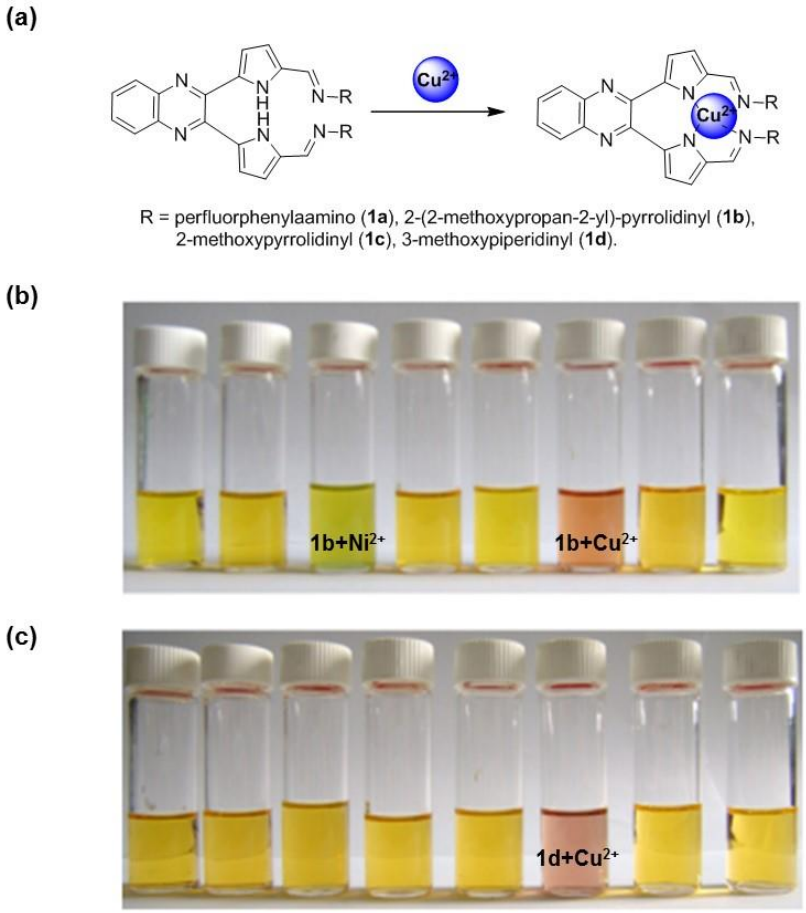

A ninhydrin–quinoxaline hybrid derivative **2** was reported by Upadhyay et al. as a potential chromogenic chemosensor for Cu^{2+} sensing in ethanol-water 1:9 v/v (Fig. 21)[131]. Compound **2** exhibited a change from olive-oil green to pink in the color of solution with the addition of Cu^{2+}, corroborating to the appearance of a band at 530 nm in the UV-vis spectra. Chemosensor **2** was found presenting high selectivity for Cu^{2+} over several other metal cations, including Na^{+}, Mg^{2+}, Al^{3+}, Co^{2+}, Fe^{3+}, Ni^{2+}, Cu^{2+}, Zn^{2+}, Cd^{2+}, Hg^{2+} and Pb^{2+} (Fig. 21). The limit of detection was 3.43×10^{-7} mol L^{-1}, and the binding mechanism involves the formation of 1:1 **2**:cation coordination complex.

Figure 21 – Binding model for reaction of chemosensor **2** and Cu^{2+} in ethanol-water 1:9 v/v.

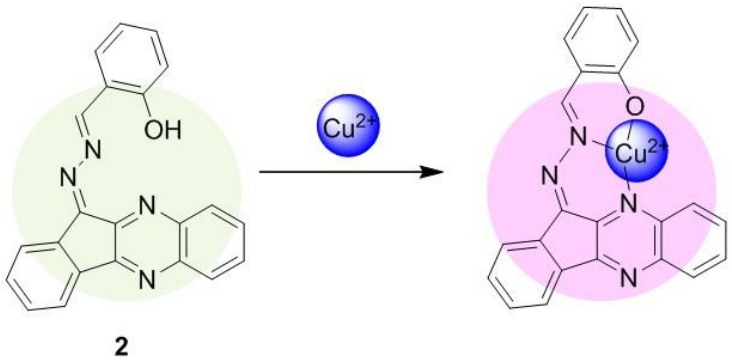

author, 2020.

Silva et al. reported two polyfunctionalized ascorbic acid-based quinoxalines (**3** and **4**) as selective chromogenic chemosensors for Cu^{2+} in methanol and aqueous methanol solutions against several other metal cations (Fig. 22)[132-134]. While compound **3** was obtained via two-step procedure, its Schiff base derivative **4** was synthesized via one-pot protocol in good yields. The presence of Cu^{2+} led to a change from colorless to yellow in the solutions containing compounds **3** and **4,** due to the formation of coordination complexes with 1:2 chemosensor-metal stoichiometry, as verified by UV-vis spectrophotometric analysis. Binding mechanisms were proposed based on infrared spectrophotometry and theoretical calculations. Furthermore, compound **3** was found to be applied as disposable sensor for Cu^{2+} in aqueous solution when adsorbed in paper[134].

Figure 22 – Binding models and colorimetric changes in Cu^{2+} sensing by compounds **3** and **4**.

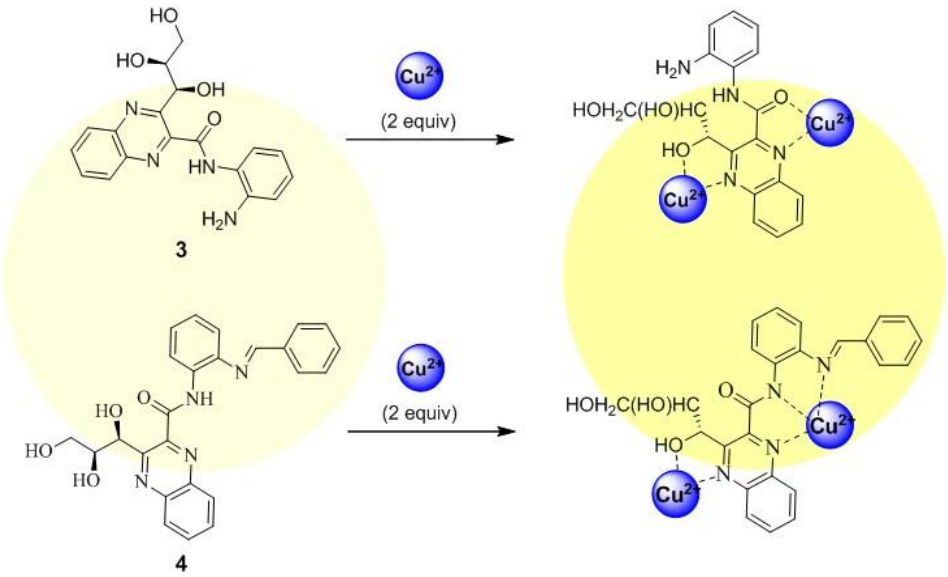

author, 2020.

Liu et al. reported the synthesis of two novel silver complexes based on quinoxaline-dibenzimidazolium salts (**5a** and **5b**), properly characterized, including by X-ray crystallography, and their potential in the chromogenic and fluorogenic selective detection of Cu^{2+} in acetonitrile (Fig. 23)[135]. The binding model involves the formation of 1:1 organometallic-Cu^{2+} complex via Cu^{2+}••• π interactions, with association constants of 1.58 x 10^4 L mol^{-1} and 3.86 x 10^4 L mol^{-1} for **5a** and **5b**, respectively.

Figure 23 – Binding model for interaction of **5a** and **5b** with Cu^{2+} in acetonitrile.

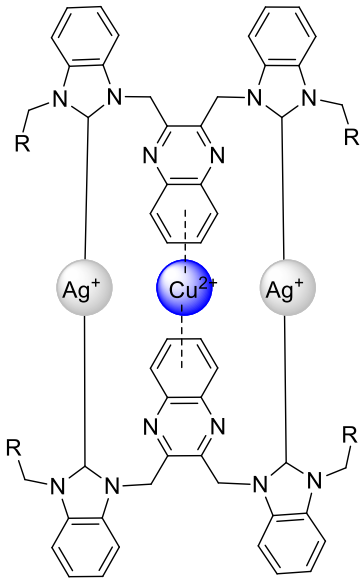

author, 2020.

Yu and coworkers have designed rhodamine-based compound **6**, which acts as chromogenic and fluorogenic optical device for effective Cu^{2+} sensing in phosphate-buffered saline solution (pH 7.4) as demonstrated in Fig. 24[136]. Naked eye analysis cleaerly demonstrated a change from colorless to pink in the solution of compound **6** after addition of Cu^{2+}. A 1:1 **6**:Cu^{2+} stoichiometry was determined from Job's plot analysis. The association constant measured in water was 0.1 µmol L^{-1} and the work concentration of Cu^{2+} ranged from 0.50 µmol L^{-1} to 5.0 µmol L^{-1}. The authors have successfully applied compound **6** in bioimaging analysis based on RAW264.7 cells enriched with Cu^{2+} investigated by laser scanning confocal microscopy.

Figure 24 – Mechanism proposal for association of **6** and Cu^{2+} in aqueous medium.

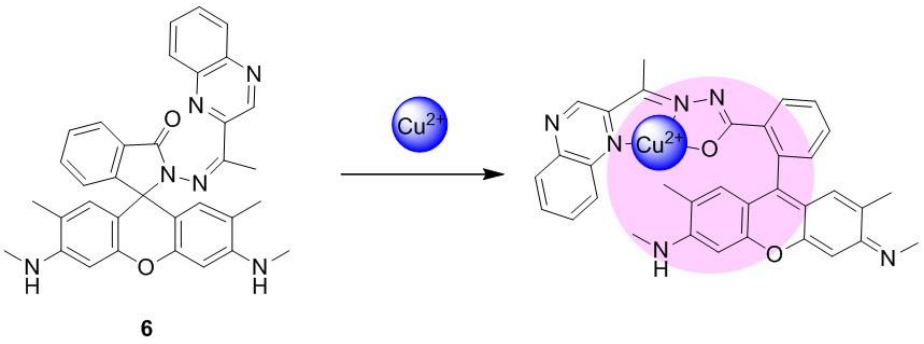

author, 2020.

Korin and coworkers have investigated the metal cation sensing ability of a series of quinoxaline derivatives bearing sulfonamide unities[137]. All compounds studied could be applied for the chromogenic and fluorogenic detection of Cu^{2+} in ethanol, due to the changes in color and red-shift in UV-vis spectra as well as fluorescence quenching in the presence of metal. Fig. 25 illustrates the results obtained for the compounds using compound **7** as example. The binding model involves an initial formation of a complex with 1:2 metal:**7** stoichiometric ratio at low concentrations of Cu^{2+}.The system obtained is then converted to a 1:1 metal:**7** complex if the metal concentration is increased. The binding constants measured for the studied compounds, between $1.15\pm0.07x10^5$ L mol^{-1} and $3.33\pm0.07x10^5$ L mol^{-1}) could be tuned based on the nature of the substituents. Interestingly, there is a Cu^{2+}-induced oxidation of **7** (and related compounds) that takes place in acetonitrile, verified by a change in color of solution from yellow to colorless, which could allow this compound useful as chemodosimeter[137].

Figure 25 – Proposed binding models for reactions between Cu^{2+} and compound **7** in ethanol and acetonitrile.

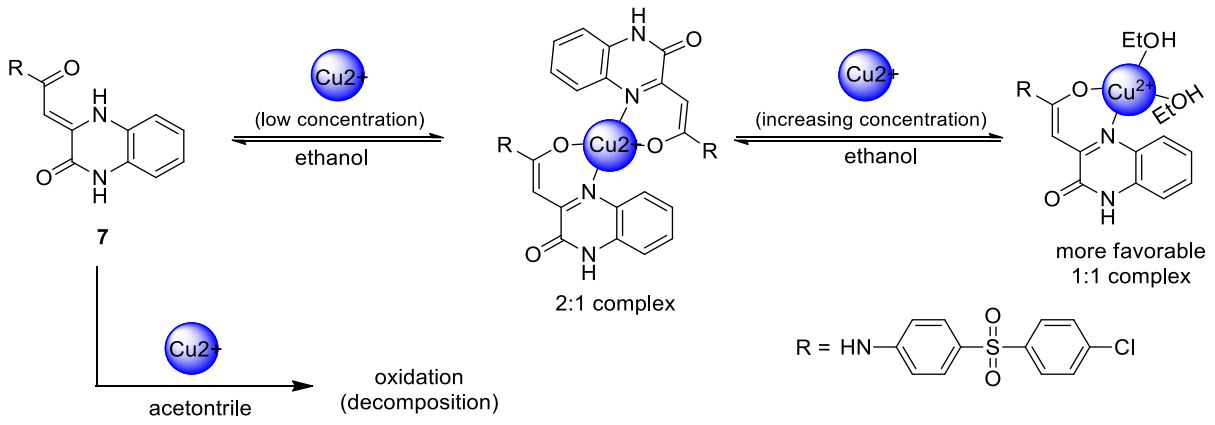

author, 2020.

2.4 *Detection of Zn^{2+}*

Zn^{2+} is also a key species in biological processes and, therefore, several supramolecular optical strategies for detection of this cation are reported in literature. Zhang and coworkers reported the synthesis and full characterization (including X-ray crystallography data) of two highly conjugated polyaza heterocyclic compounds, **8a** and **8b**, and their colorimetric and fluorimetric Zn^{2+} sensing ability in acetonitrile/water solution[138]. The mechanism proposal for the detection of the cation involves the formation of 3:1 and 2:1 metal:compound stoichiometry for **8a** and **8b**, respectively, as evidenced by spectrophotometric studies and X-ray crystallography (Fig. 26). The limits of detection were found to be 0.2 μmol L^{-1} for **8a** and 0.095 μmol L^{-1} for **8b**.

Figure 26 – Binding models, natural color change and fluorescence changes excited by UV lamp (365 nm) for compounds **8a** (a) and **8b** (b) in the presence of Zn^{2+}.[138]

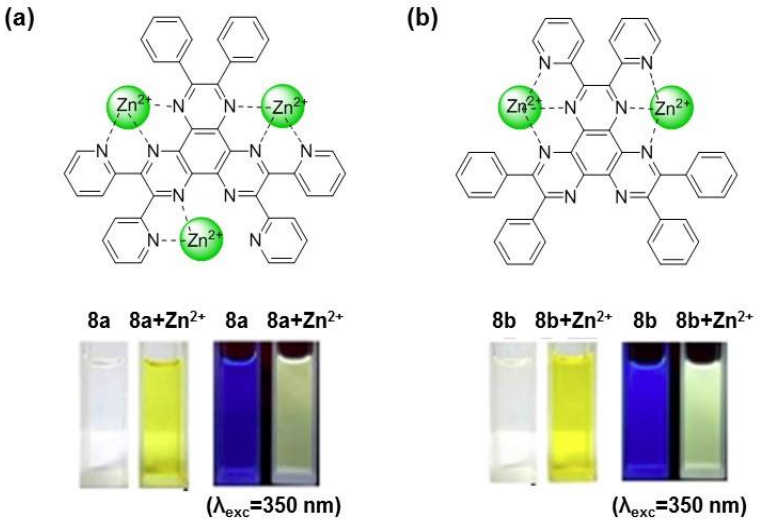

Han and colleagues recently reported the synthesis of five Y-shaped quinoxaline derivatives (**9a**-**9e**), which act as fluorogenic chemosensors for the detection of Zn^{2+} in DMF[139]. A great increase in the fluorescence emission was verified when these compounds interacted with Zn^{2+}, with the formation of coordination complexes of a 1:2 metal:chemosensor stoichiometry. The complexation of compound **9e** with Zn^{2+} is represented in Fig. 27 and induced significant fluorescence turn-on in the presence of the cation under irradiation at 365 nm. On the other hand, small fluorescence suppression was verified when Ni^{2+}, Fe^{3+}, Cu^{2+} or Co^{2+} are presented

in the medium, due to the formation of similar complexes. The chemosensors were found to be very selective for Zn^{2+} over other relevant cations. The fluorescence changes are explained based on intramolecular charge transition induced by enhanced molecular rigidity induced by coordination to Zn^{2+} (Fig. 27).

Figure 27 – Binding model and visual fluorescence change (under irradiation at 365 nm) of compound **9e** in DMF in the presence of Zn^{2+}.

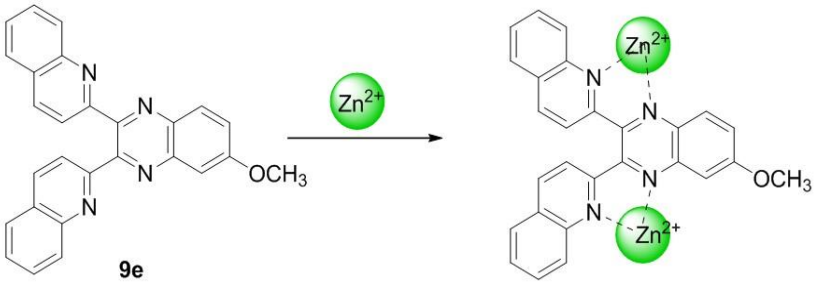

author, 2020.

Lanthanide-based coordination complexes are very interesting to many fields due their fluorescence properties, including relevant applications in biological systems. In the field of chemosensors, the europium-based coordination complex **10** was reported by Fang and colleagues as a fluorogenic probe for Zn^{2+} sensing in water, however, with optical properties also influenced by the presence of Cd^{2+} [140]. As presented in Fig. 28, the design of this functional compound involves the presence of a 1,4,7-*tris*(carboxymethyl)-1,4,7,10-tetraazacyclododecyl group to hold Eu^{3+} for fluorescence emission resource and a *bis*[(2-pyridyl)methyl]-amino unit as Zn^{2+} chelating site, besides a quinoxaline moiety acting by *antenna* effect due its dual coordination to Zn^{2+} and Eu^{3+}, *i.e.* acting as an energy transfer facilitator. The interaction of complex **10** and the cations involves 1:1 stoichiometry, and the limits of detection were found to be 5.0×10^{-7} mol L^{-1} and 1.1×10^{-6} mol L^{-1} for Zn^{2+} and Cd^{2+}, respectively.

Figure 28 – Interaction of europium complex fluorogenic chemosensor **10** with Zn^{2+} in aqueous medium.

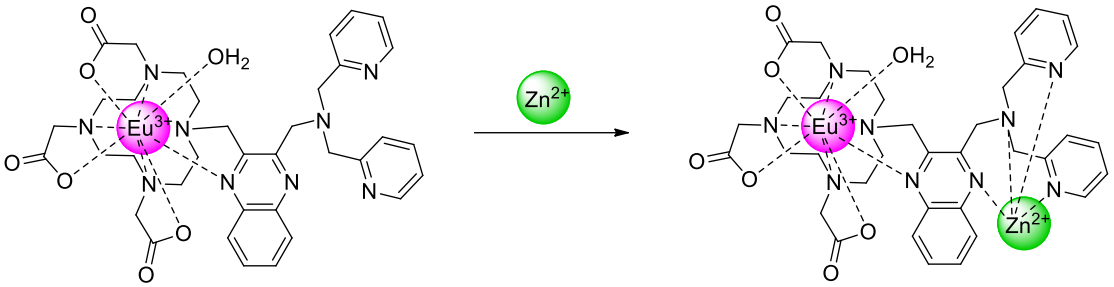

author, 2020.

Sequential detection approaches are very interesting for practical applications. In this context, Li et al. reported the synthesis of a *bis*-2,3-dipyridilquinoxaline-crown ether derivative (**11**) and its application for sequential fluorogenic detection of Zn^{2+} and K^+ in acetonitrile[141]. Binding proposal involves the initial formation of highly fluorescent Zn^{2+}:**11** complex with a 2:1 stochiometric ratio via coordination of the pyridine nitrogen atoms, followed by recognition of K^+ by the 18-crown-6 unit to afford a non-fluorescent complex (Fig. 29). Sequential detection of Zn^{2+} and K^+ proceeds *via* ICT and PET mechanisms, respectively. Authors also showed that free **11** senses the presence of K^+ due fluorescence quenching.

Figure 29 – Binding model for the sequential detection of Zn^{2+} and K^+ by probe **11.**

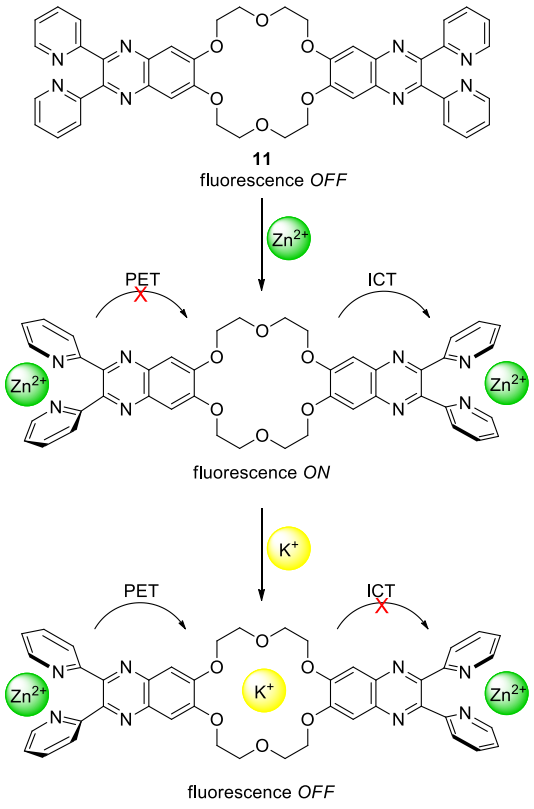

author, 2020.

Ostrowska et al. reported the synthesis and cation sensing ability of a polyfunctionalized pyrrolo[2,3-*b*]quinoxaline derivative (**12**)[142].The fluorogenic detection of Zn^{2+} by compound **12** over several other cations in acetonitrile involves the formation of a 1:1 metal:**12** complex, investigated by UV-vis spectrophotometric titration (log *K* = 6.13) and confirmed by X-ray crystallography. The chemosensor operates via an intramolecular charge transfer *off-on* type mechanism (Fig. 30). Interestingly, compound **12** was obtained along with its *Z*-isomer, however, this latter needs to undergo isomerization to *E*-isomer, and only the *E*-isomer is able to loss a proton and then coordinate Zn^{2+}.

Figure 30 – Representation of chemosensor **12** and its interaction with Zn^{2+} in acetonitrile

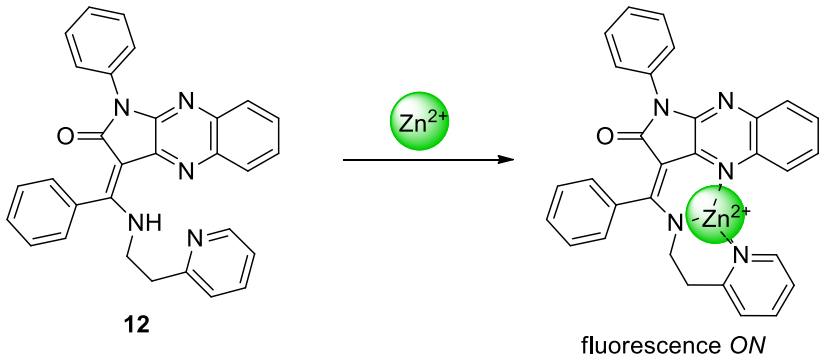

author, 2020.

2.5 *Detection of Ni^{2+}*

Nickel is a transition metal present in some relevant enzymes[143], but due their several applications in industry, Ni^{2+} represents a pollutant to the environment[144]. Therefore, the development of strategies based on optical devices for effective detection of ionic nickel is a relevant issue. Goswami *et al.* reported a series of polyfunctionalized quinoxaline derivatives, **13a**-**13c**, as chromogenic chemosensors for Ni^{2+} in solution[145-147] (Fig. 31). Compound **13a** was able to detect Ni^{2+} in CH_3CN-HEPES 9:1 v/v (pH 7.4), while compounds **13b** and **13c** detected Ni^{2+} in CH_3CN solution. Compounds **13a** and **13b** allowed naked eye detection by changes in color of their solution from colorless to yellow in the presence of Ni^{2+}, while **13c** leads to a pink solution after coordination. These features are consequence of difference in binding mechanisms in the formation of 1:2 metal-**13** complex. For **13a** and **13b**, association takes place via coordination by quinoxaline and 43ydrazine nitrogen atoms do Zn^{2+}. On the other hand, interaction between **13c** and Ni^{2+} proceeds via coordination with quinoxaline and imine

nitrogen atoms along phenolic oxygen. The limits of detection were interesting, being of 5.59 x 10^{-6} mol L^{-1} for **13b**.

Figure 31 – Binding models for interactions of ligands**13a**-**13c** and Ni^{2+}.

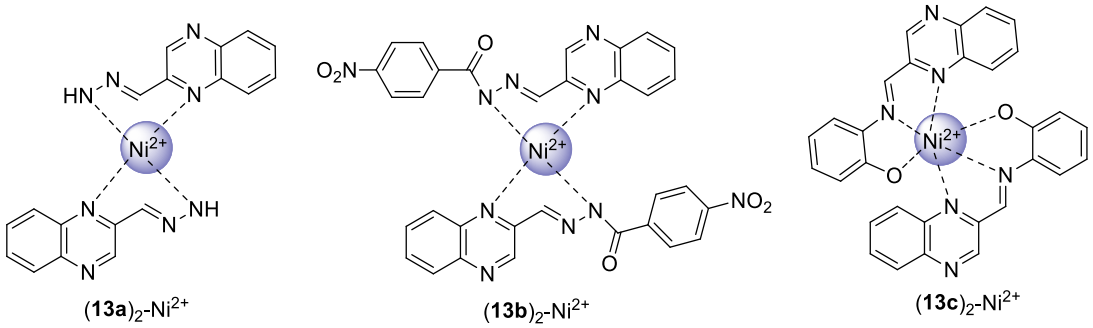

author, 2020.

Recently, Upadhyay and Karpagam reported the capacity of three novel polymers bearing quinoxaline and carbazole unities, **14a**-**14c**, in the selective fluorogenic detection of Ni^{2+} in aqueous THF solution over twelve other cations (Li^{+}, Na^{+}, K^{+}, Mg^{2+}, Ca^{2+}, Mn^{2+}, Ni^{2+}, Cd^{2+}, Cu^{2+}, Zn^{2+}, Fe^{2+} and Hg^{2+})[148] (Fig. 32). The fluorescence quenching of the polymer when Ni^{2+} is present in the medium is probably caused by energy or electron transfer reactions between the polymer backbone and binding metal complexes.

Figure 32 – Structures of polymers **14a**-**14c** (a) and their fluorescence response toward metal cations: **14a** (b); **14b** (c); and **14c** (d). C represents the polymer in the absence of metal ions[148].

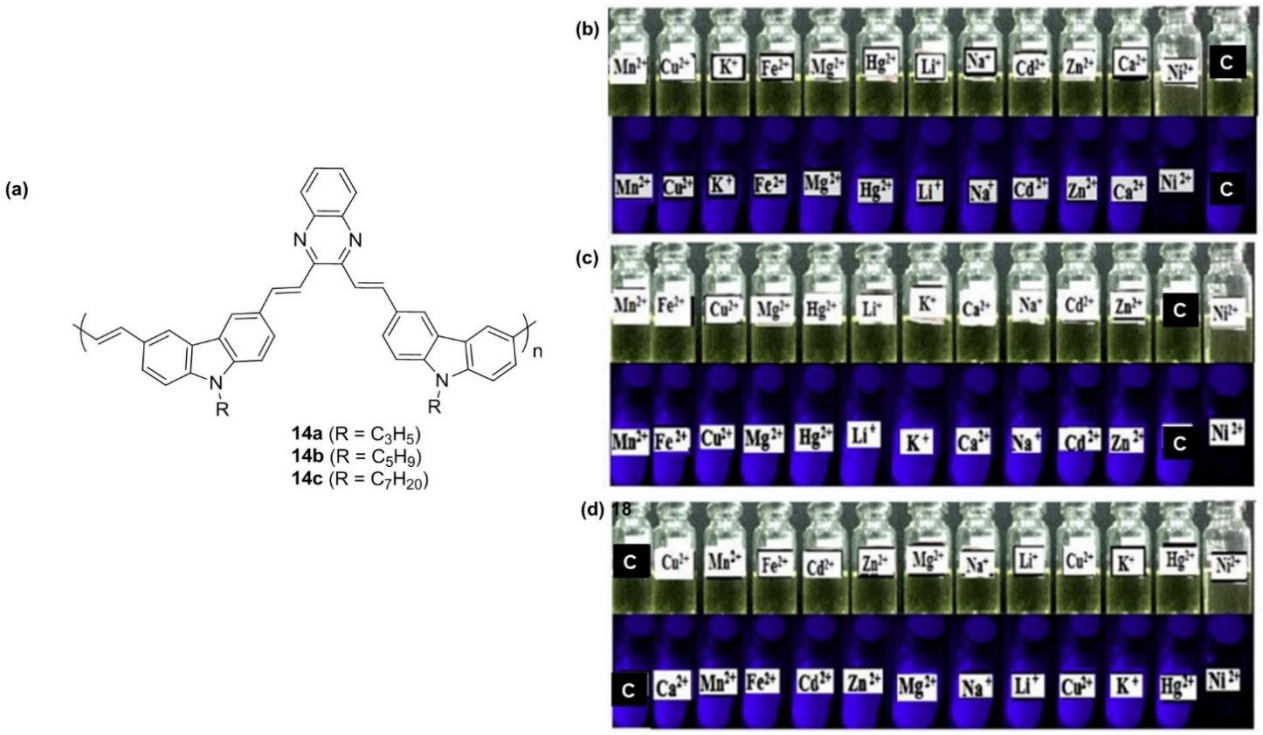

Milewska et al. reported the synthesis of *α*-aminoacid derivative *N*-Boc-3-[2-(2-quinoxalinyl)benzoxazol-5-yl]alanine methyl ester, bearing a conjugated benzoxazole-quinoxaline system as side chain, as a fluoroionophore for Ni^{2+} in acetonitrile solution[149]. Changes in the UV-vis spectrum of the compound were verified for cations, such as Cu^{2+}, Al^{3+} and Pb^{2+}, but only Ni^{2+} promoted a substantial increase of fluorescence intensity for an emission band with maximum at 460 nm. The equilibrium constant of the complex formation for Ni^{2+} to be log K = 3.61.

2.4 Detection of Hg^{2+}

Great efforts have been dispended in the development of practical protocols for fast detection of mercury in solution due its high toxicity and association to several pathologies[66]. Wang et al. reported the synthesis and selective Hg^{2+} sensing of two quinoxaline/pyrrol/imine-based macrocycles (**15a** and **15b**) in aqueous medium, *via* formation of 1:1 metal-chemosensor complexes which induce fluorescence suppression for the emission band with maximum at 358 nm [150] (Fig. 33). Chemosensors **15a** and **15b** were selective to Hg^{2+} even in competitive medium and limits of detection were measured around 1.0 x 10^{-7} mol L^{-1}.

Figure 33 – Hg^{2+} sensing by chemosensors **15a** and **15b** in aqueous medium.

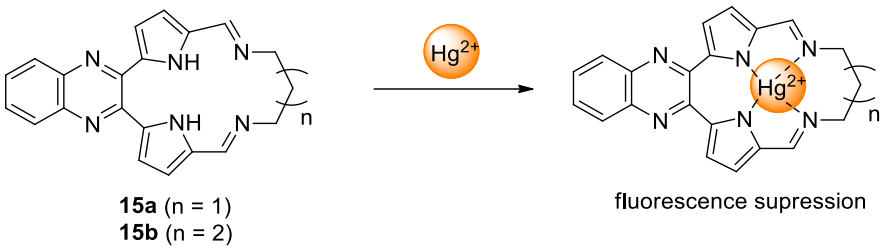

author, 2020.

Two ferrocene-based quinoxaline derivatives were reported as chemosensors for Hg^{2+} [151,152]. As reported by Zapata et al., compound **16** was verified as potential chromogenic chemosensor for Hg^{2+} in acetonitrile solution due the induced change in color of solution from orange to green after addition of the metal (Fig. 34)[154]. A 1:1 **16a**:Hg^{2+} coordination complex was proposed based on spectrofotometric data, with log K_a = 3.4 ± 0.17, and the binding model was proposed based on ^{1}H NMR experiments. The limit of detection calculated for compound **16a** reached 1,3 × 10^{-5} mol L^{-1}. As other example, Alfonso and colleagues reported the selective fluorogenic and chromogenic Hg^{2+} by 2-ferrocenyl-7,8-di-(2-pyridyl)-3*H*-imidazo[4,5-*f*]quinoxalines in CH_3CN solution[152]. The experiments suggest a 1:1 chemosensor:metal stoichiometric ratio.

Figure 34 – Interaction of chemosensor **16** with Hg^{2+} in acetonitrile, showing the visual aspect of the solution before and after the addition of the metal.

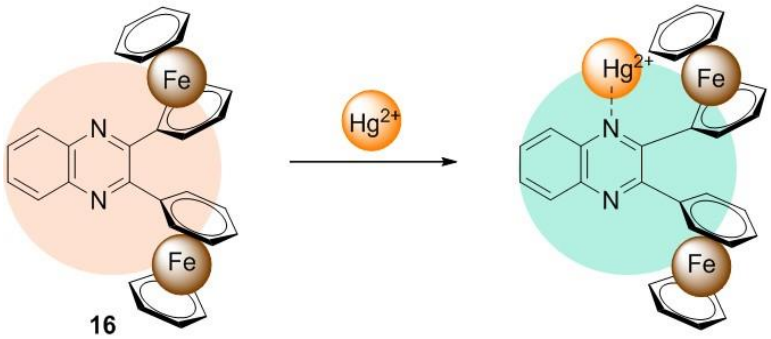

author, 2020.

The highly conjugated thiosemicarbazone Schiff base **17** was reported by Feng et al. for selective detection of Hg^{2+} in aqueous DMSO[153]. Fluorescence and UV-vis spectrophotometric studies indicated a 2:1 metal:**17** stoichiometry with association constant of 2.51 x 10^{-5} L mol^{-1}, and a relevant limit of detection of 9.07 x 10^{-7} mol L^{-1}. A binding model was proposed involving coordination of nitrogen and sulfur atoms from hydrazinecarbothioamide moieties (Fig. 35). Notably, compound **17** was effective in the quantitative determination of Hg^{2+} in different real samples (lake, tap and distilled water).

Figure 35 – Proposed structure for 1:2 ligand metal complex from compound **17** and Hg^{2+}.

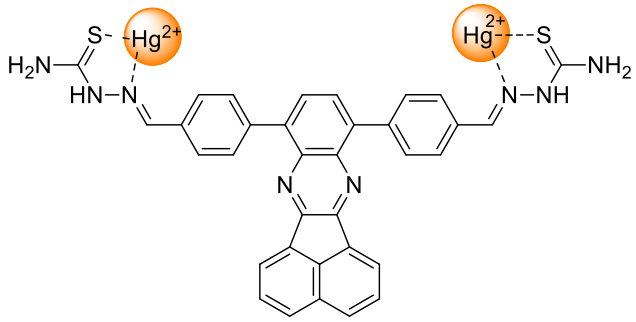

(Zn^{2+})**-17**

author, 2020.

2.5 Detection of other metal cations

The literature brings interesting examples of quinoxaline-based optical chemosensors for the detection of other metal cations. Zhao *et al*. reported the polynitrogen-based heteroaromatic compound **18** in the selective detection of Cd^{2+} in CH_2Cl_2/CH_3CN (1:9 v/v) solution[154] (Fig. 36). It was found a Cd^{2+}-induced color change in the solution containing **18**, from colorless to yellow, as well as an increase in the emission based in an intramolecular charge-transfer mechanism. The association constants for Cd^{2+} were obtained as $K_{Cd1} = 3.7x10^4$, $K_{Cd2} = 1.2x10^4$, and $K_{Cd3} = 4.1x10^3$. The formation of a 3:1 metal:**18** complex was also confirmed by X-ray crystallography. Although ligand **18** also provided a positive colorimetric response for Zn^{2+}, fluorescence properties are not affected by this ion. In further study, the authors reported that compound **18** could be used as a fluorogenic chemosensor for detection of La^{3+} over other inner transition metals (Ce^{3+}, Pr^{3+}, Nd^{3+}, Sm^{3+}, Eu^{3+}, Gd^{3+}, Tb^{3+}, Dy^{3+}, Ho^{3+}, Er^{3+}, Tm^{3+}, Yb^{3+} e Lu^{3+}) in acetonitrile[155]. Mechanism and binding model proposals are similar to those found for detection of Cd^{2+}.

Figure 36 – Binding model of chemosensor **18** in CH_2Cl_2/CH_3CN (1:9 v/v) in the presence of Cd^{2+} and photos of the solutions of 18 in the absence and in the presence of the metal ion exposed to natural light and to UV light (365 nm).

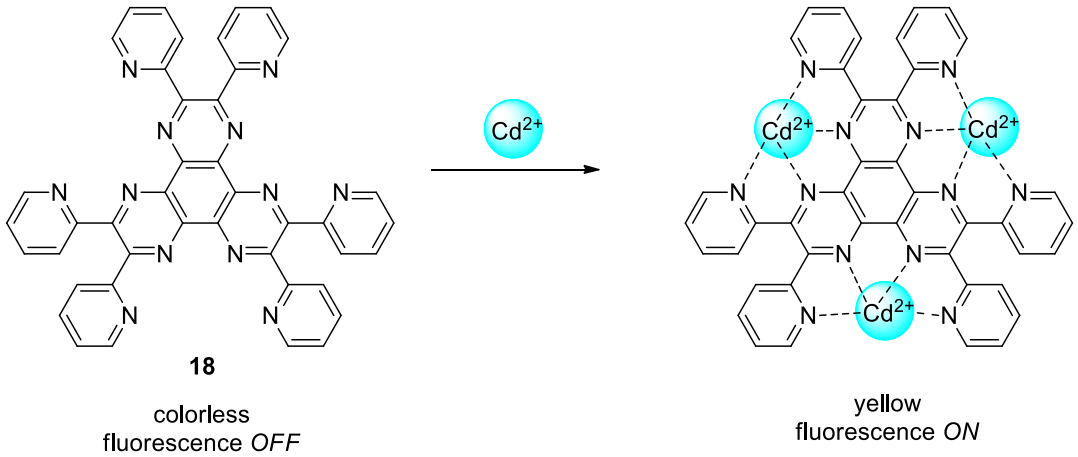

author, 2020.

Recently, Zhang et al. reported the ability of an organized metal-organic framework based on Cd^{2+}-organometallic compound **19** as functional chemosensor for Fe^{3+} sensing in DMF solution (Fig. 37)[156]. Interestingly, the resulting framework remains structurally unchanged even in DMF solution. The addition of Fe^{3+} induces an extremely significant

quenching effect on the luminescence of compound **19**, possibly due to the strong affinity of uncoordinated quinoxaline N atoms to the Fe^{3+} ion and the electron transfer from the donor groups to Fe^{3+}. The detection limit was estimated to be 2.5×10^{-6} mol L^{-1}.

Figure 37 – Representation for the structure of organometallic compound **19**.

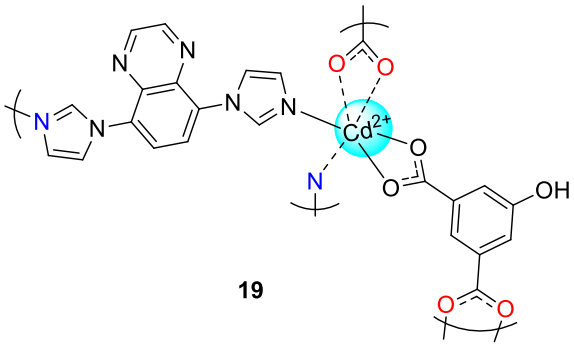

19

author, 2020.

Two quinoxaline-based conjugated polymers, **20a** and **20b**, were reported as effective in the detection of Ag^{+} ions[98,157] (Fig. 38). The presence of Ag^{+} to aqueous THF solution containing polymer **20a** leads to change in color of solution from green to red-browned. On the other hand, polymer **20b**, reported by Shi *et al.*, was also effective in the selective detection of Ag^{+} against several other cations (including Al^{3+}, Ba^{2+}, Cd^{2+}, Cu^{2+}, Hg^{2+}, Mg^{2+}, Na^{+}, Ni^{2+}, Pb^{2+} and Zn^{2+}) in aqueous solution. In both cases, metal-chemosensor associations lead to fluorescence quenching. The detection limits for chemosensors **20a** and **20b** reached $5x10^{-6}$ mol L^{-1} and 6.4×10^{-8} mol L^{-1}, respectively.

Figure 38 – Chemical structures of polymers **20a** and **20b** used as functional chemosensor for Ag^{+} sensing.

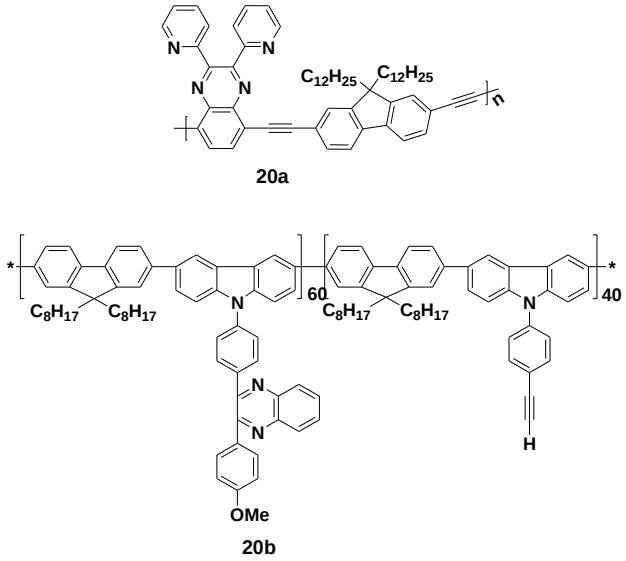

author, 2020.

Compounds **21a**-**21c** comprehend three relevant polymer-based chemosensors (Fig. 39). Zhu et al. reported the synthesis and Co^{2+} sensing ability of compound **21a** in THF solution[158]. The presence of Co^{2+} in solution induced a change from orange to green, possibly due to the formation of a core–shell structure. On the other hand, Çarbas *et al*. reported two polymeric chemosensors, **21b** and **21c**, for fluorimetric detection of Fe^{3+} ions in DMF solution[159,160]. Addition of Fe^{3+} to solution of compound **21b** leads to fluorescence quenching (excitation at 500 nm, emission at 585 nm). Fluorescence quenching was also verified for compound **23c** upon addition of Fe^{3+} (excitation at 520 nm, emission at 630 nm). Stern–Volmer constants (K_{sv}) were determined, being 5.0×10^{3} L mol^{-1} and 5.0×10^{2} L mol^{-1} for **21b** and **21c**, respectively.

Figure 39 – Structures of the polymeric sensors **21a-21c** and naked eye detection of Co^{2+} under natural light by **21a** and of Fe^{3+} by **21b** and **21c** under UV light.

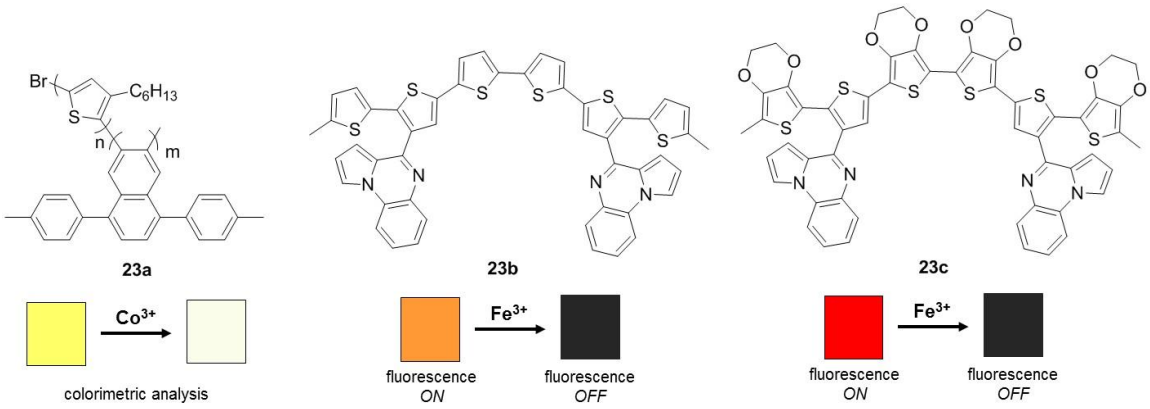

author, 2020.

3 CONCLUSIONS

This review describes the use of quinoxaline derivatives as functional plattaform in chromogenic and fluorogenic chemosensors for metal cation sensing in solution. The advances in the field were properly discussed in terms of sensing mechanisms as well as selectivity and sensitivity parameters, including detection limits and concentration ranges. Practical implementation of these reported chemosensors were also discussed when presented in original manuscripts. In agreement with a recent review focusing in quinoxaline derivatives applied in anion sensing[17], this survey confirms the versatility of this heterocycle for the development of artificial receptors for ion detection in solution.

CHAPTER 4 ONE-POT SYNTHESIS AND STRUCTURAL ELUCIDATION OF POLYFUNCTIONALIZED QUINOXALINES AND THEIR USE AS CHROMOGENIC CHEMOSENSORS FOR IONIC SPECIES

Lilian C. da Silva[1], Alexandra Lindner[2], Lívia N. Cavalcanti,[1] Erivaldo P. da Costa[1], Mireia M. Azevedo[1], Renata M. Araújo[1], Gutto R.S. de Freitas[3], Miguel A. F. de Souza[1], Vanderlei G. Machado[2] and Fabrício G. Menezes[1]*

[1] *Federal University of Rio Grande do Norte, Institute of Chemistry, PPGQ, Biological Chemistry and Chemometrics,59072-970 Natal, RN, Brazil*

[2] *Departamento de Química, Universidade Federal de Santa Catarina, Florianópolis, SC, 88040-900, Brazil*

[3] *Federal Institute of Rio Grande do Norte, Currais Novos, RN, 59380-000, Brazil*

Manuscript of the article: Journal of Molecular Structure 1195 (2019) 936e943

Contributions:

- Synthesis of compounds
- Spectroscopic Experiments for sensor of Cu^{2+}
- NMR elucidation

1 INTRODUCTION

The development of synthetic receptors for recognizing ionic substrates in solution is one of the main targets in supramolecular chemistry[7,161], and represents an important basis for developing optical devices for the selective detection of analytes with practical importance[162-168]. Advances in this field have attracted many research groups to studies related to the design of chromogenic chemosensors, especially due to the fact that the analysis involves both simple implementation and low-cost procedures, including the possibility of naked-eye detection[169].

Two important targets associated to ion detection are Cu^{2+} and F^- due to their abundance in nature and relevance in different fields. For example, Cu^{2+} is essential to several biological processes since it is present in many important enzymes. However, when in abnormal levels it may lead to toxicity and damaging conditions, which are associated to several pathologies[119,131,170-172]. On the other hand, F^- plays relevant role in treatment and prevention of dental damage as well as osteoporosis, but it may be associated to many diseases in overexposure situations[77,173-175]. Furthermore, is associated to military proposes, including refinement of uranium and as a hydrolysis product of Sarin, a nerve agent used in terrorist incidents[174].

Aromatic heterocycles are commonly explored as signaling unities in artificial receptors due to their relevant electronic properties, which can be affected by interaction with specific analytes. In this context, several synthetic chemosensors for both cations and anions have been developed based on quinoxaline derivatives[14,78,80,131,132,136,176]. Synthetic methodologies based on one-pot procedures have attracted attention in the last decades due to environmental concerns, economics, and time-dependence, among other issues[14]. In this context, some interesting examples are reported in literature in which quinoxaline derivatives of relevant applications are synthesized via one-pot procedures[12,127,177,178].

This paper reports the effective *one-pot* synthesis of nine polyfunctionalized quinoxaline derivatives starting from *L*-ascorbic acid. Furthermore, a detailed NMR spectrometric study was performed and the data brought to the light relevant information associated to the target-molecules. Two selected products were investigated as chromogenic chemosensors for detecting ions in solution. While compound **22a** was found to be selective for detection of Cu^{2+} in aqueous medium (methanol-water 4:1), compound **22b** was able to perform selective recognition of F^- in DMSO and aqueous DMSO solution. These sensing-ability studies were performed based on UV-vis, as well as theoretical calculations or NMR spectrometry as supporting data.

2 EXPERIMENTAL

2.1 General

All reagents, solvents and other materials were purchased from commercial sources and used without purification. Inorganic salts $CuCl_2$, $CoCl_2.6H_2O$, $SnCl_2.2H_2O$, $MgCl_2.6H_2O$, $Ba(NO_3)_2$, $SrCl_2.H_2O$, $Pb(NO_3)_2$, $Zn(NO_3)_2.6H_2O$, $NiCl_2$, $FeSO_4.7H_2O$, $AlCl_3$, $CdSO_4.8H_2O$, NaCl, LiCl, $AgNO_3$ and $Cr(NO_3)_3.9H_2O$, were used in this work. All anions (HO^-, HSO_4^-, $H_2PO_4^-$, NO_3^-, CN^-, $HCOO^-$, F^-, Cl^-, Br^-, and I^-) were used as tetra-*n*-butylammonium salts. Melting points were acquired on a Microquímica MQAPF0301 instrument and were not corrected. Elemental analyses were performed using an E-1110 Carlo Erba instrument. Infrared spectra were acquired using a PerkinElmer model 283 equipment. NMR spectra were performed on a Varian Mercury Plus 400 MHz or Bruker Avance DPX 300 MHz, DMSO-d_6 as solvent.

*2.2 One-pot procedure for obtainment of compounds **22a-22i***

In a round bottom flask, a solution of 0.20 g (1.14 mmol) of *L*-ascorbic acid in 20 mL of ethanol was stirred at 60 ^oC until total homogenization. Then 0.12 g (1.14 mmol) of benzoquinone was added and resulting solution was stirred at 60 ^oC for 2h. After that, 0.24 g (2.20 mmol) of *o*-phenylenediamine was added and the resulting solution was kept in the same reactional condition for 3 h. Then, the appropriate aldehyde (1.25 mmol) and 0.1 mL of glacial acetic acid were added to the reactional flask, and the final solution was maintained at 60 ^oC for 4-20 h. After this time, half of solvent was withdrawn under vacuum, cold water was added and the solution was kept in ice bath. The resulting precipitate was collected by filtration as pure product. Detailed information is given in Table 2. Melting points, infrared spectroscopy and elemental analysis data are presented below, and ^1H and ^{13}C NMR data are given in Table 2 and Table 3, respectively.

N-[(*E*)-2-*(phenylmethylidene)amino)phenyl]-3-(1,2,3-trihydroxypropyl)naphthalene-2-carboxamide* (**22^a**): m.p.: *203 °C; IR* (KBr, $\bar{\nu}_{max}/cm^{-1}$): 3361, 1679, 1585, 1514, 1450, 1058, 763. Elemental analysis for $C_{25}H_{22}N_4O_4$: C, 67.86; H, 5.01; N, 12.66; found: C, 67.78; H, 5.08; N, 12.70.

N-[(*E*)-2-(4-nitrobenzylidene-amino)phenyl]-3-((1*S*,2*S*)-1,2,3-trihydroxypropyl)quinoxaline-2-carboxamide (**22b**): m.p.: 220 ºC; IR (KBr, $\bar{\nu}_{max}$/cm^{-1}): 3390, 1640, 1515, 1340, 802. Elemental analysis for $C_{25}H_{21}N_5O_6$: C, 61.60; H, 4.34; N, 14.37; found: C, 61.59; H, 4.38; N, 14.39.

N-[*(E)-2*-(4-fluorophenyl)methylidene)amino)phenyl]-3-((1*S*,2*S*)-1,2,3-trihydroxypropyl)quinoxaline-2-carboxamide (**22c**): m.p.: 210 °C; IR (KBr, $\bar{\nu}_{max}$/cm^{-1}): 3432, 3297, 1678, 1579, 1509, 1451, 1220, 1043, 826. Elemental analysis for $C_{25}H_{21}FN_4O_4$: C, 65.21; H, 4.60; N, 12.17; found: C, 65.28; H, 4.70; N, 12.21.

N-[*(E)-2*-(4-bromophenyl)methylidene)amino)phenyl]-3-((1*S*,2*S*)-1,2,3-trihydroxypropyl)quinoxaline-2-carboxamide (**22d**): m.p.: 231 °C; IR (KBr, $\bar{\nu}_{max}$/cm^{-1}): 3350, 3285, 1664, 1582, 1514, 1448, 1029, 754. Elemental analysis for $C_{25}H_{21}BrN_4O_4$: C, 57.59; H, 4.06; N, 10.75; found: C, 57.57; H, 4.11; N, 10.79.

N-[(*E*)-2-(3-hydroxyphenyl)methylidene)amino)phenyl]-3-((1*S*,2*S*)-1,2,3-trihydroxypropyl)quinoxaline-2-carboxamide (**22e**): m.p.: 232 °C; IR (KBr, $\bar{\nu}_{max}$/cm^{-1}): 3519, 3276, 3170, 1655, 1588, 1515, 1059, 769. Elemental analysis for $C_{25}H_{22}N_4O_5$: C, 65.49; H, 4.84; N, 12.22; found: C, 65.51; H, 4.89; N, 12.25.

N-[(*E*)-2-(4-hydroxyphenyl)methylidene)amino)phenyl]-3-((1*S*,2*S*)-1,2,3-trihydroxypropyl)quinoxaline-2-carboxamide (**22f**): m.p.: 220 °C; IR (KBr, $\bar{\nu}_{max}$/cm^{-1}): 3432, 3304, 1662, 1600, 1576, 1512, 1448, 1059, 810, 746. Elemental analysis for $C_{25}H_{22}N_4O_5$: C, 65.49; H, 4.84; N, 12.22; found: C, 65.50; H, 4.87; N, 12.27.

N-[(*E*)-2-(4-methoxyphenyl)methylidene)amino)phenyl]-3-((1*S*,2*S*)- 1,2,3-trihydroxypropyl)quinoxaline-2-carboxamide (**22g**): m.p.: 211 °C; IR (KBr, $\bar{\nu}_{max}$/cm^{-1}): 3450, 3304, 1687, 1660, 1580, 1505, 1450, 1263, 1035, 833, 769. Elemental analysis for $C_{26}H_{24}N_4O_5$: C, 66.09; H, 5.12; N, 11.86; found: C, 66.11; H, 5.15; N, 11.90.

N-[(*E*)-2-(4-hydroxy-3-methoxyphenyl)methylidene)amino)phenyl]-3-((1*S*,2*S*)-1,2,3-trihydroxypropyl)quinoxaline-2-carboxamide (**22h**): m.p.: 205 °C; IR (KBr, $\bar{\nu}_{max}$/cm^{-1}): 3536, 3370, 3298, 1679, 1568, 1506, 1442, 1211, 1021, 769, 755. Elemental analysis for $C_{26}H_{24}N_4O_6$: C, 63.93; H, 4.95; N, 11.47; found: C, 63.91; H, 4.97; N, 11.50.

N-[(*E*)-2-(4-(dimethylamino)phenyl)methylidene)amino)phenyl]-3-((1*S*,2*S*)-1,2,3-trihydroxypropyl)quinoxaline-2-carboxamide (**22i**): m.p.: 197 °C; IR (KBr, $\bar{\nu}_{max}$/cm^{-1}): 3403, 3259, 1666, 1604, 1584, 1503, 1448, 1167, 817, 762. Elemental analysis for $C_{27}H_{27}N_5O_4$: C, 66.79; H, 5.61; N, 14.42; found: C, 66.76; H, 5.65; N, 14.45.

2.3 Chemosensor assay

2.3.1 Cu^{2+} detection

Naked-eye and UV-vis studies aiming ion detection were performed by analyzing changes in the color of solutions containing compound **22a**, in methanol, before and after addition of 10 equiv of selected cations in water. Photographs were taken and UV-vis spectra were obtained for each final solution after 60 min. Spectrophotometric titration was performed by addition of Cu^{2+} (0 to 5 equiv) in water to a methanolic solution of **22a**. In all experiments, the final solution of **22a** was fixed at 4x10^{-5} mol L^{-1} and methanol-water 4:1 *v/v* as the final solvent system.

2.3.2 F^- detection

Naked-eye and UV-vis experiments were performed by analyzing changes in the color of solutions containing compound **22b** (4.0×10^{-5} mol L^{-1}) in the absence and presence of anionic species in DMSO and in DMSO containing 2.5% (v/v) water. Titration experiments were performed with the preparation of solution of **22b** as described previously. This solution was used to prepare the stock anion solutions in flasks which were closed with rubber stoppers and the titrations were carried out by adding small amounts (2–50 μL) of the salt solution with a microsyringe to closed quartz cuvettes containing the solution of compound **22b**. UV–vis spectra were obtained after each addition and the absorbance values were collected at 440 nm in DMSO and at 434 nm in DMSO containing 2.5% (v/v) water.

2.4 Computational calculations

The computational methodology employed for obtainment of structural parameters of compound **1a** was B3LYP combined with 6-311++G(d,p) basis set[179], and the calculations were performed using a Gaussian software[180]. All optimized structures were found as minimum at

the potential energy surface since vibrational frequencies did not indicate imaginary frequencies. The conductor-like polarizable continuum model (CPCM) solvation method was employed in order to verify the solvent effect[181,182].

3. RESULTS AND DISCUSSION

3.1 Synthesis and general structural analysis

The overview of the protocol for the one-pot synthesis of nine polyfunctionalized quinoxalines is presented in Table 1. Compounds 22a-22i were obtained in good yields (65-84 %) for an interesting scope of commercially available aldehydes. Ethanol was selected as solvent for this protocol due to its low toxicity and high availability. All products were collected by direct filtration from the solution, i.e. not requiring any purification process. Mechanistically, the reaction starts by oxidation of L-ascorbic acid by the action of benzophenone to its dehydro-derivative, which then reacts with two equivalents of o-phenylenediamine to give both quinoxaline and amide unities. Lastly, condensation of aromatic amine with appropriate aldehydes affords the final products. As expected, reactions were affected by the nature of the aldehydes. In this context, while the reaction involving 4-nitrobenzaldehyde was found to be the fastest one, those involving aromatic aldehydes bearing electron releasing groups required longer periods of time to provide the products in comparable yields.

Table 1 – Protocol for the one-pot synthesis of polyfunctionalized quinoxalines **22a-22i**.

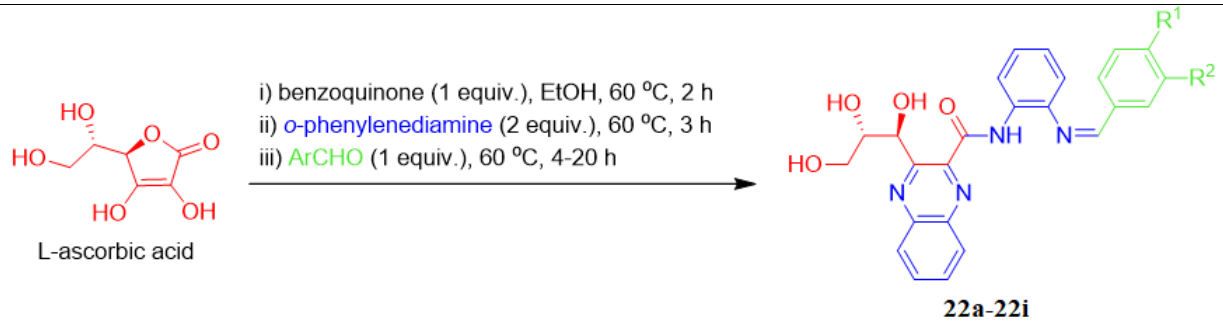

22a-22i

Entry	R^1	R^2	Time (h)[a]	Yield (%)[b]	Entry	R^1	R^2	Time (h)[a]	Yield (%)[b]
22a	H	H	5	84%	**22f**	OH	H	15	68%
22b	NO_2	H	4	81%	**22g**	OMe	H	16	80%
22c	F	H	7	78%	**22h**	OH	Ome	20	75%
22d	Br	H	9	82%	**22i**	Nme_2	H	20	65%
22e	H	OH	14	71%					

[a] after addition of aldehyde;

[b] relative to L-ascorbic acid.

All compounds were obtained as yellow or orange solids with well-defined melting points. Compounds **22a**-**22i** are found to be very structurally interesting due their high degree of functionalization, which includes the presence of a trihydroxypropyl group, quinoxaline moiety, and amide and imine groups. IR analysis of compounds **22a**-**22i** showed amide C═O axial stretching bands between 1656 cm^{-1} and 1688 cm^{-1} in the spectra of the synthesized Schiff bases. Bands relative to C═N imine stretching were assigned in the IR spectra between 1600 and 1568 cm^{-1}. Computational analysis using B3LYP combined with 6-311++G(d,p) basis set provided the optimized structures of compound **22a** (Fig. 40). An extended conjugated system comprising quinoxaline, amide, benzene ring and imine moieties was found, including two intramolecular hydrogen bonds involving amide proton and nitrogen atoms from both imine and quinoxaline moieties (Fig. 40a). These intramolecular interactions are supposed to provide an additional stabilization to the molecule, as well as a high degree of planarity to the system (Fig. 40b).

Figure 40 – (a) and side (b) views of optimized structure of compound 1a obtained using B3LYP combined with 6e311++G(d,p) basis set in the Gaussian software.

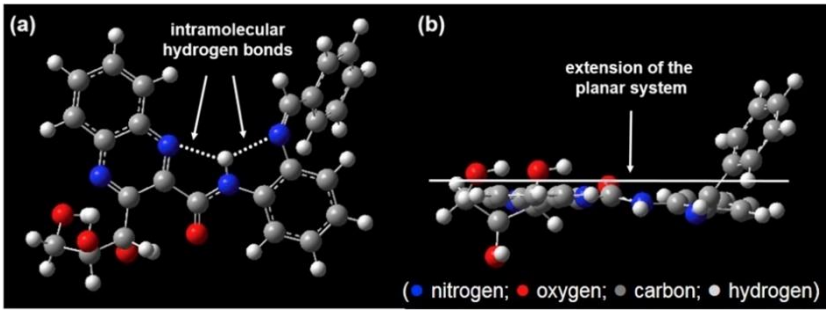

author, 2020.

3.2 NMR characterization

Structural elucidation of all novel Schiff bases was based on an extensive NMR study, including one-dimensional ^{1}H and ^{13}C, as well as two-dimensional HSQC, HMBC and COSY analysis. ^{1}H and ^{13}C NMR data are summarized in Table 2 and Table , respectively. Our initial analysis was concerned with the amide and imine hydrogens, which, as expected, are placed in the lowest field on the spectra, between δ 11.29 and 11.61 ppm, and 8.67 and 8.95 ppm, respectively. The aromatic portion originated from the aldehydes was found presenting usual multiplicity patterns for substituted benzene rings, as well as their chemical shifts displacing to

a lower field due to the presence of electron-withdrawing groups and to a higher field in the presence of electron-donating substituents.

Compound **22h** originating from a reaction with vaniline was selected for further discussions involving NMR analysis (figure 41). COSY and ^{1}H NMR analysis of aromatic portion of compound **22h** evidenced a close relation of H10 and H11 set at δ 7.48 ppm as doublet of doublets, and δ 7.21 ppm as triplet of doublets, respectively. This was also found for H12 (triplet of doublets at δ 7.33 ppm) and H13 (doublet of doublets at δ 8.58 ppm). This latter is found in the lowest field between aromatic hydrogens due to the anisotropic effect originated from the imine group. These anisotropic hydrogens influenced by imine group are set between δ 8.62 and 8.56 ppm in all compounds. There is a clear correlation involving H20 and H21 observed as doublet at δ 7.02 ppm and multiplet at δ 7.69 ppm, respectively, with the former being in a higher field due to the electron-releasing effect of *orto*-hydroxyl group, and less resonance effect related to C═N bond due to their *meta* relation. Quinoxaline moiety is associated to two doublets of doublets at δ 8.23 and 8.13 ppm for H7 and H4, respectively, and two triplets of doublets at δ 8.03 and 7.98 ppm for H6 and H5, respectively.

Figure 41 – Expansion of COSY spectrum of compound **22h** and correlations.

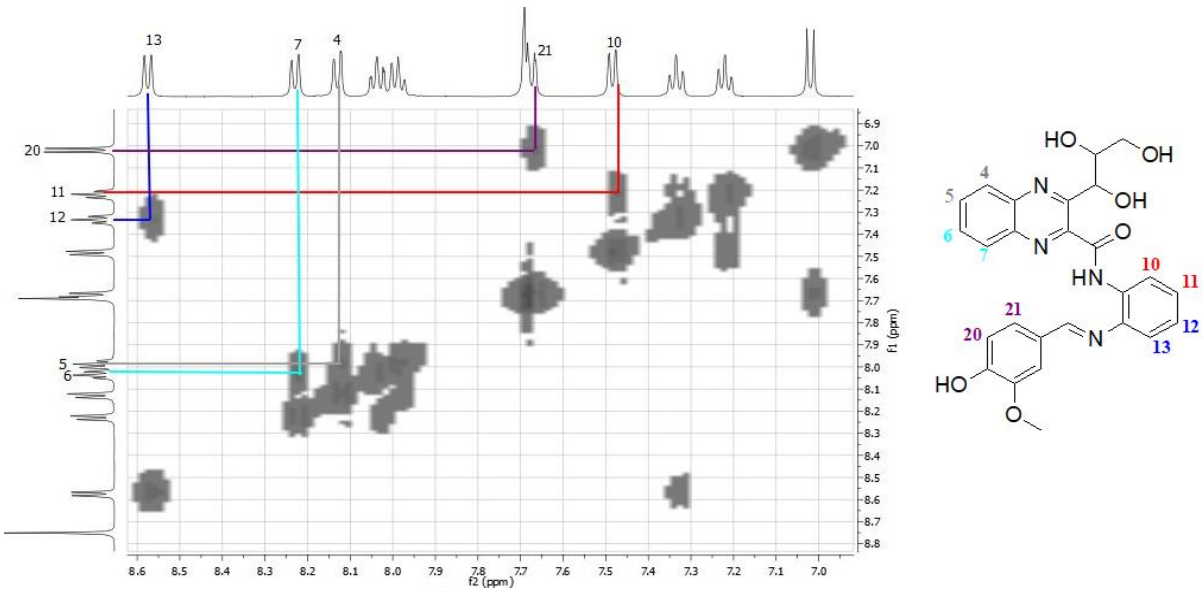

author, 2020.

The assignment of the saturated portion of compound **22h** was based on HSQC spectra (Fig. 42). It first detaches in the presence of two diastereotopic hydrogens in the methylene unit (C24), observed as two multiplets centered at δ 3.63 and 3.49 ppm. This pattern was found in ^{1}H NMR spectra of all compounds as a clear consequence of remaining chiral centers from *L*-

ascorbic acid. Hydrogens of the methynic groups in C22 and C23 were set at δ 5.93 ppm (as doublet of doublets) and δ 4.02 ppm (as multiplet), respectively. The position in the lowest field of the former is due to the adjacent electron-deficient quinoxaline moiety. Hydroxyl hydrogens from alcoholic moiety were easily identified since no correlation was found in HSQC spectra (Fig. 42), and their individual attribution was based on the multiplicity patterns and coupling constant values related to hydroxyl hydrogens.

Figure 42 – Expansion of HSQC spectrum of compound **22e** and correlations.

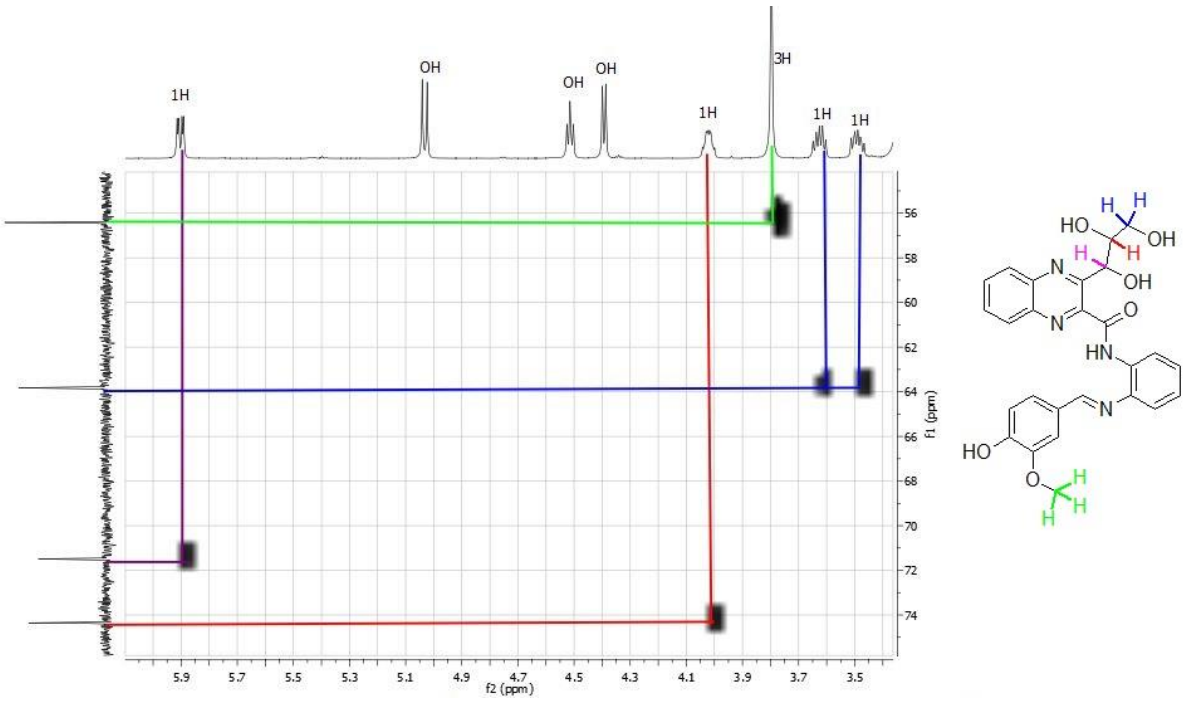

author, 2020.

Some interesting features emerge from analyzing substituents originated from the aldehydes. Compounds **22f** and **22e** have phenolic hydroxyl groups in *para* and *meta* positions relative to imine carbon set at δ 10.30 and 9.87 ppm, respectively. This difference is due to the higher resonance effect of the *para*-substituted derivative (signal in lower field). Hydrogens from methoxy and dimethylamine moieties (in compounds **22g** and **22i**, respectively) are also visualized as expected in the spectra, at δ 3.89 and 3.06 ppm.

Table 2 – ^{1}H NMR data for compounds **22a-22i**.

Position	**22a**	**22b**	**22c**	**22d**	**22e**	**22f**	**22g**	**22h**	**22i**
4	8.24 (*m*)	8.22 (m)	8.21 (*m*)	8.11 (*m*)	8.23 (*t*, 8.3)	8.24 (*m*)	8.21 (*m*)	8.13 (*dd*, 8.2, 0.8)	8.24 (*m*)
5	8.19 (*m*)	8.03 (m)	8.07 (*m*)	8.07 (*m*)	8.04 (*t*, 7.0)	8.07 (*m*)	8.05 (*m*)	7.98 (*td*, 7.6, 1.3)	8.04 (*m*)
6	8.19 (*m*)	8.03(m)	8.07 (*m*)	8.07 (*m*)	7.98 (*t*, 7.3)	8.07 (*m*)	8.05 (*m*)	8.03 (*td*, 7.6, 1.3)	8.04 (*m*)
7	8.24 (*m*)	8.20 (m)	8.21 (*m*)	8.21 (*m*)	8.31 (*d*, 8.3)	8.18 (*m*)	8.15 (*m*)	8.23 (*dd*, 8.2, 0.8)	8.24 (*m*)
10	7.61 (*d*, 7.8)	7.6 (d, 7.9)	7.52 (*d*, 8.0)	7.53 (*d*, 7.8)	7.56 (*d*, 7.9)	7.51 (*d*, 7.9)	7.53 (*d*, 7.9)	7.48 (*dd*, 8.0, 0.9)	7.47 (*d*, 7.5)
11	7.26 (*t*, 7.6)	7.25 (t, 7.6)	7.21 (*t*, 7.5)	7.21 (*t*, 7.6)	7.23 (*t*, 7.5)	7.29 (*t*, 7.5)	7.19 (*m*)	7.21 (*td*, 6.7, 1.1)	7.17 (*t*, 7.5)
12	7.40 (*t*, 7.6)	7.42 (t, 7.5)	7.36 (*t*, 7.5)	7.37 (*t*, 7.6)	7.38 (*t*, 7.5)	7.34 (*t*, 7.4)	7.34 (*m*)	7.33 (*td*, 7.2, 0.8)	7.30 (*t*, 7.5)
13	8.60 (*d*, 8.0)	8.56 (d, 8.1)	8.57 (*d*, 8.0)	8.56 (*d*, 8.1)	8.61 (*d*, 8.1)	8.58 (*d*, 8.0)	8.59 (*d*, 7.2)	8.58 (*dd*, 8.1, 0.9)	8.58 (*d*, 7.8)
15	8.95 (*s*)	9.03 (s)	8.84 (*s*)	8.84 (*s*)	8.83 (*s*)	8.76 (*s*)	8.82 (*s*)	8.75 (*s*)	8.67 (*s*)
17	8.08 (*m*)	8.30 (m)	8.04 (*m*)	8.07 (*m*)	7.67 (*s*)	8.07 (*m*)	7.19 (*m*)	7.69 (*m*)	8.04 (*m*)
18	7.66 (*m*)	8.42 (d, 7.9)	7.47 (*t*, 8.5)	7.80 (*d*, 8.3)	–	7.02 (*d*, 8.5)	8.15 (*m*)	–	6.86 (*d*, 8.7)
19	7.66 (*m*)	–	–	–	7.07 (*d*, 7.9)	–	–	–	–
20	7.66 (*m*)	7.25 (t, 7.6)	7.47 (*t*, 8.5)	7.80 (*d*, 8.3)	7.45 (*t*, 7.9)	7.02 (*d*, 8,5)	8.15 (*m*)	7.02 (*d*, 8.0)	6.86 (*d*, 8.7)
21	8.08 (*m*)	8.09 (m)	8.07 (*m*)	8.07 (*m*)	7.63 (*d*, 7.5)	8,07 (*m*)	7.19 (*m*)	7.69 (*m*)	8.04 (*m*)
22	5.96 (*dd*, 8.8, 2.0)	5.88 (d, 8.7)	5.94 (*d*, 8.5)	5.92 (*dd*, 8.8, 2.4)	5.99 (*d*, 6.7)	5.98 (*d*, 8.4)	5.96 (*d*, 6.9)	5.93 (*dd*, 8.8, 2.8)	5.98 (*dd*, 8.4, 2.1)
22–OH	5.03 (*d*, 8.8)	5.06 (d, 8.8)	5.03 (*d*, 8.8)	5.03 (*d*, 8.9)	5.05 (*d*, 8.5)	5.05 (*d*, 8,5)	5.04 (*d*, 8.4)	5.04 (*d*, 6.1)	5.05 (*d*, 8.7)
23	4.02 (*m*)	3.90 (m)	4.02 (*m*)	4.03 (*m*)	4.04 (*m*)	4.04 (*m*)	4.03 (*m*)	4.02 (*m*)	4.04 (*m*)
23–OH	4.38 (*d*. 6.0)	4.44 (d, 6.0)	4.38 (*d*, 6.0)	4.38 (*d*, 6.2)	4.39 (*m*)	4.39 (*d*, 5.6)	4.52 (*m*)	4.39 (*d*, 6.1)	4.38 (*d*, 5.7)
24a	3.66 (*m*)	3.64 (m)	3.67 (*m*)	3.67 (*m*)	3.66 (*m*)	3.67 (*m*)	3.64 (*m*)	3.63 (*m*)	3.66 (*m*)
24b	3.52 (*m*)	3.54 (m)	3.54 (*m*)	3.54 (*m*)	3.53 (*m*)	3.54 (*m*)	3.52 (*m*)	3.49 (*m*)	3.56 (*m*)
24–OH	4.54 (*t*, 5.7)	4.58 (t, 5.4)	4.53 (*t*, 4.5)	4.53 (*t*, 5.7)	4.54 (*s*)	4.53 (*m*)	4.36 (*s*)	4.51 (*t*, 5.6)	4.54 (*t*, 5.1)
NH	11.54 (*s*)	11.35 (s)	11.39 (*s*)	11.38 (*s*)	11.54 (*s*)	11.53 (*s*)	11.51 (*s*)	11.29 (*s*)	11.61 (*s*)
C18–OH	–	–	–	–	9.87 (*s*)	–	–	–	–
C18–OMe	–	–	–	–	–	–	–	3.79 (*s*)	–
C19–OH	–	–	–	–	–	10.30 (*s*)	–	9.93 (*s*)	–
C19–OMe	–	–	–	–	–	–	3.89 (*br*, *s*)	–	–
C19–NMe_2	–	–	–	–	–	–	–	–	3.06 (*br*, *s*)

[a] Chemical shifts are given in ppm; multiplicity and coupling constants (*J*, in Hz) are given in parentheses. The abbreviations *s*, *d*, *t*, *q*, *dd*, *m* and *br* denote singlet, doublet, triplet, quartet, doublet of doublets, multiplet and broad, respectively.

The ^{13}C NMR data of compounds **22a**-**22i** are presented in Table 3. All spectra have all signals expected for the number of carbons in each molecular structure. Carbonyl and imine carbons are found between δ 161.4 – 162.2 ppm and δ 159.1 – 160.4 ppm, respectively. ^{13}C DEPT-135 spectra were fundamental to the assignment of aromatic carbons, and are also interesting for distinguishing methylene carbon of the aliphatic portion of the molecules. ^{13}C NMR spectroscopy was found to be interesting in the analysis of the aromatic portions originated from the aldehyde reagent. In the absence of any substituent, carbon in *para* position relative to imine was set at δ 132.1 ppm. On the other hand, the carbons adjacent to fluoride and bromide in compounds **22c** and **22d** were set at δ 163.8 and 126.1 ppm, respectively. This difference reflects the prevailing electron withdrawing inductive effect of fluoride, while a mesomeric effect is more prominent for bromide. As expected, the presence of phenolic hydroxyl groups in **22f** and **22e** at *para* and *meta* position, respectively, relative to the imine moiety, led to lower chemical shift to the adjacent carbons (δ 161.7 ppm for C19 in **22f**, and δ 158.4 ppm for C18 in **22e**).

Table 3 – ^{13}C NMR data for compounds **22a**-**22i**.

Position	22a	22b	22c	22d	22e	22f	22g	22h	22i
1	156.4	156.4	156.8	156.8	156.9	156.9	156.9	156.9	156.9
2	142.4	142.7	142.9	142.9	142.7	143.0	142.9	143,4	142.9
3	138.3	138.1	138.8	138.6	138.9	139.0	139.0	139.0	139.0
4	128.8	128.8	129.0	129.0	128.9	129.0	129.0	129.0	129.0
5	132.4	132.6	132.8	132.8	132.9	132.9	132.9	132.8	132.8
6	131.1	131.3	131.5	131.6	131.3	131.4	131.2	131.3	131.1
7	128.9	129.8	129.1	129.1	129.5	129.1	129.1	129.1	129.1
8	138.5	138.7	139.0	139.0	139.0	139.3	139.2	139.8	139.8
9	133.1	133.5	133.6	133.6	133.5	133.3	133.4	133.1	133.2
10	117.1	117.5	117.5	117.6	117.6	117.2	117.4	117.6	117.4
11	124.3	124.6	124.7	124.8	124.8	124.7	124.7	124.9	124.7
12	127.7	128.6	128.1	128.3	128.0	127.3	127.2	127.2	127.3
13	118.5	119.2	119.1	119.2	119.8	118.9	118.9	119.0	118.7
14	141.3	141.4	141.7	141.7	141.8	141.8	141.8	141.8	141.7
15	159.8	158.1	158.9	159.1	160.4	159.5	159.5	160.3	159.3
16	135.9	133.4	133.5	135.5	137.8	127.3	129.3	128.2	124.1
17	128.6	129.8	131.6	130.9	119.0	127.9	131.6	112.8	131.5
18	128.5	124.2	116.5	132.4	158.4	116.3	114.9	148.5	111.9
19	132.1	149.2	163.8	126.1	115.3	161.7	162.9	151.5	153.3
20	128.5	124.2	131.7	132.4	130.3	116.3	114.9	116.2	111.9
21	128.5	129.8	116.6	130.9	120.8	129.9	131.6	124.2	131.5
22	70.9	71.1	71.5	71.5	71.4	71.5	71.5	71.4	71.5
23	73.8	74.0	74.4	74.3	74.3	74.3	74.4	74.3	74.4
24	63.3	64.8	63.9	63.9	63.8	63.9	63.9	63.8	63.9
C=O	161.4	161.7	161.8	161.9	161.8	161.8	161.8	162.2	161.8
C18─OMe	─	─	─	─	─	─	─	56.4	─
C19─NMe_2	─	─	─	─	─	─	─	─	40.2

[a] Chemical shifts given in ppm.

*3.3 Compound **22a** as chemosensor for Cu^{2+}*

Two selected products, **22a** and **22b**, derived from benzaldehyde and 4-nitrobenzaldehyde, respectively, were selected to be investigated as potential chromogenic chemosensors for selective detection of ions in solution. Initially, the addition of several metal cations (including Na^{+}, Li^{+}, Ag^{+}, Cu^{2+}, Sr^{2+}, Fe^{2+}, Pb^{2+}, Mg^{2+}, Ni^{2+}, Zn^{2+}, Sn^{2+}, Cd^{2+}, Ba^{2+}, Co^{2+}, Al^{3+} and Cr^{3+}), in water, to a methanolic solution of compound **22a** ($4x10^{-5}$ mol L^{-1}) was investigated. Naked eye analysis shows that only Cu^{2+} ions induces a color change (Fig. 4a), and this result is in agreement with the UV-vis analysis (Fig. 43), as a new band emerges in the visible region of the spectrum. Spectrophotometric titration suggests that interaction of **22a** and Cu^{2+} involves a 2:1 metal-ligand coordination complex since the absorbance at 467 nm increases by addition of Cu^{2+} until saturation at approximately $8x10^{-5}$ mol L^{-1} (Fig. 43 – insert).

Figure 43 – Methanol-water (4:1 v/v) solutions of compound **22a** ($4x10^{-5}$ mol L^{-1}) in the absence and in the presence of cationic species (10 equiv) after 60 min: (a) naked-eye detection of Cu^{2+}; (b) UV-vis spectra of the final solutions. Insert: Titration curve obtained on addition of Cu^{2+} (0 to 5 equiv) to solutions of compound **22a** (4×10^{-5} mol L^{-1}).

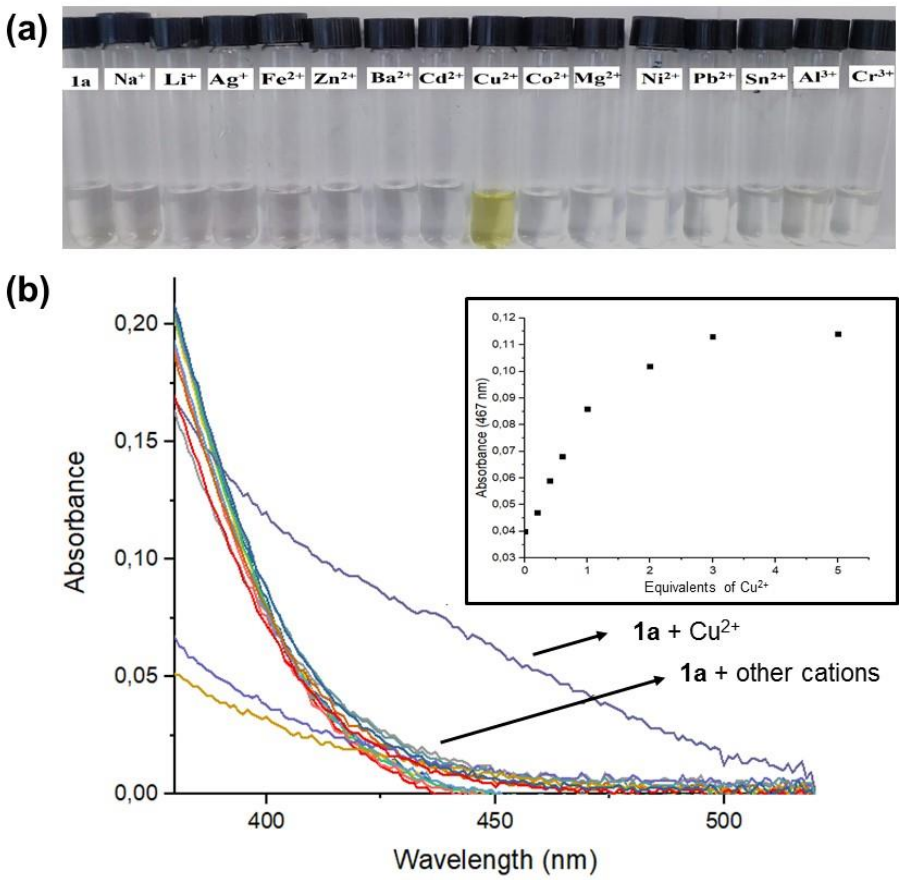

author, 2020.

FTIR analysis of free 1a and 1a-Cu2+ complex (Fig. S1, supporting information) shows only a slight shift in the band associated to C═O stretching after the addition of Cu^{2+} from 1672 cm^{-1} to 1681 cm^{-1}, which rules out the possibility of coordination through amide oxygen[183,184]. On the other hand, bands in the region between 1400-1650 cm^{-1} becoming broader suggest coordination involving nitrogen atoms from both imine and quinoxaline moieties. Based on our previously report[132] and spectroscopic data, interactions involve two different sites. Firstly, nitrogen atoms from quinoxaline, amide and imine coordinate simultaneously to Cu^{2+}, leading to the formation of two five-membered rings. As consequence, there are losses of planarity and hydrogen bonding in the conjugated system, which is consistent with a relatively low rate of the complex formation. A second coordination may involve the other quinoxaline nitrogen as well as one hydroxyl group from the alcoholic portion of the ligand.

*3.4 Compound **22b** as chemosensor for F^-*

The behavior of compound **22b** as chemosensor for anions was investigated. Figs. 6a and 6b show naked-eye analyses of compound **22b** against the excess of ten anionic species, including F^-, HSO_4^-, $H_2PO_4^-$, NO_3^-, CN^-, $HCOO^-$, Cl^-, Br^-, I^- and HO^-, in pure DMSO and in the presence of 2.5% (*v/v*) water, respectively. The results clearly indicate that **22b** is very sensitive to the presence of F^- in both solvent systems. The naked-eye analyses are consistent with the UV-vis spectrophotometric data (Fig. 44c and Fig. 44d), in which a band in the visible region of the spectra (maximum at 440 nm) only emerges in the presence of F^-. In DMSO, the intensity of absorption in the presence of F^- was found to be close to that verified for the hydroxide anion. On the other hand, interactions of chemosensor **22b** and F^- decrease considerably in the presence of 2.5% (*v/v*) water, and this behavior is naturally expected due to the highly competitive aqueous media.

Figure 44 – Chemosensor **22b** (4.0×10^{-5} mol L^{-1}) in the absence (a) and presence of 25 equiv of HO^-, HSO_4^-, $H_2PO_4^-$, NO_3^-, CN^-, $HCOO^-$, F^-, Cl^-, Br^-, and I^-, as tetra-n-butylammonium salts: naked-eye analysis in DMSO and (a) 2.5% (v/v) water (b); UV analysis in DMSO (c) 2.5% (v/v) water (d).

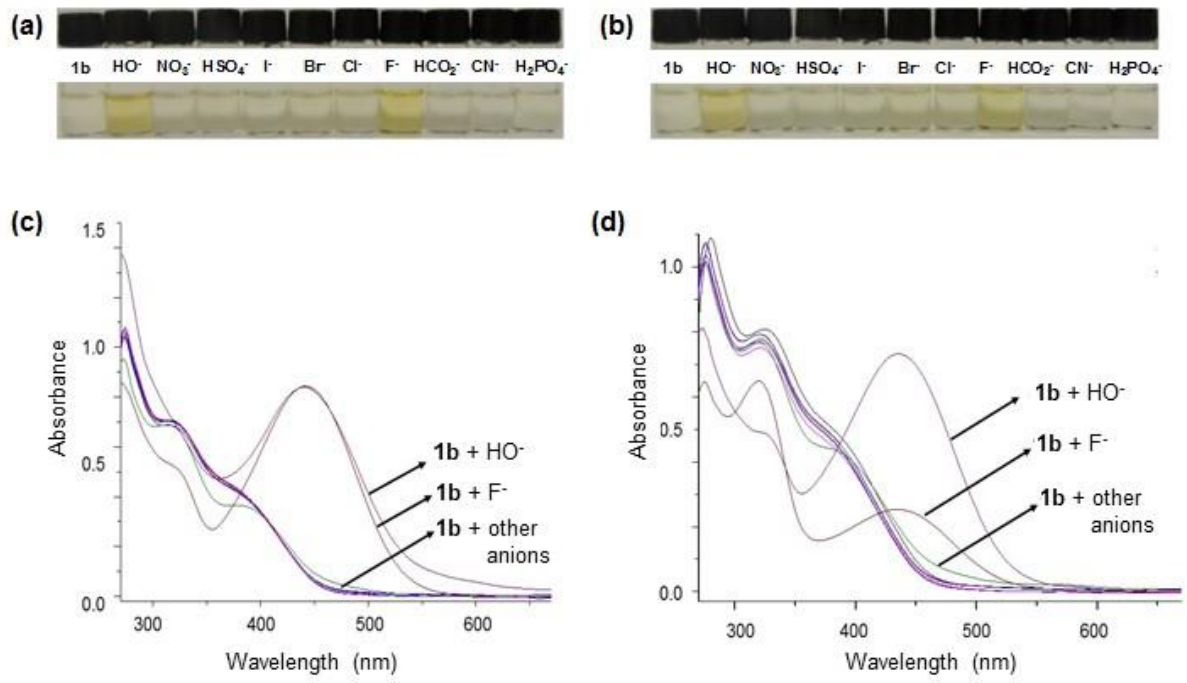

author, 2020.

Spectrophotometric titrations were performed in attempt to study the mechanism of interaction between **22b** and F^- (Fig. S2). As the concentration of anionic species in solution becomes higher in pure DMSO, the intensity of the band at 434 nm increases considerably (Fig. S2a). An isosbestic point at 406 nm was verified until the addition of 5 equiv of F^- (Fig. S2b), which is then lost as *c* (F^-) increased. The non-trivial form of the titration curve considering absorbance values at 440 nm (Fig. S2c) suggests that the anion may not only interact with the reaction center in compound **22b,** but also in other hydrogen bond donor sites in the molecule.

In the next step, the effect of adding water on the sensing ability of chemosensor **22b** was investigated (Fig. S3). In the presence of 2.5% (v/v) water, a new absorption band (maximum at 434 nm) clearly emerges with the addition of the anion, however, it is less pronounced than the change verified in pure DMSO. These results in aqueous medium are due to the limitation in F^- detection by hydrogen-bond donor chemosensors in aqueous competitive medium[173,175], since the high hydration energy of F^- (-465 kJ mol^{-1})[185] makes the anion less able to act as a base[186] .

The interaction of chemosensor **1b** and F^- was investigated by ^{1}NMR spectrometry in DMSO-d_6. Fig. 45 presents ^{1}H NMR spectra of compound **1b** before and after the addition of

1, 3 and 7 equiv of F^-. Signals associated to hydrogens from amide (δ 11.35 ppm) and imine (δ 9.02 ppm) groups disappear after the addition of the first equivalent of fluoride, indicating that these two sites act as hydrogen-bond donor groups. As expected, the signal associated to the aromatic hydrogens becomes broader and shifts to a higher field after interaction with F^- due to the increased electronic density of the chemosensor after interaction with the anionic species.

Figure 45 – ^{1}H NMR spectra (DMSO-d_6, 200 MHz) of chemosensor **22b** (7.0 mol L^{-1}) in the absence and presence of 1, 3 and 7 equiv of tetra-*n*-butylammonium fluoride.

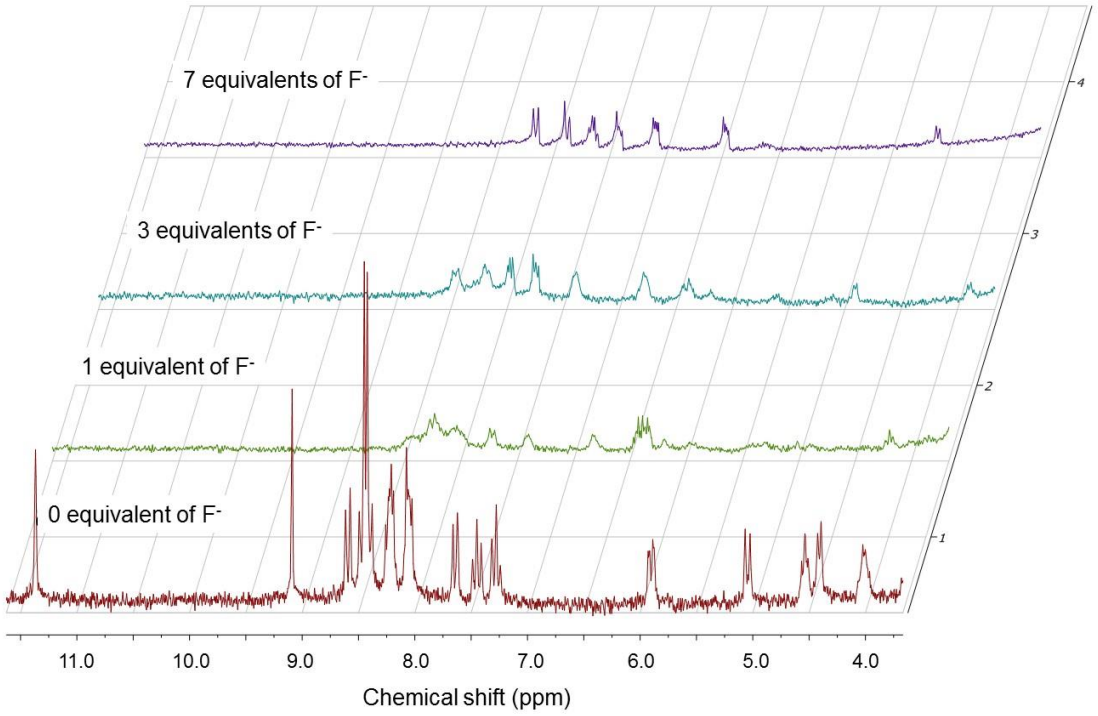

author, 2020.

4 CONCLUSIONS

This paper reports the one-pot synthesis of nine novel polyfunctionalized quinoxaline derivatives starting from *L*-ascorbic acid. Reaction products were obtained in 65-84 % after four synthetic transformations for an interesting scope of commercially available aldehydes. Combined unidimensional ^{1}H, ^{13}C. DEPT-135, as well as bidimensional COSY and HSQC techniques provided all evidence for NMR assignment for these molecules. The main features of NMR spectra include diastereotopic hydrogens in C24, low field N─H and C─H of amide and imine groups, respectively, as well as patterns of aromatic and heteroaromatic unities. In addition, polyol moiety was found to present an expected but interesting multiplicity patterns for C─H and O─H groups. Compound **22a** was able to selectively detect Cu^{2+} ions in aqueous solution by forming a 2:1 Cu^{2+}-**22a** complex. On the other hand, compound **22b** was found to be effective in the fast recognition of F^{-} in pure DMSO and in the presence of 2.5% (v/v) water, in which NMR data indicated that both amide and imine hydrogen could interact with the anionic species. These results can be used as reference for further studies of this molecular skeleton in developing new chromogenic chemosensors for other ionic species.

SUPPORTING INFORMATION

1. Supplementary figures cited in the manuscript

Fig S1 – FTIR spectra of compound **22a** (blue line) and its Cu^{2+} complex (red line).

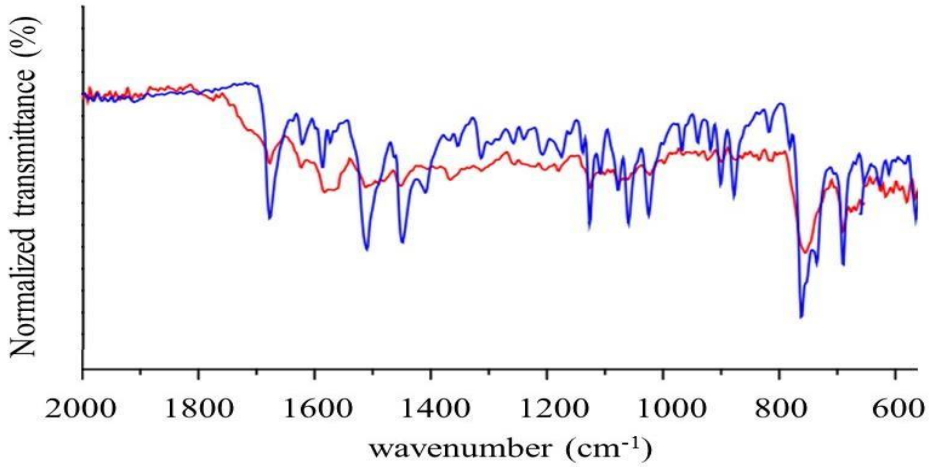

Fig. S2 – UV-vis spectrophotometric study of the interactions of **22b** (4.0×10^{-5} mol L^{-1}) with F^- (as tetra-*n*-butylammonium salt) in DMSO: (a) consecutive spectra from 0 to 42 equivalents; (b) consecutive spectra in which the isosbestic point occurs; (c) titration curve.

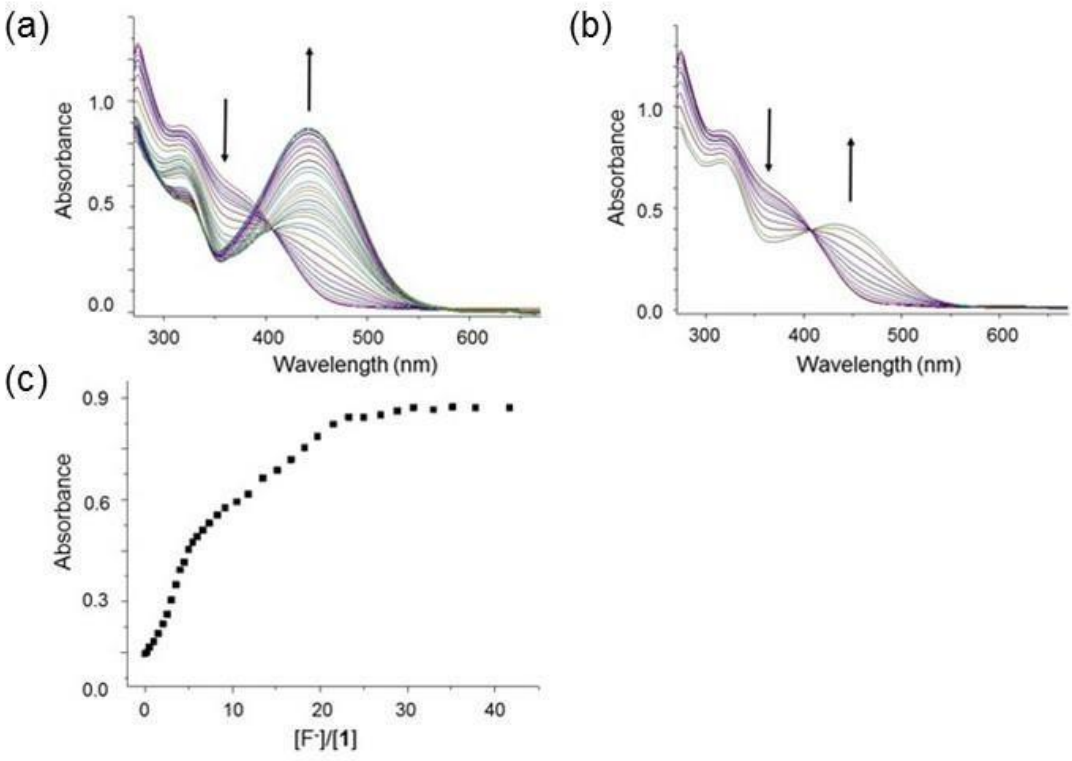

Fig. S3 – UV-vis spectra for the titration of **22b** (4.0×10^{-5} mol L^{-1}) with tetra-*n*butylammonium fluoride (0-54 equiv) in DMSO containing 2.5% water.

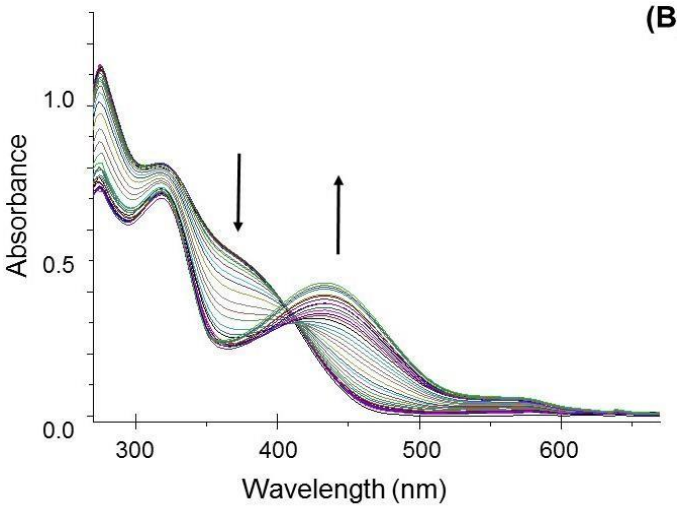

2. ^{1}H and ^{13}C NMR spectra of compounds 22a-22i

Fig. S4 – ^{1}H NMR (DMSO-d_6, 500 MHz) spectrum of compound **22a**.

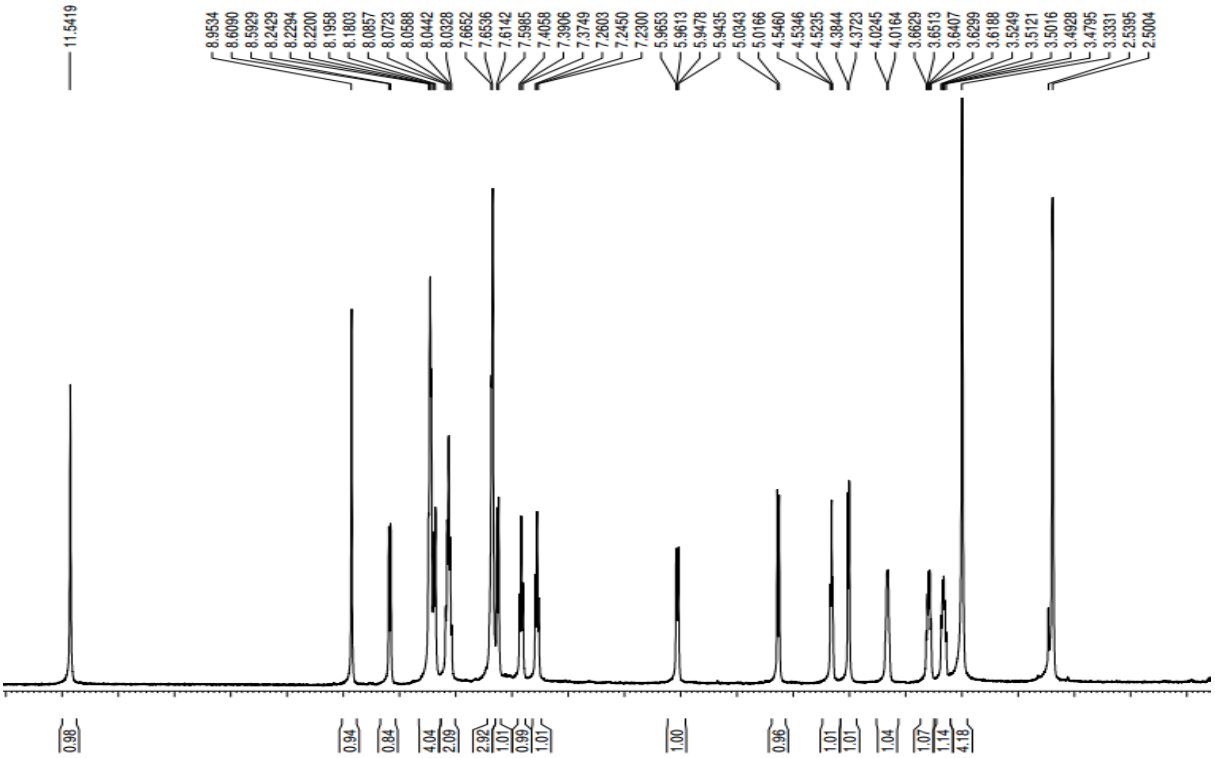

Fig. S5 – ^{13}C NMR and DEPT-135 (DMSO-d_6, 125 MHz) spectrum of compound **22a**.

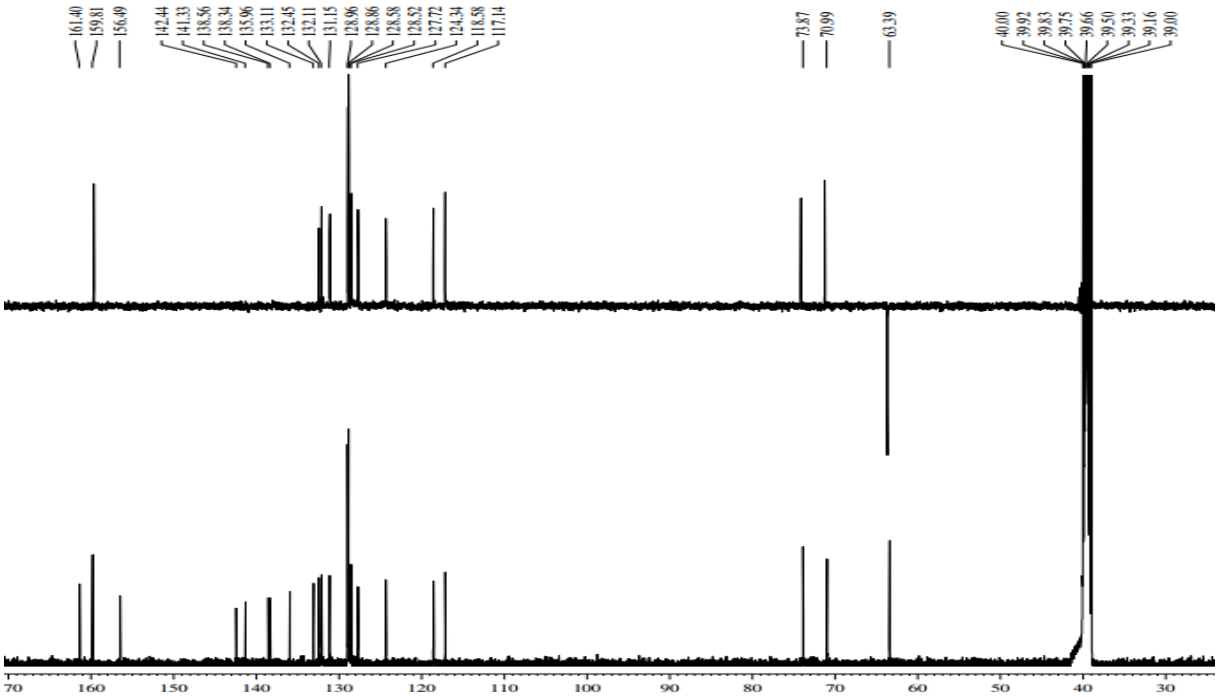

Fig. S6 – Two-dimensional NMR Spectrum – HSQC (DMSO-d6, 500 MHz) and compound correlations **22a.**

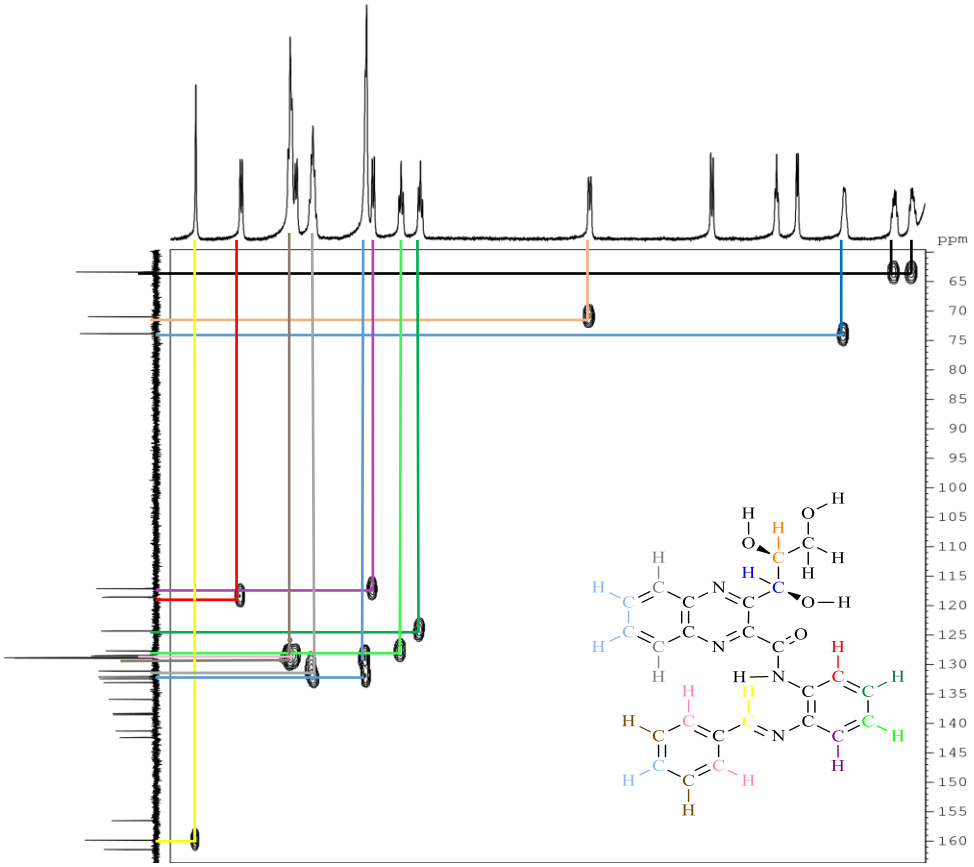

Fig. S7 – Two-dimensional NMR Spectrum – HMBC (DMSO-d6, 500 MHz) and compound correlations **22a.**

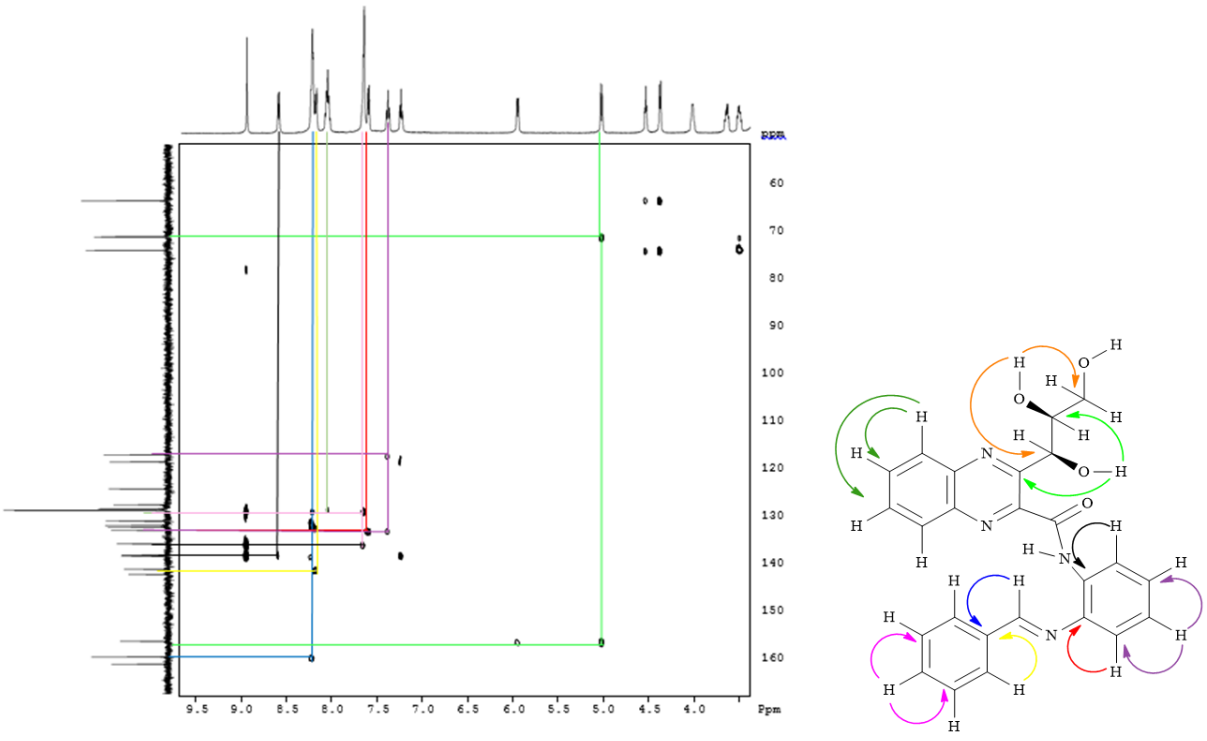

Fig. S8 – Two-dimensional NMR Spectrum – COSY (DMSO-d6, 500 MHz) and compound correlations **22a.**

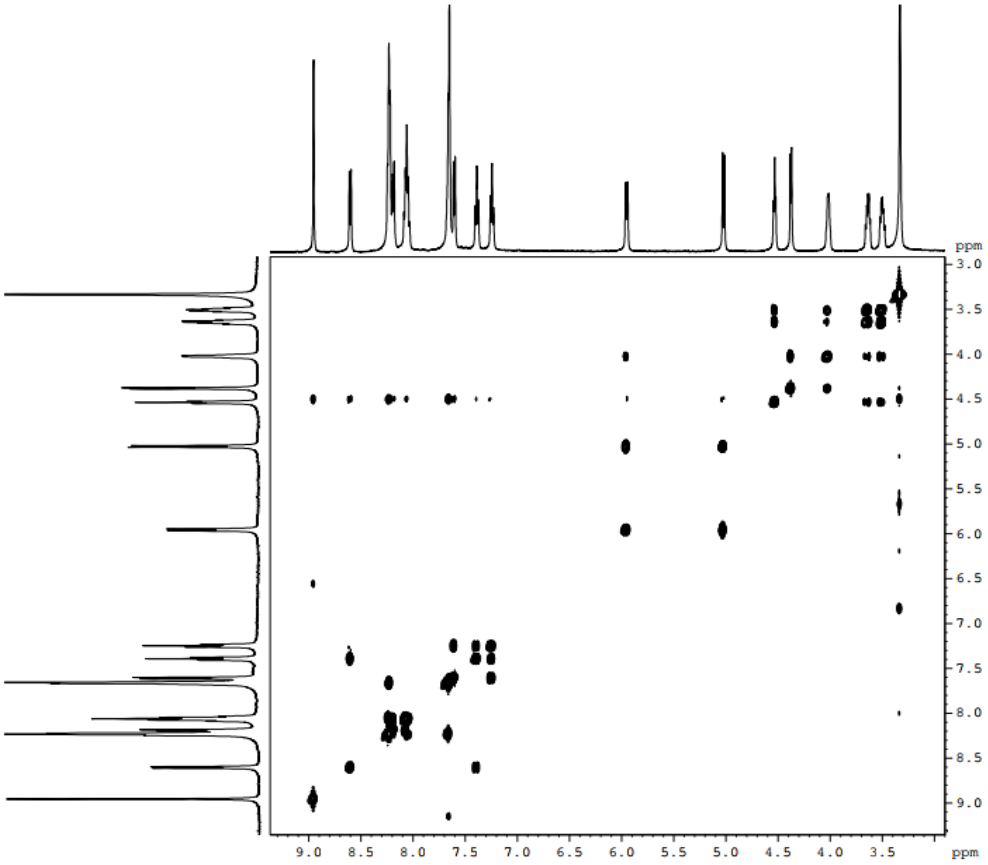

Fig. S9 – ^{1}H NMR (DMSO-d_6, 500 MHz) spectrum of compound **22c**.

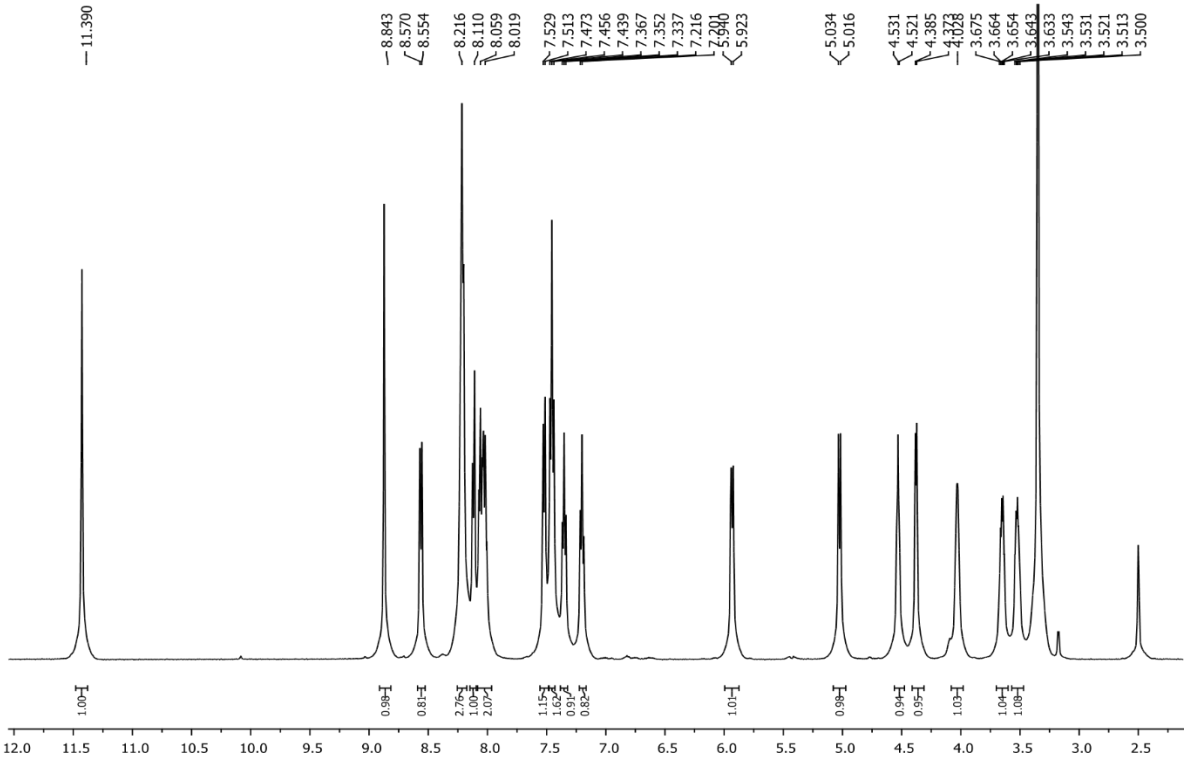

Fig. S10 – ^{13}C NMR (DMSO-d_6, 125 MHz) spectrum of compound **22c**.

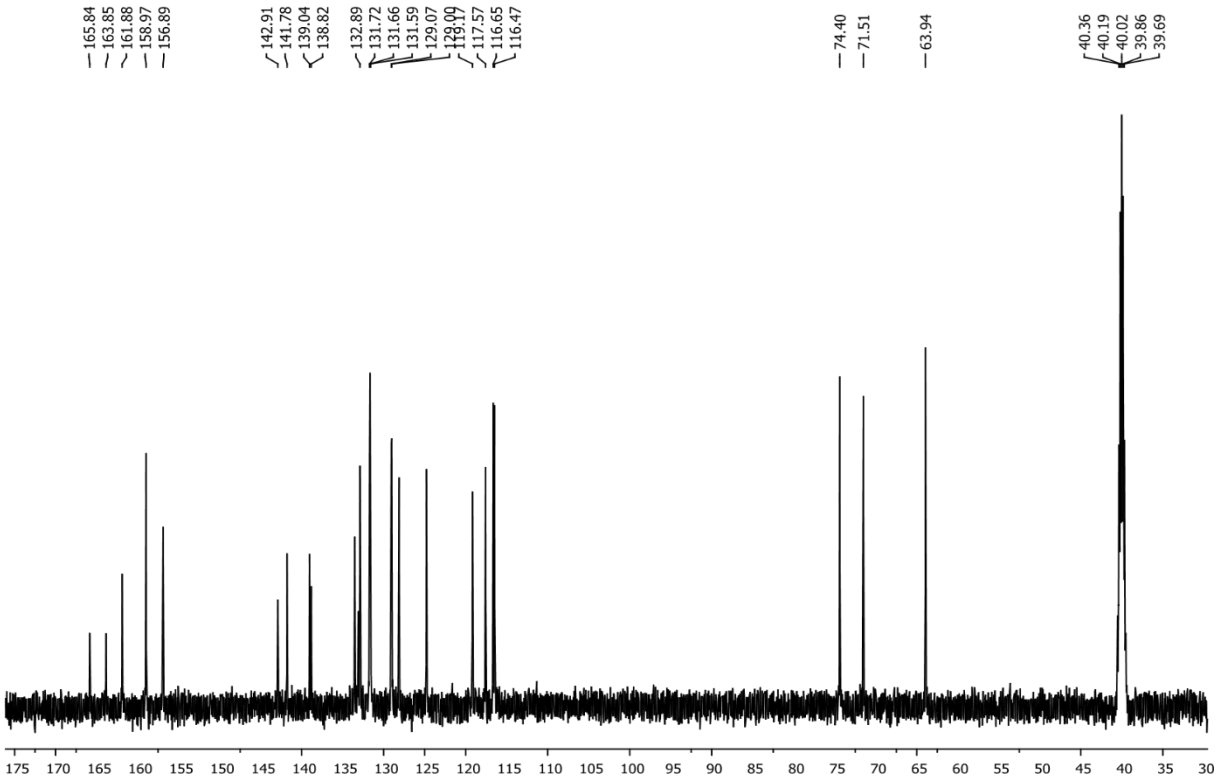

Fig. S11 – ^{1}H NMR (DMSO-d_6, 500 MHz) spectrum of compound **22d**.

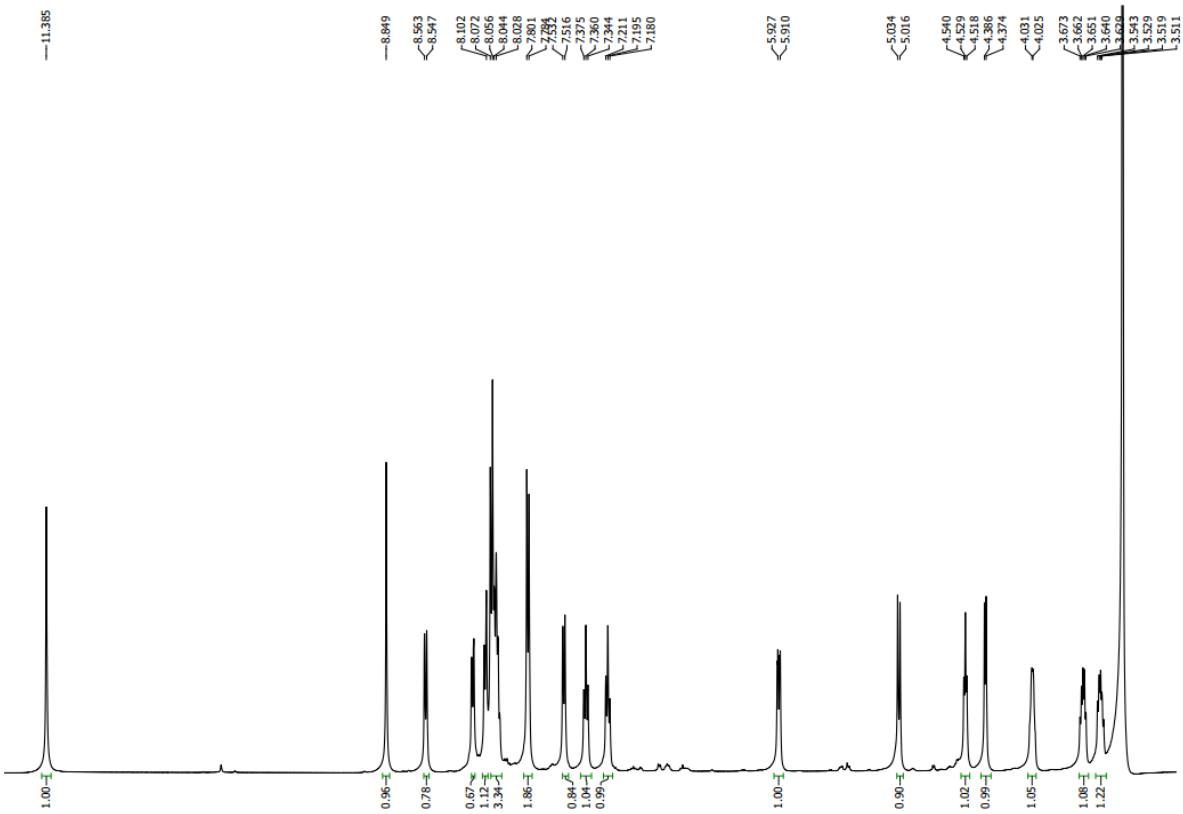

Fig. S12 – ^{13}C NMR (DMSO-d_6, 125 MHz) spectrum of compound **22d**.

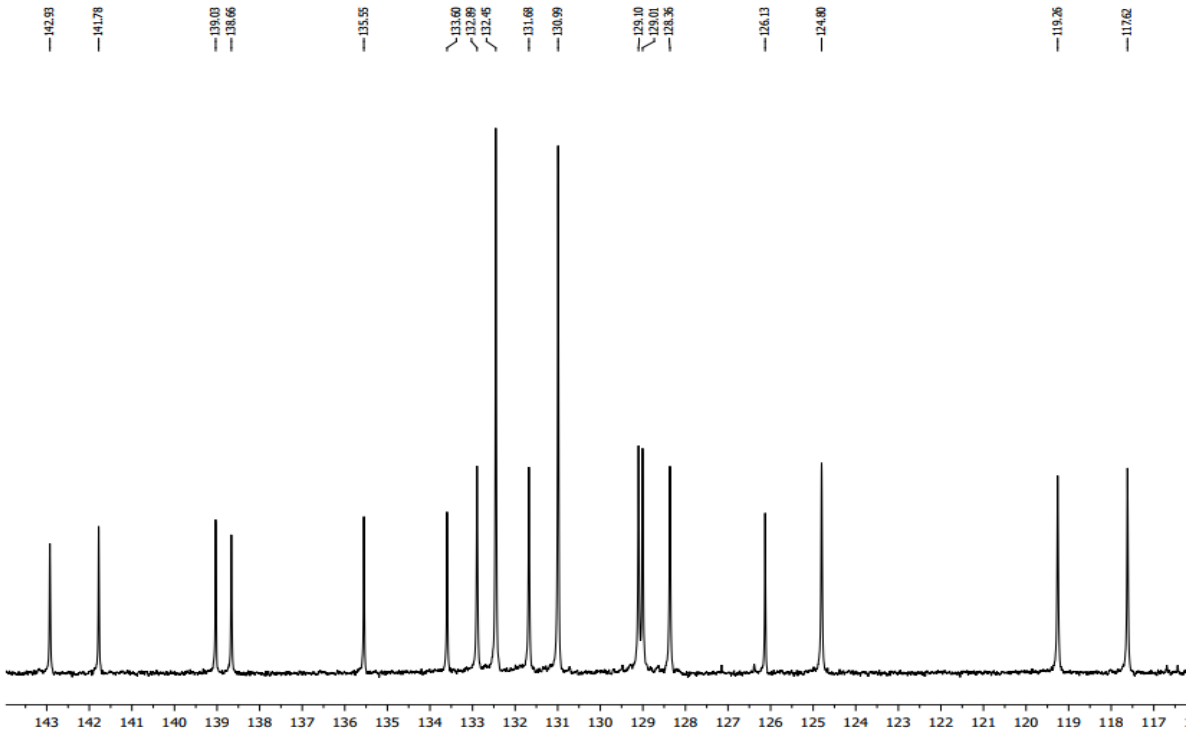

Fig. S13 – ^{1}H NMR (DMSO-d_6, 300 MHz) spectrum of compound **22e**.

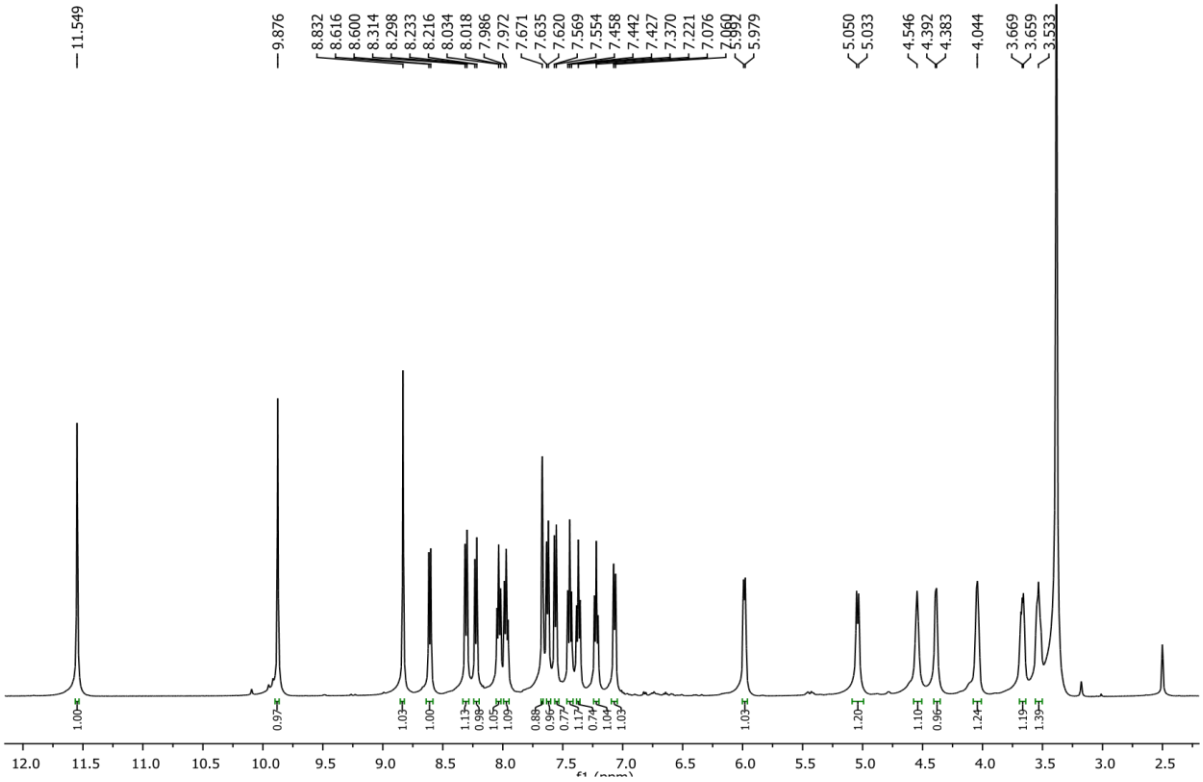

Fig. S14 – ^{13}C NMR (DMSO-d_6, 75 MHz) spectrum of compound **22e**.

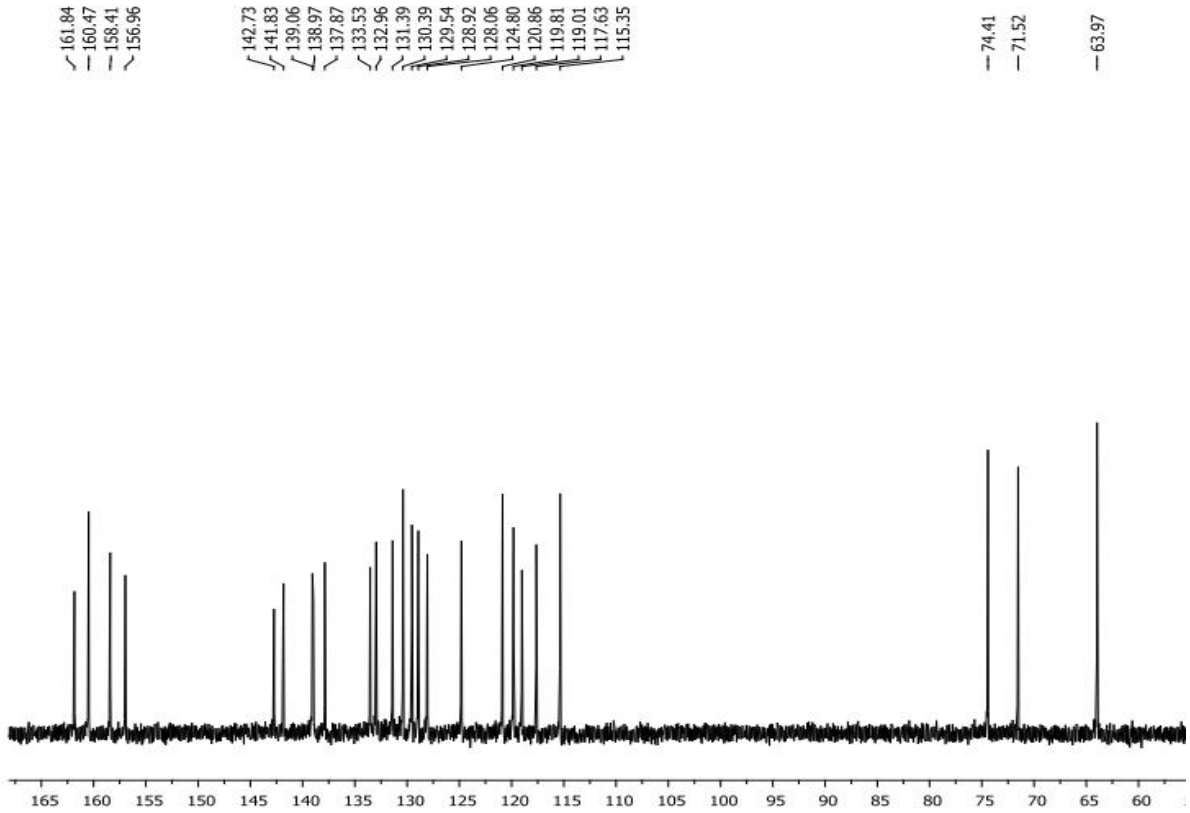

Fig. S15 – ^{1}H NMR (DMSO-d_6, 300 MHz) spectrum of compound **22g**.

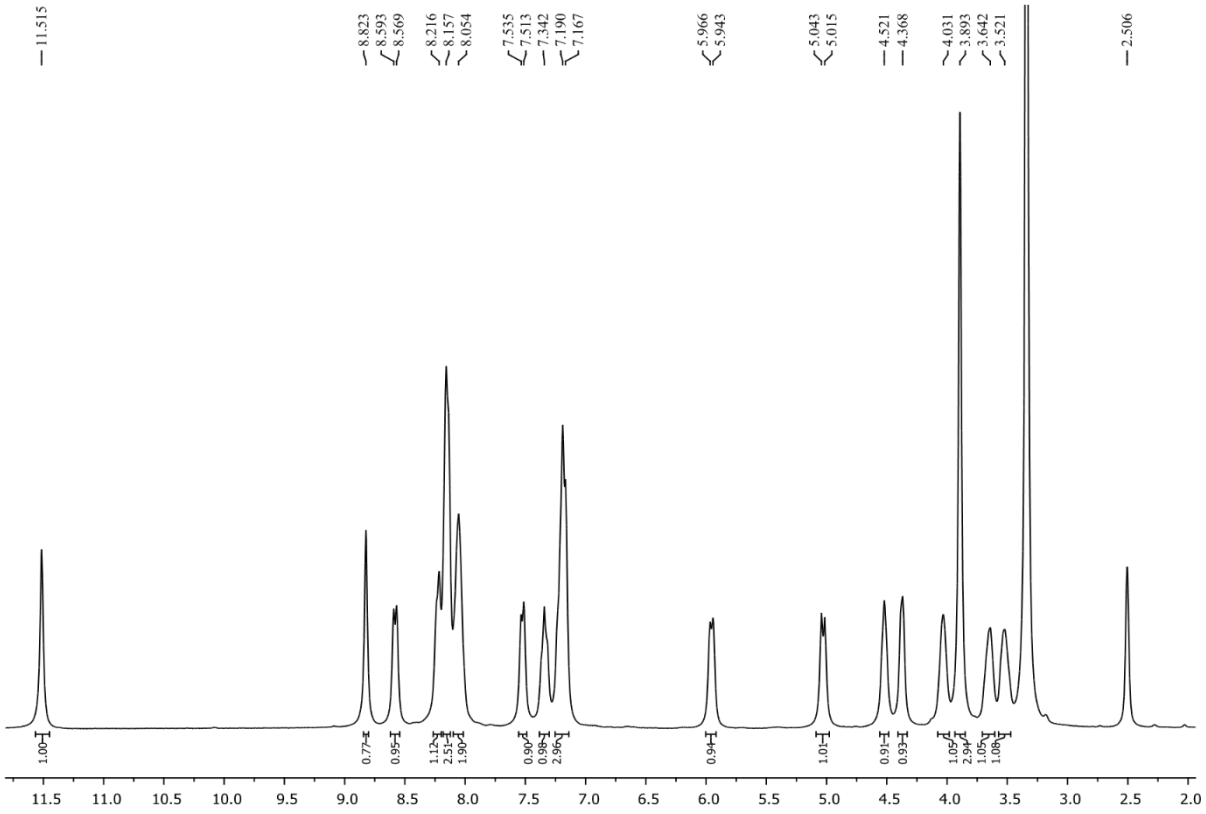

Fig. S16 – ^{13}C NMR (DMSO-d_6, 75 MHz) spectrum of compound **22g**.

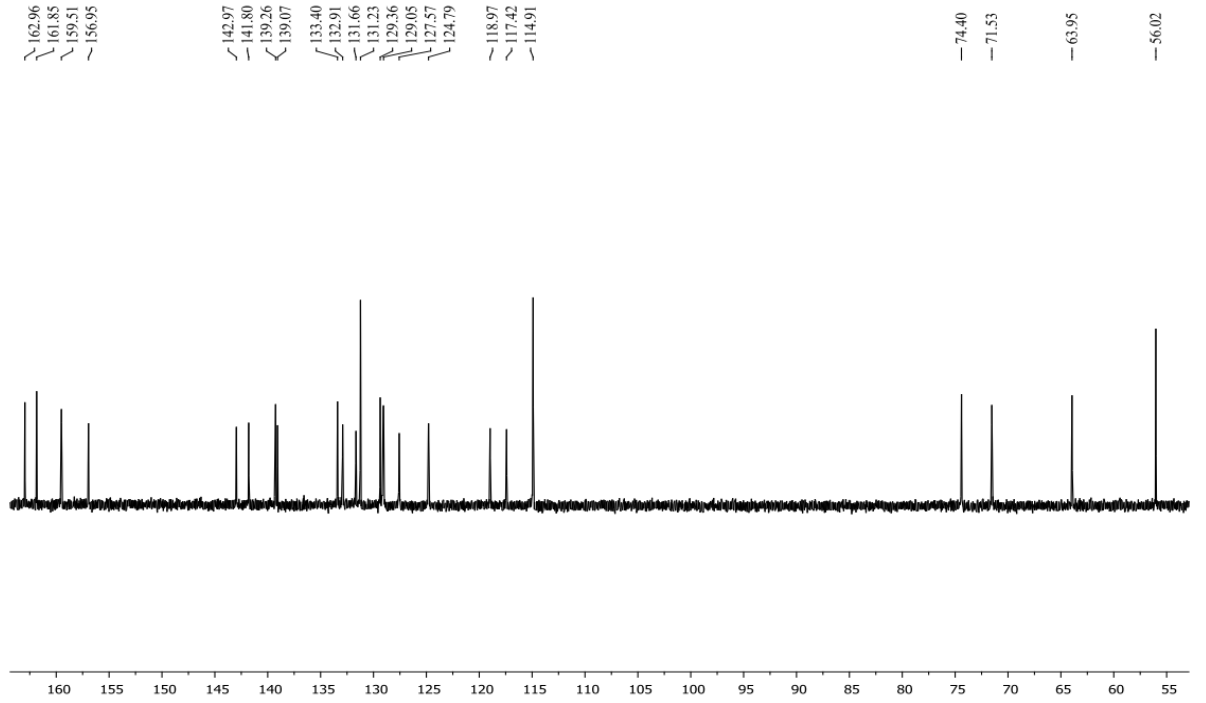

Fig. S17 – ^{1}H NMR (DMSO-d_6, 500 MHz) spectrum of compound **22h**.

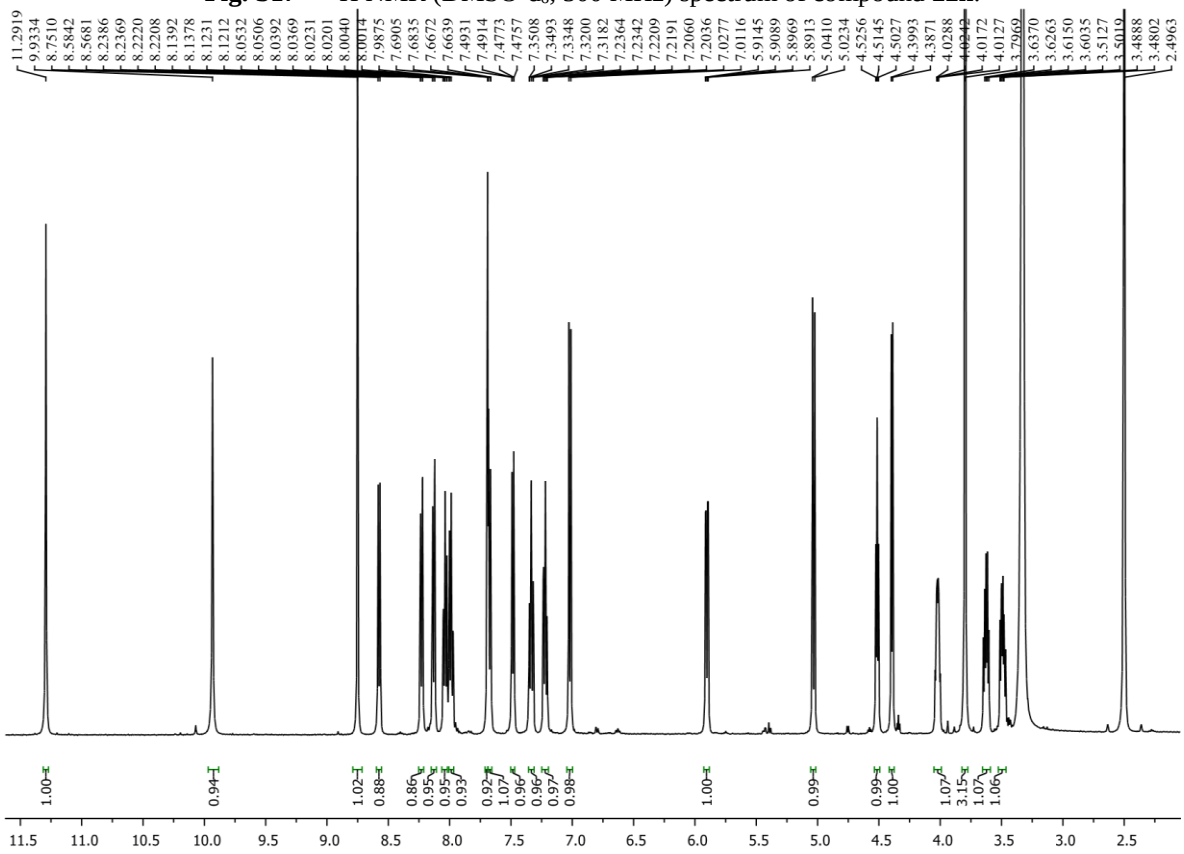

Fig. S18 – ^{13}C NMR – DEPT-135 (DMSO-d_6, 125 MHz) spectrum of compound **22h**.

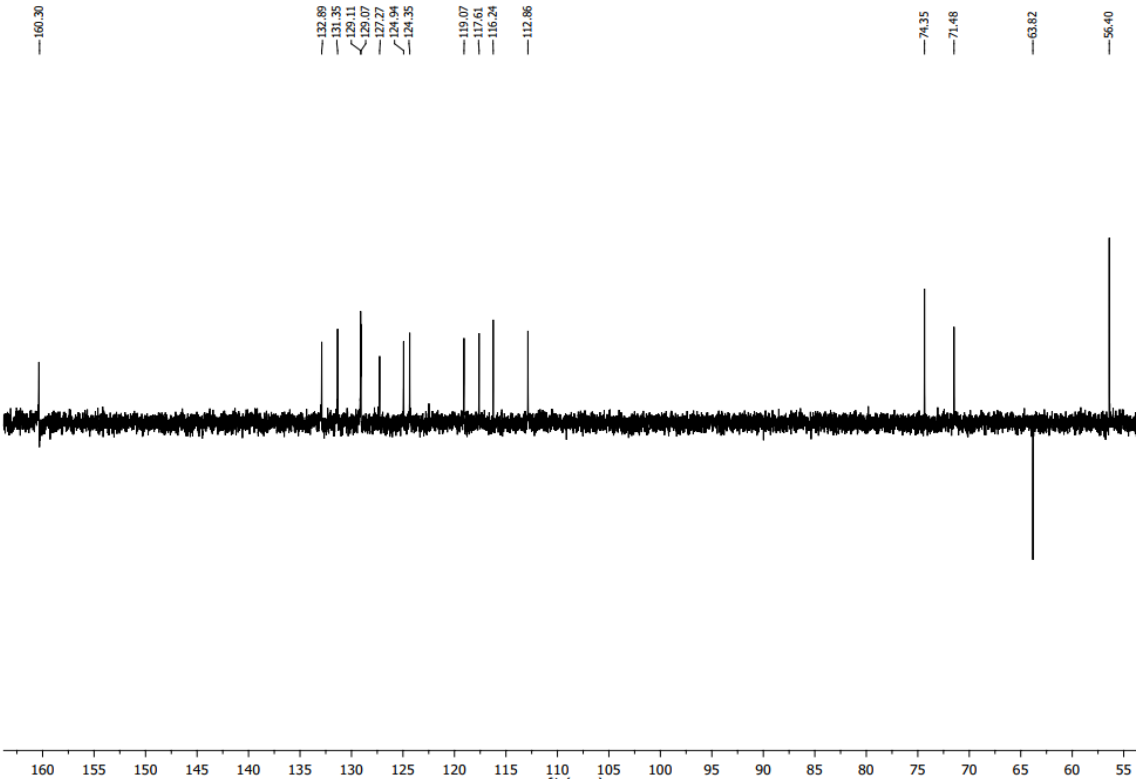

Fig. S19 – ^{1}H NMR (DMSO-d_6, 300 MHz) spectrum of compound **22i**.

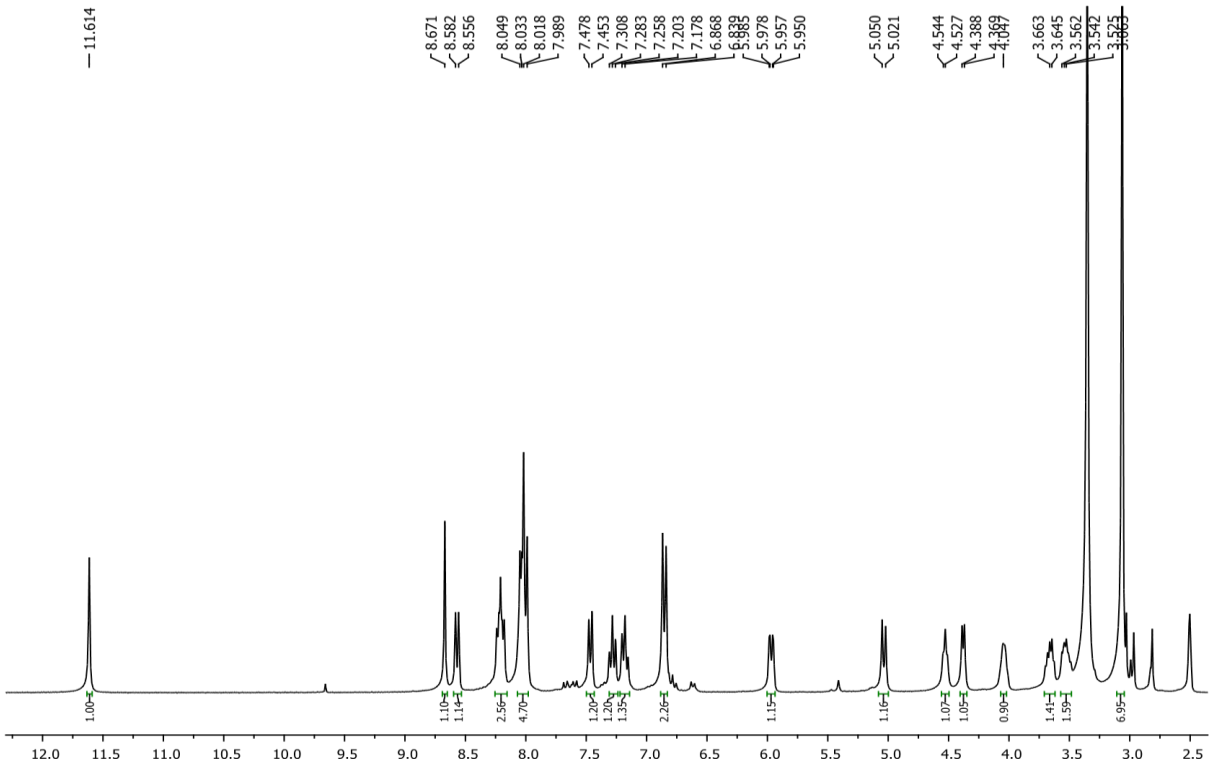

Fig. S20 – ^{13}C NMR (DMSO-d_6, 75 MHz) spectrum of compound **22i**

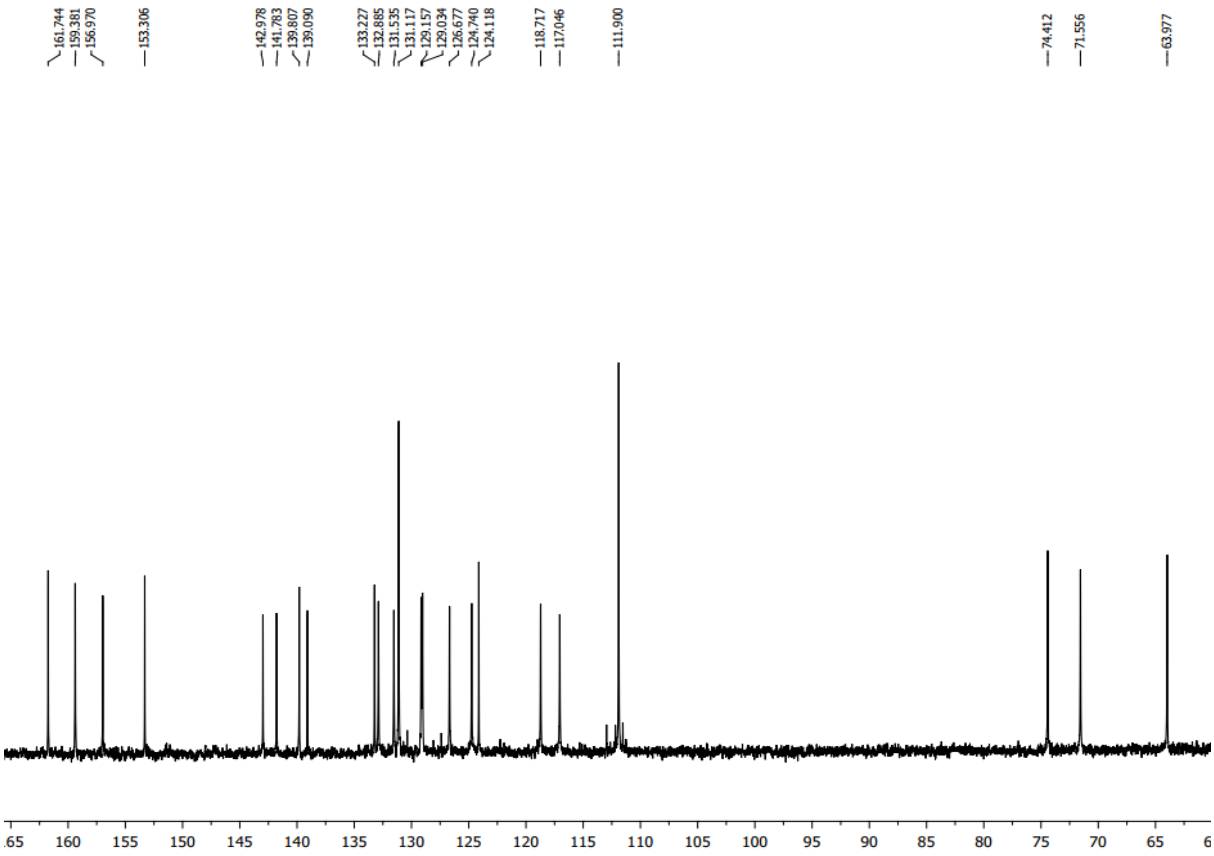

CHAPTER 5 $(QUERCETIN)_2Al^{3+}$ COMPLEX AS CHEMOSENSOR FOR F^- IN AQUEOUS SOLUTION: A MULTIDISCIPLINARY PROJECT FOR CHEMISTRY CLASSES

Lilian C. da Silva[1], Gizely V. L. Cavalcante[1], Alane P. A. dos Santos[1], Miguel A. F. de Souza[1], Lívia N. Cavalcanti[1], Renata M. Araújo[1], Fabrício G. Menezes[1]

[1]*Federal University of Rio Grande do Norte, Institute of Chemistry, 59072-970 Natal, RN, Brazil*

Manuscript in finalization

Contributions:

- Synthesis of compounds
- Spectroscopic Experiments
- NMR elucidation

Experiments being conducted by collaborators:

- Theoretical calculations

Writing to be finalized:

- Discussion of computational calculation results
- Conclusions

1 INTRODUCTION

The scientific challenges of the modern society require intensive interdisciplinary approaches, but which face considerable obstacles, including traditional structure of universities and colleges[187,188]. In fact, most of chemistry undergraduate courses in this 21st century still presents a curricular structure based on main braches of chemistry as separate areas (organic chemistry, inorganic chemistry, physical chemistry and analytical chemistry)[189]. Therefore, there is a need in presenting strategies for a unified view of traditional subdisciplines of chemistry[190]. In this context, the design of new multidisciplinary strategies for educational purposes is essential to provide a broad vision for chemistry to undergraduate students [191–197].

This work presents a biotechnological-based mini project proposal combining different branches of chemistry, including natural products, synthetic modification, coordination chemistry, spectroscopic characterization, qualitative analysis and computational chemistry. More specifically, it is aimed the application of a Quercetin-based-Al^{3+} coordination complex as chromogenic chemosensor for F^- in aqueous solution. The proposal may be adapted for three to five classes depending mainly on laboratorial structure.

1.1 Theoretical basis

Flavonoids comprise an extensive group of polyphenolic-based secondary metabolites found in many fruits, vegetable, roots, wine, to cite a few, which are very popular due their presence in nutraceutical, pharmaceutical and cosmetic formulations besides several medicinal goals due the proven activities against several pathologies such inflammatory processes, obesity, diabetes, allergy and cancer[103,198-205]. Among different classes of flavonoids, flavonols are characterized as 3-hydroxyflavone derivatives, and some relevant examples including 3-[α-L-rhamnopyranosyl-(1→6)-β-D-glucopyranosyloxy]) and (2-(3,4-dihydroxyphenyl)-3,5,7-trihydroxy-4H-chromen-4-one), popularly known as Rutin (RUT) and Quercetin (QCT), respectively, which are isolated from several natural plants[206-209]. Notably, RUT can be obtained from *Bredemeyera floribunda* Willd (Polygalaceae) in appreciable yields (*ca* 22%, mass per mass) [209], which widely stimulates its use in biotechnological research. Subsequently, QCT can be obtained directly form the acid hydrolysis of RUT in affordable yield (Fig. 46)[210].

Figure 46 – Hydrolysis of RUT to generate QCT[210].

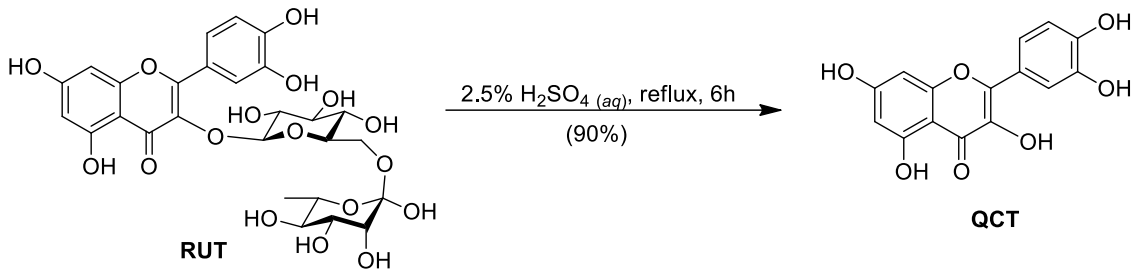

Due their notable structural features, flavonoids are particularly interesting in coordination chemistry, providing organometallic compounds from reactions with different cations and stoichiometry. There are interesting reports focusing on coordination of QCT and different cations, including Al^{3+}, Fe^{3+}, Fe^{2+}, Cd^{2+}, Ca^{2+}, Co^{2+}, Ni^{2+}, Mg^{2+}, Pb^{2+}, Pd^{2+} and La^{3+}, in both aqueous or organic medium and their applications in many fields[183,211-218]. Sathish et al reported the use of Al^{3+}-based coordination compound from anionic 3-hydroxyflavone (3HF) as chromogenic and fluorogenic chemosensor for the detection of F^- anions in solution[183]. The mechanistic proposal is based on the initial formation of colored (yellow) and slightly fluorescence $Al^{3+}(3HF)_2$, which in the presence of F^- leads to colorless and highly fluorescence $Al^{3+}(HF)F_3$ complex.

Detection of F^- in aqueous solution is very relevant due its role in the prevention and treatment of dental caries and osteoporosis, and especially due its classification as pollutant rather than nutrient[184], and also its association to refinement of uranium and decomposition of chemical weapon such as the compound 2-[fluoro(methyl)phosphoryl]oxypropane (known as Sarin)[174]. Therefore, a proposal concerned on the development of artificial receptors for the detection of F^- in aqueous medium in the sense of biotechnological approach becomes very attractive to undergraduate in chemistry courses.

1.2 The proposal

Initially, for this proposal, a natural product-based chemistry is involved in the isolation of RUT from ethanolic extract of the roots of the *Bredemeyera floribunda* Willd (Polygalaceae) (however, in case of impossibility in performing this step, RUT is easily purchase in drugstores and associated stores with affordable prices). The next step involves the hydrolysis of RUT to obtainment of QCT. In both stages, NMR analysis is very interesting and

may be of broad interest for undergraduate chemistry students. With pure QCT in hands, students are able to perform the synthesis of $(QCT)_2Al^{3+}$ according to literature[186] which can be followed by UV-Vis spectroscopy, and then apply it for the qualitative detection of F^- in aqueous solution toward other anionic halides by naked-eye as well as UV-Vis spectroscopy and fluorescence analysis. Lastly, students will be able to enter into computational chemistry by modelling the structures of the coordination complexes generated during the process and to simulate their energies and UV-Vis spectra. All stages of this multidisciplinary proposal can be properly discussed by students and professors, which may provide additional stimulus for the students in this academic.

2. RESULTS AND DISCUSSION

2.1 Classes 1 and 2: isolation of rutin and obtainment of quercetin

RUT was first obtained from the ethanolic extract of the roots from *Bredemeyera floribunda* Willd (Polygalaceae), a plant found in many locations of Northeast region of Brazil. The compound was purification by molecular exclusion chromatography on sephadex LH-20 using methanol as solvent, yielding 22% in mass (1.32 g) of RUT. As previously mentioned, in the absence of the referred plant, RUT is easily acquired in drugstores and associated stores with affordable prices (30 capsules, 500 mg each – R$ 46.00, U$ 11.62). With RUT in hands, next stage involved its conversion in QCT *via* C─O bond cleavage under aqueous acidic medium [210]. Mechanistically, this reaction proceeds similarly to an acid-mediated acetal hydrolysis in carbohydrates (disaccharides or higher).

Fig. 47 shows ^{1}H NMR spectra of RUT and QCT. The ^{1}H NMR spectrum of RUT (Fig. 47a) can be divided in two main regions: from δ 3.08 to 5.45 ppm, associated to carbohydrate hydrogens; and from δ 6.20 to 7.59 ppm, comprising typical absorptions of hydrogen atoms bonded directly to aromatic rings. Hydrogens H6 and H8 (flavonoid ring "A") were verified as two doublets (^{4}J = 3.0 Hz) at δ 6.20 ppm and δ 6.40 ppm, respectively. There are three other absorptions in aromatic region of the spectra relative to hydrogens of flavonoid ring "B", at δ 7.59 ppm (^{4}J = 3.0 Hz) and δ 6.86 ppm (^{3}J = 9.0 Hz), associated to hydrogens H2´ and H5´, respectively. As expected, ^{1}H NMR spectrum of QCT does not present absorptions related to hydrogens of a carbohydrate moiety. The hydroxyl proton at C5 position is associated to a well-defined singlet at δ 12.49 ppm and are not equivalent to other hydroxyl protons due to "chelating effect" originated from interaction with oxygen adjacent to C4. This hydrogen has a lifetime larger than the other protons OH and appears in spectra of RUT and QCT. However, other hydroxyl protons appear only as a broad signal in spectrum of RUT but in spectrum of QCT other signs of hydroxyl protons are present in the spectrum (H7, H3', H4' and H3). The phenolic hydrogen (H7) appears at δ 10.82 ppm. The signal in δ 9.61 ppm appears as a broad signal and is assigned to H3 and the hydrogen of the catechol (ring "B") appears in a single signal (multiplet) at δ 9.35 ppm. Both flavonoids, RUT and QCT, were also characterized by ^{13}C NMR.

Figure 47 – NMR spectra (DMSO-d6, 300 MHz) of RUT (a) and QCT (b).

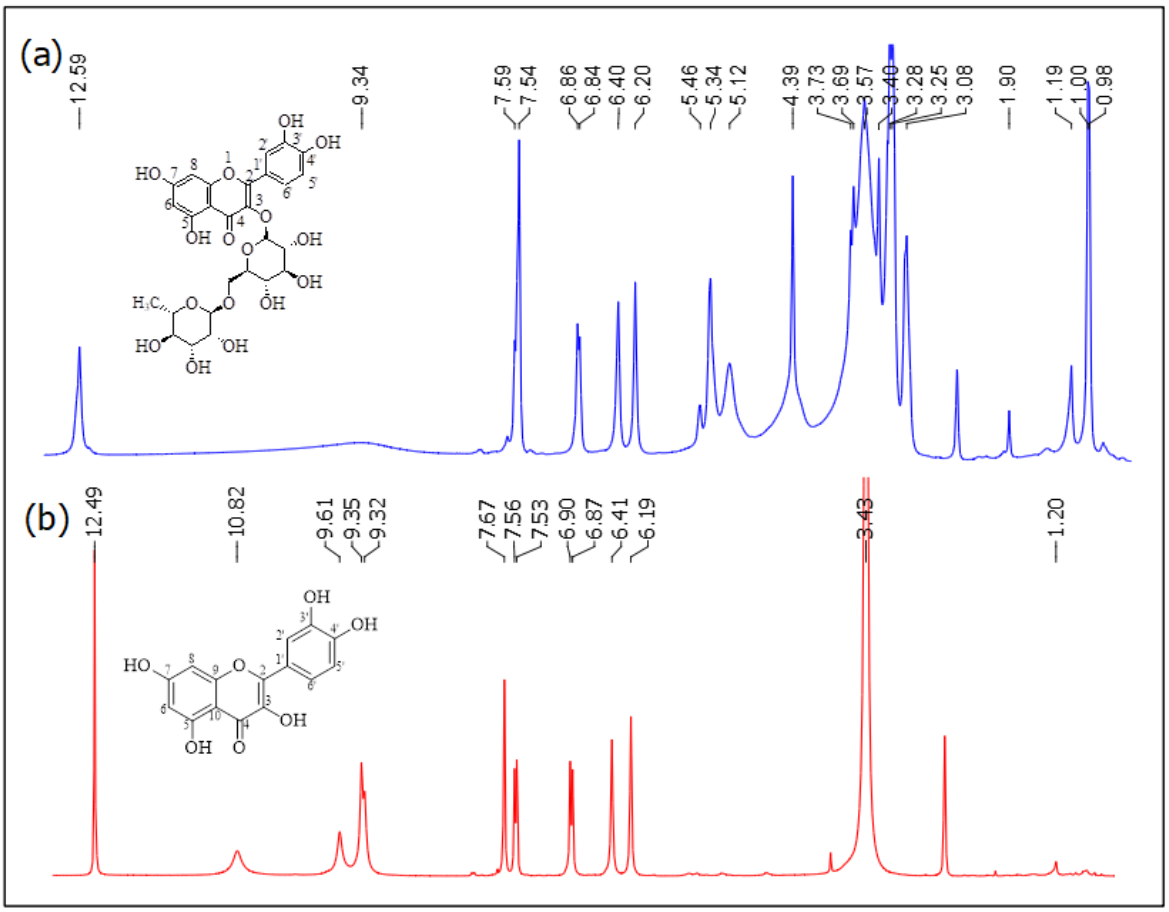

author, 2020.

2.2 Classes 3 and 4: synthesis of QCT_2Al^{3+} complex and its evaluation in qualitative detection of F^- in aqueous medium

The complex $(QCT)_2Al^{3+}$ was synthesized from reaction of $Al(NO_3)_3.9H_2O$ with two equivalents of QCT and evaluated as chromogenic chemosensor for F^- in aqueous medium (Fig. 48). The final product can be isolated as a yellow solid.

Figure 48 – Synthesis of complex QCT_2Al^{3+} and its and $Al(QCT)F_3$.

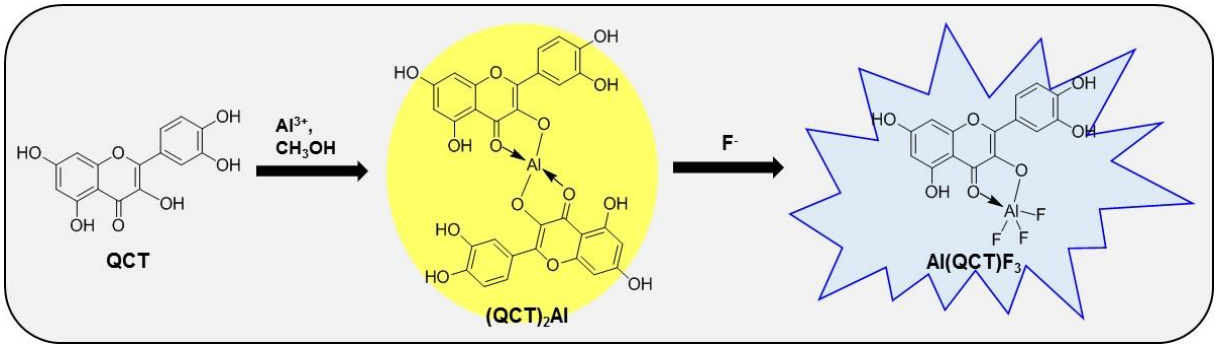

author, 2020.

Although isolable, complex $(QCT)_2Al^{3+}$ was used *in situ* int eh subsequent anion detection experiment. The effect of addition of different halide (I^-, Br^-, Cl^-, and F^-; 10 equivalents) to solutions of complex QCT_2Al^{3+} (0.1 μM) in methanol-water 9:1 *v/v* was investigated by naked eye as well as UV-Vis and fluorescence spectroscopies. Only addition of F^- induces a change from yellow to colorless in solution containing QCT_2Al^{3+} (Fig. 49a) and this result is consistent to UV-Vis analysis since there is a considerable decreasing in the band at 435 nm concomitantly to a new band emerging at 375 nm (Fig. 49b). Furthermore, fluorescence analysis clearly indicates singular effect of F^- over other halides characterized by a showy change in color (Fig. 49c) and increasing in the intensity of the band at 480 nm under irradiation at 375 nm (Fig. 49d). These colorimetric and spectroscopic changes can be comprehended in terms of high affinity of F^-, a hard base, to Al^{3+} cation, a hard acid, as well as poor and soft basicity of Cl^-, Br^- and I^- [219]. The recognition of metals using water as a solvent is of great importance even in small proportions of water in another organic solvent due to the possibility of using real samples. This advantage can be used in other experiments by students with the possibility of samples collected in the environment.

Figure 49 – Effect of addition of ten equivalents of selected anions (F^-, Cl^-, Br^- and I^-) to solution QCT_2Al^{3+} (0.1 μM) in methanol-water 9:1 v/v: (a) naked eye analysis; (b) UV-Vis spectra; (c) fluorescence spectra

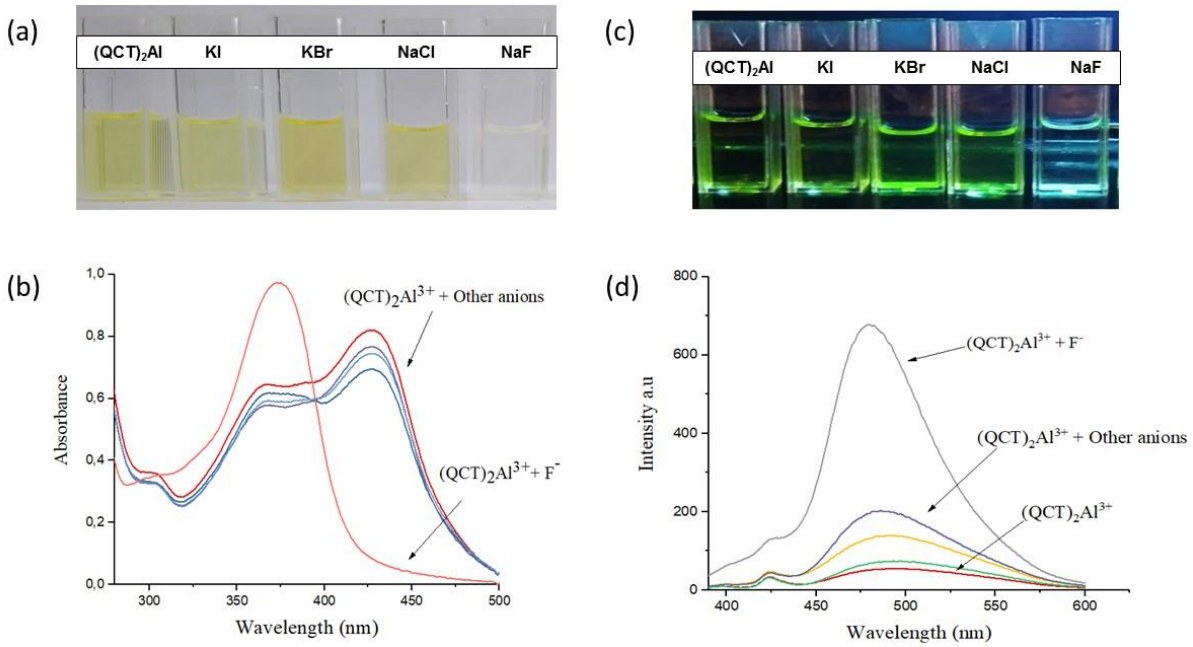

author, 2020.

CHAPTER 6 FINAL CONSIDERATIONS

The synthesis of new quinoxaline derivatives has been promising throughout the work done by our research group, mainly because these molecules present relevant applications. The studies conducted by our group with ascorbic acid (AA) as a precursor began with the search for new chemosensors, resulting in the synthesis of a new Cu^{2+} sensor, AAQX[132], published in a first work as previously mentioned. Besides, the synthesized sensor (AAQX) was immobilized on strips of paper and in collaboration with the Biological Chemistry and Chemistry research group, was quantified using a low-cost reflectometer[134].

The studies on quinoxaline-derived chemosensors resulted in a review article dealing with these sensors applied to cations. At the beginning of the research, there was a need for writing sensors applied to cations and anions. However, during the studies, it was possible to notice the recent publication of the review article focused on quinoxaline-derived chemosensors applied to anions[17]. Therefore, the review article in this paper deals only with quinoxaline-derived chemosensors applied to cations, bringing a relevant contribution to the literature since this report does not exist.

The dedication of this work was focused on chemosensors, having first resulted in nine unpublished compounds in the literature, which were duly characterized using one-dimensional and two-dimensional NMR spectra (COSY, HSQC, and HMBC), two of which were applied as Cu^{2+} sensors and F^-. The other compounds have not been tested for ionic analytes, however, due to their similar structures to the characterized sensors, are potential candidates in the application as new sensors.

Finally, a multidisciplinary proposal for chemistry lectures was built aiming to bring to the students, new experiences and stimulate them for scientific research. The proposal is interesting from a biotechnological point of view, integrating the field of chemosensors, natural products, organic synthesis, and computational chemistry in a single project. The work presented good results where it was possible the synthesis of the quercetin complex with the aluminum ion (Al^{3+}) and the application of this complex as F^- chemosensor. In this project, quercetin was obtained through Rutin hydrolysis, but it can also be easily found commercially and at affordable prices. Another interesting fact is that, in addition to the characterization by spectroscopic methods (UV-vis. or fluorescence), the detection can be observed with the naked eye by the students, because the solution coloration in the presence of the F^- ion is changed from

yellow to colorless. The possible adaptations show that the project can be applied even in environments where it is not possible to use spectroscopic equipment, bringing a relevant contribution to the teaching area with new practices.

REFERENCES

1. S. UPADHYAY, A. SINGH, R. SINHA, S. OMER, K. NEGI, Colorimetric chemosensors for d-metal ions: A review in the past, present, and future prospect, J. Mol. Struct. 1193 (2019) 89–102. https://doi.org/10.1016/j.molstruc.2019.05.007.

2. S. DHIMAN, M. AHMAD, N. SINGLA, G. KUMAR, P. SINGH, V. LUXAMI, N. KAUR, S. KUMAR, Chemodosimeters for optical detection of fluoride anion, Coord. Chem. Rev. 405 (2020) 213138. https://doi.org/10.1016/j.ccr.2019.213138.

3. A. PATIL, S. SALUNKE-GAWALI, Overview of the chemosensor ligands used for selective detection of anions and metal ions (Zn^{2+}, Cu^{2+}, Ni^{2+}, Co^{2+}, Fe^{2+}, Hg^{2+}), Inorganica Chim. Acta. 482 (2018) 99–112. https://doi.org/10.1016/j.ica.2018.05.026.

4. G. SIVARAMAN, M. INIYA, T. ANAND, N.G. KOTLA, O. SUNNAPU, S. SINGARAVADIVEL, A. GULYANI, D. CHELLAPPA, Chemically diverse small molecule fluorescent chemosensors for copper ion, Coord. Chem. Rev. 357 (2018) 50–104. https://doi.org/10.1016/j.ccr.2017.11.020.

5. A.L. BERHANU, GAURAV, I. MOHIUDDIN, A.K. MALIK, J.S. AULAKH, V. KUMAR, K.H. KIM, A review of the applications of Schiff bases as optical chemical sensors, TrAC - Trends Anal. Chem. 116 (2019) 74–91. https://doi.org/10.1016/j.trac.2019.04.025.

6. R. GULIYEV, Design strategies for chemosensors and their applications in molecular scale logic gates. Dissertation, Bilkent University, 2013. http://www.thesis.bilkent.edu.tr/0006231.pdf.

7. B. WANG, E. V. ANSLYN, Chemosensors: Principles, Strategies, and Applications, 2011. https://doi.org/10.1002/9781118019580.

8. P. WANG, D. ZHOU, B. CHEN, High selective and sensitive detection of Zn(II) using tetrapeptide-based dansyl fluorescent chemosensor and its application in cell imaging, Spectrochim. Acta - Part A Mol. Biomol. Spectrosc. 204 (2018) 735–742. https://doi.org/10.1016/j.saa.2018.07.001.

9. A. ALIBERTI, P. VAIANO, A. CAPORALE, M. CONSALES, M. RUVO, A. CUSANO, Fluorescent chemosensors for Hg^{2+} detection in aqueous environment, Sensors Actuators, B Chem. 247 (2017) 727–735. https://doi.org/10.1016/j.snb.2017.03.026.

10. P. TANG, G. SUN, Highly sensitive colorimetric paper sensor for methyl isothiocyanate (MITC): Using its toxicological reaction, Sensors Actuators, B Chem. 261 (2018) 178–187. https://doi.org/10.1016/j.snb.2018.01.086.

11. U. RAJAJI, A. MUTHUMARIYAPPAN, S.M. CHEN, T.W. CHEN, R.J. RAMALINGAM, A novel electrochemical sensor for the detection of oxidative stress and cancer biomarker (4-nitroquinoline N-oxide) based on iron nitride nanoparticles with multilayer reduced graphene nanosheets modified electrode, Sensors Actuators, B Chem. 291 (2019) 120–129. https://doi.org/10.1016/j.snb.2019.04.041.

12. Y. HAYASHI, Pot economy and one-pot synthesis, Chem. Sci. 7 (2016) 866–880. https://doi.org/10.1039/c5sc02913a.

13. J.S. DA ROSA, R.L. DE O. GODOY, J. OIANO NETO, R. DA S. CAMPOS, V.M. DA MATTA, C.A. FREIRE, A.S. DA SILVA, R.S. DE SOUZA, Desenvolvimento de um método de análise de vitamina C em alimentos por cromatografa líquida de alta eficiência e exclusão iônica, Ciência e Tecnol. Aliment. 27 (2007) 837–846. https://doi.org/10.1590/s0101-20612007000400025.

14. L.C. DA SILVA, D.F. DE LIMA, J.A. SILVA, C.L.M. DE MORAIS, B.L. ALBUQUERQUE, A.J. BORTOLUZZI, J.B. DOMINGOS, R.M. ARAÚJO, F.G. MENEZES, K.M.G. LIMA, Quantification of synthetic amino-nitroquinoxaline dyes: An approach using image analysis, J. Braz. Chem. Soc. 27 (2016) 1067–1077. https://doi.org/10.5935/0103-5053.20160002.

15. E.S.H.E. ASHRY, K.F. ATTA, S. ABOUL-ELA, R. BELDI, MAOS of quinoxalines, conjugated pyrazolylquinoxalines and fused pyrazoloquinoxalines from L-ascorbic and D-isoascorbic acid, J. Carbohydr. Chem. 26 (2007) 1–16. https://doi.org/10.1080/07328300701252359.

16. C. HENNING, K. LIEHR, M. GIRNDT, C. ULRICH, M.A. GLOMB, Extending the spectrum of α-dicarbonyl compounds in vivo, J. Biol. Chem. 289 (2014) 28676–28688. https://doi.org/10.1074/jbc.M114.563593.

17. S.K. DEY, M. AL KOBAISI, S. V. BHOSALE, Functionalized Quinoxaline for Chromogenic and Fluorogenic Anion Sensing, ChemistryOpen. 7 (2018) 934–952. https://doi.org/10.1002/open.201800163.

18. D. DAMASCENO, L. FERREIRA, D. LIMA, N. ARCÂNGELA, R. DE SÁ, G. TETAPING, A. CLARA, A. FERREIRA, B. GERALDO, S. SANT, Ó. PESSOA, A. CAMPBELL, T. CRISTINA, M. NOGUEIRA, M. VINÍCIUS, N. DE SOUZA, J. RICARDO, D. FIGUEIREDO, A. PAULA, R. RODRIGUES, Research in Veterinary Science Response of preantral follicles exposed to quinoxaline : A new compound with anticancer potential, Res. Vet. Sci. 128 (2020) 261–268. https://doi.org/10.1016/j.rvsc.2019.12.010.

19. P.J. LINDSAY-SCOTT, P.T. GALLAGHER, Synthesis of heterocycles from arylacetonitriles: Powerful tools for medicinal chemists, Tetrahedron Lett. 58 (2017) 2629–2635. https://doi.org/10.1016/j.tetlet.2017.05.089.

20. M. MONIER, A. EL-MEKABATY, D. ABDEL-LATIF, K.M. ELATTAR, Heterocyclic steroids : E ffi cient routes for annulation of pentacyclic steroidal pyrimidines, Steroids. 154 (2019) 108548. https://doi.org/10.1016/j.steroids.2019.108548.

21. S. ZHOU, G. HUANG, G. CHEN, Design, synthesis and biological activity of a novel ethylenediamine derivatives as H1 receptor antagonists, Bioorganic Med. Chem. 27 (2019) 115127. https://doi.org/10.1016/j.bmc.2019.115127.

22. D.J. BROWN, Quinoxalines - Supplement II, 2004.

23. V.A. MAMEDOV, Quinoxalines: Synthesis, reactions, mechanisms and structure, 2016. https://doi.org/10.1007/978-3-319-29773-6.

24. Y. V.D. NAGESWAR, K. HARSHA VARDHAN REDDY, K. RAMESH, S. NARAYANA MURTHY, Recent developments in the synthesis of quinoxaline derivatives by green synthetic approaches, Org. Prep. Proced. Int. 45 (2013) 1–27. https://doi.org/10.1080/00304948.2013.743419.

25. R.B. BAUDY, L.P. GREENBLATT, I.L. JIRKOVSKY, M. CONKLIN, R.J. RUSSO, D.R. BRAMLETT, T.A. EMREY, J.T. SIMMONDS, D.M. KOWAL, R.P. STEIN, R.P. TASSE, Potent Quinoxaline-Spaced Phosphono α-Amino Acids of the AP-6 Type as Competitive NMDA Antagonists: Synthesis and Biological Evaluation, J. Med. Chem. 36 (1993) 331–342. https://doi.org/10.1021/jm00055a004.

26. T.B. NGUYEN, L. ERMOLENKO, A. AL-MOURABIT, Sodium sulfide: A sustainable solution for unbalanced redox condensation reaction between *o*-nitroanilines and alcohols catalyzed by an iron-sulfur system, Synth. 47 (2015) 1741–1748. https://doi.org/10.1055/s-0034-1380134.

27. B. SAHA, B. MITRA, D. BRAHMIN, B. SINHA, P. GHOSH, 2-Iodo benzoic acid: An unconventional precursor for the one pot multi-component synthesis of quinoxaline using organo Cu (II) catalyst, Tetrahedron Lett. 59 (2018) 3657–3663. https://doi.org/10.1016/j.tetlet.2018.08.051.

28. V.A. SAMSONOV, Furazan ring opening upon treatment of benzofurazan with ethanolamine to yield quinoxalines, Russ. Chem. Bull. 56 (2007) 2510–2512. https://doi.org/10.1007/s11172-007-0400-x.

29. C. WALCZAK, T.J. PAYNE, C.B. WADE, M. YONKEY, M. SCHEID, A. BADOUR, D.K. MOHANTY, The thermal instability of 2,4 and 2,6-*N*-alkylamino-disubstituted and 2-*N*-alkylamino-substituted nitrobenzenes in weakly alkaline solution: Sec-amino effect, J. Heterocycl. Chem. 52 (2015) 681–687. https://doi.org/10.1002/jhet.2154.

30. J.M. PARK, C.Y. JUNG, Y. WANG, H.D. CHOI, S.J. PARK, P. OU, W.D. JANG, J.Y. JAUNG, Effect of additional phenothiazine donor and thiophene π-bridge on photovoltaic performance of quinoxaline cored photosensitizers, Dye. Pigment. 170 (2019) 107568. https://doi.org/10.1016/j.dyepig.2019.107568.

31. D.H. KIM, Y.W. HAN, D.K. MOON, A comparative investigation of dibenzo[a,c]phenazine and quinoxaline donor–acceptor conjugated polymers: Correlation of planar structure and intramolecular charge transfer properties, Polymer (Guildf). 185 (2019) 121906. https://doi.org/10.1016/j.polymer.2019.121906.

32. B. ALAMEDDINE, N. BAIG, S. SHETTY, S. AL-MOUSAWI, Conjugated copolymers bearing 2,7-di(thiophen-2-yl)phenanthrene-9,10-dione units and alteration of their emission via functionalization of the ortho-dicarbonyl groups into quinoxaline and phenazine derivatives, Polymer (Guildf). 178 (2019) 121589. https://doi.org/10.1016/j.polymer.2019.121589.

33. S. BHARGAVA, P. SONI, D. RATHORE, An environmentally benign attribute for the expeditious synthesis of quinoxaline and its derivatives, J. Mol. Struct. 1198 (2019) 1256758. https://doi.org/10.1016/j.molstruc.2019.07.005.

34. H.M. BACHHAV, S.B. BHAGAT, V.N. TELVEKAR, Efficient protocol for the synthesis of quinoxaline, benzoxazole and benzimidazole derivatives using glycerol as green solvent, Tetrahedron Lett. 52 (2011) 5697–5701. https://doi.org/10.1016/j.tetlet.2011.08.105.

35. L.M. ANDERSON, A.R. BUTLER, A Mechanistic Study of Quinoxaline Formation, J. Chem. Soc. Perkin Trans. 2. 2 (1994) 323–326.

36. K. AGHAPOOR, H.R. DARABI, F. MOHSENZADEH, Y. BALAVAR, H. DANESHYAR, Zirconium(IV) chloride as versatile catalyst for the expeditious synthesis of quinoxalines and pyrido[2,3-b]pyrazines under ambient conditions, Transit. Met. Chem. 35 (2010) 49–53. https://doi.org/10.1007/s11243-009-9294-9.

37. J.J. CAI, J.P. ZOU, X.Q. PAN, W. ZHANG, Gallium(III) triflate-catalyzed synthesis of quinoxaline derivatives, Tetrahedron Lett. 49 (2008) 7386–7390. https://doi.org/10.1016/j.tetlet.2008.10.058.

38. W.H. CHEESEMAN, P.D. ROY, C.H. ROAD, PreparationPreparation and reactions of pyrrolo[1,2-a]quinoxalinesulphonic acids, J. Chem. Soc. C Org. 5 (1969) 856–860.

39. A.A. ABU-HASHEM, Synthesis, Reactions and Biological Activity of Quinoxaline Derivatives, ChemInform. 5 (2015) 14–56. https://doi.org/10.1002/chin.201532244.

40. C.A. OBAFEMI, W. PFLEIDERER, Permanganate Oxidation of Quinoxaline and Its Derivatives, Helv. Chim. Acta. 77 (1994) 1549–1556. https://doi.org/10.1002/hlca.19940770610.

41. T. KAUSHAL, G. SRIVASTAVA, A. SHARMA, A. SINGH NEGI, An insight into medicinal chemistry of anticancer quinoxalines, Bioorganic Med. Chem. 27 (2019) 16–35. https://doi.org/10.1016/j.bmc.2018.11.021.

42. M. MONTANA, F. MATHIAS, T. TERME, P. VANELLE, Antitumoral activity of quinoxaline derivatives: A systematic review, Eur. J. Med. Chem. 163 (2019) 136–147. https://doi.org/10.1016/j.ejmech.2018.11.059.

43. S. TARIQ, K. SOMAKALA, M. AMIR, Quinoxaline: An insight into the recent pharmacological advances, Eur. J. Med. Chem. 143 (2018) 542–557. https://doi.org/10.1016/j.ejmech.2017.11.064.

44. S.R. SAGAR, D.P. SINGH, R.D. DAS, N.B. PANCHAL, V. SUDARSANAM, M. NIVSARKAR, K.K. VASU, Pharmacological investigation of quinoxaline-bisthiazoles as multitarget-directed ligands for the treatment of Alzheimer's disease, Bioorg. Chem. 89 (2019) 102992. https://doi.org/10.1016/j.bioorg.2019.102992.

45. Y. YUAN, Z. WANG, R. YANG, T. QIAN, Q. ZHOU, Naphthyl quinoxaline thymidine conjugate is a potent anticancer agent post UVA activation and elicits marked inhibition of tumor growth through vaccination, Eur. J. Med. Chem. 171 (2019) 255–264. https://doi.org/10.1016/j.ejmech.2019.03.051.

46. T. AFROUGH, M. BAKAVOLI, H. ESHGHI, H. BEYZAEI, M. MOGHADDAM-MANESH, Synthesis, Characterization and In Vitro Antibacterial Evaluation of Novel 4-(1-(Pyrimidin-4-yl)Ethyl)-12 H -Pyrimido[4′,5′:5,6][1,4]Thiazino[2,3- b]Quinoxaline Derivatives, Polycycl. Aromat. Compd. (2019) 1–11. https://doi.org/10.1080/10406638.2019.1614640.

47. J. COGO, J. CANTIZANI, I. COTILLO, D.P. SANGI, A.G. CORRÊA, T. UEDA-NAKAMURA, B.P.D. FILHO, J.J. MARTÍN, C.V. NAKAMURA, Quinoxaline derivatives as potential antitrypanosomal and antileishmanial agents, Bioorganic Med. Chem. 26 (2018) 4065–4072. https://doi.org/10.1016/j.bmc.2018.06.033.

48. H.M. PATEL, V. BHARDWAJ, P. SHARMA, M.N. NOOLVI, S. LOHAN, S. BANSAL, A. SHARMA, Quinoxaline-PABA bipartite hybrid derivatization approach: Design and search for antimicrobial agents, J. Mol. Struct. 1184 (2019) 562–568. https://doi.org/10.1016/j.molstruc.2019.02.074.

49. S. TARIQ, O. ALAM, M. AMIR, Synthesis, anti-inflammatory, p38α MAP kinase inhibitory activities and molecular docking studies of quinoxaline derivatives containing triazole moiety, Bioorg. Chem. 76 (2018) 343–358. https://doi.org/10.1016/j.bioorg.2017.12.003.

50. P. GĄSIORSKI, M. MATUSIEWICZ, E. GONDEK, M. POKLADKO-KOWAR, P. ARMATYS, K. WOJTASIK, A. DANEL, T. UCHACZ, A. V. KITYK, Efficient green electroluminescence from 1,3-diphenyl-1H-pyrazolo[3,4-b]quinoxaline dyes in dye-doped polymer based electroluminescent devices, Dye. Pigment. 151 (2018) 380–384. https://doi.org/10.1016/j.dyepig.2018.01.002.

51. M. DUDA, M. RĄPAŁA-KOZIK, K.M. STADNICKA, B. MUSIELAK, P. GOSZCZYCKI, Ł.J. WITEK, M. ZAWROTNIAK, M. GONZÁLEZ-GONZÁLEZ, K. OSTROWSKA, Application of pyrrolo[2,3-b]quinoxaline with an N,N-bis(pyridin-2-ylmethyl)ethylenediamine chain for Zn(II) detection in Candida albicans and fibroblast cells, J. Photochem. Photobiol. A Chem. 382 (2019) 111944. https://doi.org/10.1016/j.jphotochem.2019.111944.

52. J.M. PARK, C.Y. JUNG, J.H. CHO, D.H. KIM, Y. WANG, J.Y. JAUNG, Synthesis of new di-anchoring organic sensitizer based on quinoxaline acceptor for dye-sensitized solar cells, Tetrahedron Lett. 59 (2018) 3322–3325. https://doi.org/10.1016/j.tetlet.2018.07.049.

53. J.Y. JAUNG, Synthesis and halochromism of new quinoxaline fluorescent dyes, Dye. Pigment. 71 (2006) 245–250. https://doi.org/10.1016/j.dyepig.2005.07.008.

54. X. LAI, G. QIU, Q. YE, R. WANG, J.-B. LIU, A reaction-based fluorescent probe for detecting o-phenylenediamine in water and lateritic soil samples, J. Photochem. Photobiol. A Chem. 386 (2020) 112101. https://doi.org/10.1016/j.jphotochem.2019.112101.

55. A. ZARROUK, A. DAFALI, B. HAMMOUTI, H. ZARROK, S. BOUKHRIS, M. ZERTOUBI, Synthesis, characterization and comparative study of functionalized quinoxaline derivatives towards corrosion of copper in nitric acid medium, Int. J. Electrochem. Sci. 5 (2010) 46–55.

56. L.O. OLASUNKANMI, E.E. EBENSO, Experimental and computational studies on propanone derivatives of quinoxalin-6-yl-4 , 5-dihydropyrazole as inhibitors of mild steel corrosion in hydrochloric acid, J. Colloid Interface Sci. 561 (2020) 104–116. https://doi.org/10.1016/j.jcis.2019.11.097.

57. J. SARANYA, P. SOUNTHARI, K. PARAMESWARI, S. CHITRA, Acenaphtho[1,2-b]quinoxaline and acenaphtho[1,2-b]pyrazine as corrosion inhibitors for mild steel in acid medium, Meas. J. Int. Meas. Confed. 77 (2016) 175–186. https://doi.org/10.1016/j.measurement.2015.09.008.

58. M. FINŠGAR, J. JACKSON, Application of corrosion inhibitors for steels in acidic media for the oil and gas industry: A review, Corros. Sci. 86 (2014) 17–41. https://doi.org/10.1016/j.corsci.2014.04.044.

59. A.W. CZARNIK, Supramolecular Chemistry, Fluorescence, and Sensing, in: 1993. https://doi.org/10.1021/bk-1993-0538.ch001.

60. D. WU, A.C. SEDGWICK, T. GUNNLAUGSSON, E.U. AKKAYA, J. YOON, T.D. JAMES, Fluorescent chemosensors: The past, present and future, Chem. Soc. Rev. 45 (2017) 7105–7123. https://doi.org/10.1039/c7cs00240h.

61. C.J. PEDERSEN, The Discovery of Crown Ethers (Noble Lecture), Angew. Chemie Int. Ed. English. 27 (1988) 1021–1027. https://doi.org/10.1002/anie.198810211.

62. B. KAUR, N. KAUR, S. KUMAR, Colorimetric metal ion sensors – A comprehensive review of the years 2011–2016, Coord. Chem. Rev. 358 (2018) 13–69. https://doi.org/10.1016/j.ccr.2017.12.002.

63. L. FABBRIZZI, A. POGGI, Sensors and switches from supramolecular chemistry, Chem. Soc. Rev. 24 (1995) 197–202. https://doi.org/10.1039/CS9952400197.

64. M. FORMICA, V. FUSI, L. GIORGI, M. MICHELONI, New fluorescent chemosensors for metal ions in solution, Coord. Chem. Rev. 256 (2012) 170–192. https://doi.org/10.1016/j.ccr.2011.09.010.

65. B. VALEUR, M.N. BERBERAN-SANTOS, Molecular Fluorescence: Principles and Applications, Second Edition, 2012. https://doi.org/10.1002/9783527650002.

66. H.V. MONTEIRO, THAÍS HELENA, Funções Plenamente Reconhecidas de Nutrientes Fósforo, 2010.

67. D.H. DE F. MUNIZ, E.C. OLIVEIRA-FILHO, Metais pesados provenientes de rejeitos de mineração e seus efeitos sobre a saúde e o meio ambiente, Univ. Ciências Da Saúde. 4 (2008) 83–100. https://doi.org/10.5102/ucs.v4i1.24.

68. S.L. SENSI, A. GRANZOTTO, M. SIOTTO, R. SQUITTI, Copper and Zinc Dysregulation in Alzheimer's Disease, Trends Pharmacol. Sci. 39 (2018) 1049–1063. https://doi.org/10.1016/j.tips.2018.10.001.

69. D.J. WAGGONER, T.B. BARTNIKAS, J.D. GITLIN, The role of copper in neurodegenerative disease, Neurobiol. Dis. 6 (1999) 221–230. https://doi.org/10.1006/nbdi.1999.0250.

70. M.S. KIM, S.Y. LEE, J.M. JUNG, C. KIM, A new Schiff-base chemosensor for selective detection of Cu2+ and Co2+ and its copper complex for colorimetric sensing of S2- in aqueous solution, Photochem. Photobiol. Sci. 16 (2017) 1677–1689. https://doi.org/10.1039/c7pp00229g.

71. K.B. KIM, H. KIM, E.J. SONG, S. KIM, I. NOH, C. KIM, A cap-type Schiff base acting as a fluorescence sensor for zinc(ii) and a colorimetric sensor for iron(ii), copper(ii), and zinc(ii) in aqueous media, Dalt. Trans. 42 (2013) 16569. https://doi.org/10.1039/c3dt51916c.

72. Y. ZHOU, X. BAO, Synthesis, recognition and sensing properties of dipyrrolylmethane-based anion receptors, Spectrochim. Acta - Part A Mol. Biomol. Spectrosc. 210 (2019) 1–8. https://doi.org/10.1016/j.saa.2018.10.056.

73. X. JIA, Y. YANG, Y. HE, Q. MA, Y. LIU, Theoretical study on the sensing mechanism of a fluorescence chemosensor for the cyanide anion, Spectrochim. Acta - Part A Mol. Biomol. Spectrosc. 216 (2019) 258–264. https://doi.org/10.1016/j.saa.2019.03.034.

74. M. MOHAPATRA, S. ANAND, B.K. MISHRA, D.E. GILES, P. SINGH, Review of fluoride removal from drinking water, J. Environ. Manage. 91 (2009) 67–77. https://doi.org/10.1016/j.jenvman.2009.08.015.

75. M. CAMETTI, K. RISSANEN, Recognition and sensing of fluoride anion, Chem. Commun. 20 (2009) 2809–2829. https://doi.org/10.1039/b902069a.

76. K.C. CHANG, S.S. SUN, M.O. ODAGO, A.J. LEES, Anion recognition and sensing by transition-metal complexes with polarized NH recognition motifs, Coord. Chem. Rev. 284 (2015) 111–123. https://doi.org/10.1016/j.ccr.2014.09.009.

77. C.Y. CHEN, T.P. LIN, C.K. CHEN, S.C. LIN, M.C. TSENG, Y.S. WEN, S.S. SUN, New chromogenic and fluorescent probes for anion detection: Formation of a [2 + 2] supramolecular complex on addition of fluoride with positive homotropic cooperativity, J. Org. Chem. 73 (2008) 900–911. https://doi.org/10.1021/jo7019916.

78. C.B. BLACK, B. ANDRIOLETTI, A.C. TRY, C. RUIPEREZ, J.L. SESSLER, Dipyrrolylquinoxalines: Efficient sensors for fluoride anion in organic solution [12], J. Am. Chem. Soc. 121 (1999) 10438–10439. https://doi.org/10.1021/ja992579a.

79. R. POHL, D. ALDAKOV, P. KUBÁT, K. JURSÍKOVÁ, M. MARQUEZ, P. ANZENBACHER, Strategies toward improving the performance of fluorescence-based sensors for inorganic anions, Chem. Commun. 11 (2004) 1282–1283. https://doi.org/10.1039/b315268e.

80. P. ANZENBACHER, A.C. TRY, H. MIYAJI, K. JURSIKOVA, V.M. LYNCH, M. MARQUEZ, J.L. SESSLER, Fluorinated calix[4]pyrrole and dipyrrolylquinoxaline: Neutral anion receptors with augmented affinities and enhanced selectivities, J. Am. Chem. Soc. 122 (2000) 10268–10272. https://doi.org/10.1021/ja002112w.

81. C.Y. WU, M.S. CHEN, C.A. LIN, S.C. LIN, S.S. SUN, Photophysical studies of anion-induced colorimetric response and amplified fluorescence quenching in dipyrrolylquinoxaline-containing conjugated polymers, Chem. - A Eur. J. 12 (2006) 2263–2269. https://doi.org/10.1002/chem.200500804.

82. J. YOO, M.S. KIM, S.J. HONG, J.L. SESSLER, C.H. LEE, Selective sensing of anions with Calix[4]pyrroles strapped with chromogenic dipyrrolylquinoxalines, J. Org. Chem. 74 (2009) 1065–1069. https://doi.org/10.1021/jo802059c.

83. C. BEJGER, J.S. PARK, E.S. SILVER, J.L. SESSLER, Tetrathiafulvalene diindolylquinoxaline: A dual signaling anion receptor with phosphate selectivity, Chem. Commun. 46 (2010) 7745–7747. https://doi.org/10.1039/c0cc02934c.

84. C. PARTHIBAN, S. CIATTINI, L. CHELAZZI, K.P. ELANGO, Colorimetric sensing of anions by Cu(II), Co(II), Ni(II) and Zn(II) complexes of naphthoquinone-imidazole hybrid - Influence of complex formation on selectivity and sensing medium, Sensors Actuators, B Chem. 231 (2016) 768–778. https://doi.org/10.1016/j.snb.2016.03.106.

85. S. MADHUPRIYA, K.P. ELANGO, Spectrophotometric and spectrofluorimetric studies on the selective sensing of fluoride ions by Co(II) and Ni(II) complexes of naphthoquinone derivative possessing enhanced H-bonding property, Spectrochim. Acta - Part A Mol. Biomol. Spectrosc. 97 (2012) 429–434. https://doi.org/10.1016/j.saa.2012.06.020.

86. A.C. BOUDET, J.P. CORNARD, J.C. MERLIN, Conformational and spectroscopic investigation of 3-hydroxyflavone-aluminum chelates, Spectrochim. Acta - Part A Mol. Biomol. Spectrosc. 56 (2000) 829–839. https://doi.org/10.1016/S1386-1425(99)00284-X.

87. M.D. ENGELMANN, R. HUTCHESON, I.F. CHENG, Stability of ferric complexes with 3-hydroxyflavone (flavonol), 5,7-dihydroxyflavone (chrysin), and 3′,4′-dihydroxyflavone, J. Agric. Food Chem. 53 (2005) 2953–2960. https://doi.org/10.1021/jf048298q.

88. L. DANGLETERRE, J.P. CORNARD, Interaction of lead (II) chloride with hydroxyflavones in methanol: A spectroscopic study, Polyhedron. 24 (2005) 1593–1598. https://doi.org/10.1016/j.poly.2005.04.019.

89. J.P. CORNARD, L. DANGLETERRE, C. LAPOUGE, DFT and TD-DFT investigation and spectroscopic characterization of the molecular and electronic structure of the Zn(II)-3-hydroxyflavone complex, Chem. Phys. Lett. 419 (2006) 304–308. https://doi.org/10.1016/j.cplett.2005.11.101.

90. A.S. ROY, D.R. TRIPATHY, S. SAMANTA, S.K. GHOSH, S. DASGUPTA, DNA damaging, cell cytotoxicity and serum albumin binding efficacy of the rutin-Cu(II) complex, Mol. Biosyst. 12 (2016) 1687–1701. https://doi.org/10.1039/c6mb00161k.

91. J.P. CORNARD, J.C. MERLIN, Spectroscopic and structural study of complexes of quercetin with Al(III), J. Inorg. Biochem. 92 (2002) 19–27. https://doi.org/10.1016/S0162-0134(02)00469-5.

92. G. CERCHIARO, A.M.D.C. FERREIRA, Oxindoles and copper complexes with oxindole-derivatives as potential pharmacological agents, J. Braz. Chem. Soc. 17 (2006) 1473–1485. https://doi.org/10.1590/S0103-50532006000800003.

93. Y.H. HUNG, A.I. BUSH, R.A. CHERNY, Copper in the brain and Alzheimer's disease, J. Biol. Inorg. Chem. 15 (2010) 61–76. https://doi.org/10.1007/s00775-009-0600-y.

94. B. I., R. A., Visions & Reflections (Minireview) Menkes disease, Cell. Mol. Life Sci. 65 (2007) 89–91. https://doi.org/10.1007/s00018-007-7439-6.

95. E. GAGGELLI, H. KOZLOWSKI, D. VALENSIN, G. VALENSIN, Copper homeostasis and neurodegenerative disorders (Alzheimer's, prion, and Parkinson's diseases and amyotrophic lateral sclerosis), Chem. Rev. 106 (2006) 1995–2044. https://doi.org/10.1021/cr040410w.

96. S. ERDEMIR, B. TABAKCI, Selective and Sensitive Fluorescein-Benzothiazole Based Fluorescent Sensor for Zn2+ Ion in Aqueous Media, J. Fluoresc. 27 (2017) 2145–2152. https://doi.org/10.1007/s10895-017-2153-8.

97. A. BUDIMIR, Metal ions, Alzheimer's disease and chelation therapy, Acta Pharm. 61 (2011) 1–14. https://doi.org/10.2478/v10007-011-0006-6.

98. W. SHI, Y. LEI, Y. HUI, H. MI, F. MA, Y. TIAN, Z. XIE, Aqueous nanodispersion of acetylene tethered, quinoxaline-containing conjugated polymer as fluorescence probe for Ag+, New J. Chem. 38 (2014) 4730–4735. https://doi.org/10.1039/c4nj00492b.

99. A.E. KANDJANI, Y.M. SABRI, M. MOHAMMAD-TAHERI, V. BANSAL, S.K. BHARGAVA, Detect, remove and reuse: A new paradigm in sensing and removal of Hg (II) from wastewater via SERS-active ZnO/Ag nanoarrays, Environ. Sci. Technol. 49 (2015) 1578–1584. https://doi.org/10.1021/es503527e.

100. M.T. KACZMAREK, M. ZABISZAK, M. NOWAK, R. JASTRZAB, Lanthanides: Schiff base complexes, applications in cancer diagnosis, therapy, and antibacterial activity, Coord. Chem. Rev. 370 (2018) 42–54. https://doi.org/10.1016/j.ccr.2018.05.012.

101. FARZANEH SHEMIRANIA, M. BAGHDADIA, M. RAMEZANIB, M.R. JAMALI, Determination of ultratrace amounts of bismuth in water samples by electrothermal atomic absorption spectrometry (ET-AAS) after cloud point extraction, Anal. Chim. Acta. 534 (2005) 163–169. https://doi.org/10.1016/j.aca.2004.06.036.

102. R. MOHAMED, B.H. ZAINUDIN, A.S. YAAKOB, Method validation and determination of heavy metals in cocoa beans and cocoa products by microwave assisted digestion technique with inductively coupled plasma mass spectrometry, Food Chem. 303 (2020) 125392. https://doi.org/10.1016/j.foodchem.2019.125392.

103. G.J. SHI, Y. LI, Q.H. CAO, H.X. WU, X.Y. TANG, X.H. GAO, J.Q. YU, Z. CHEN, Y. YANG, In vitro and in vivo evidence that quercetin protects against diabetes and its complications: A systematic review of the literature, Biomed. Pharmacother. 109 (2019) 1085–1099. https://doi.org/10.1016/j.biopha.2018.10.130.

104. J. WU, B. KWON, W. LIU, E. V. ANSLYN, P. WANG, J.S. KIM, Chromogenic/Fluorogenic Ensemble Chemosensing Systems, Chem. Rev. 115 (2015) 7893–7943. https://doi.org/10.1021/cr500553d.

105. T.L. MAKO, J.M. RACICOT, M. LEVINE, Supramolecular luminescent sensors, Chem. Rev. 119 (2019) 322–477. https://doi.org/10.1021/acs.chemrev.8b00260.

106. G. ARAGAY, J. PONS, A. MERKOÇI, Recent trends in macro-, micro-, and nanomaterial-based tools and strategies for heavy-metal detection, Chem. Rev. 111 (2011) 3433–3458. https://doi.org/10.1021/cr100383r.

107. D.T. QUANG, J.S. KIM, Fluoro- and chromogenic chemodosimeters for heavy metal ion detection in solution and biospecimens, Chem. Rev. 110 (2010) 6280–6301. https://doi.org/10.1021/cr100154p.

108. R. KUMAR, A. SHARMA, H. SINGH, P. SUATING, H.S. KIM, K. SUNWOO, I. SHIM, B.C. GIBB, J.S. KIM, Revisiting Fluorescent Calixarenes: From Molecular Sensors to Smart Materials, Chem. Rev. 119 (2019) 9657–9721. https://doi.org/10.1021/acs.chemrev.8b00605.

109. D. CAO, Z. LIU, P. VERWILST, S. KOO, P. JANGJILI, J.S. KIM, W. LIN, Coumarin-Based Small-Molecule Fluorescent Chemosensors, Chem. Rev. 119 (2019) 10403–10519. https://doi.org/10.1021/acs.chemrev.9b00145.

110. J. LI, D. YIM, W.D. JANG, J. YOON, Recent progress in the design and applications of fluorescence probes containing crown ethers, Chem. Soc. Rev. 46 (2017) 2437–2458. https://doi.org/10.1039/c6cs00619a.

111. Y. DING, W.H. ZHU, Y. XIE, Development of Ion Chemosensors Based on Porphyrin Analogues, Chem. Rev. 117 (2017) 2203–2256. https://doi.org/10.1021/acs.chemrev.6b00021.

112. R. PAOLESSE, S. NARDIS, D. MONTI, M. STEFANELLI, C. DI NATALE, Porphyrinoids for Chemical Sensor Applications, Chem. Rev. 117 (2017) 2517–2583. https://doi.org/10.1021/acs.chemrev.6b00361.

113. W. SUN, S. GUO, C. HU, J. FAN, X. PENG, Recent Development of Chemosensors Based on Cyanine Platforms, Chem. Rev. 116 (2016) 7768–7817. https://doi.org/10.1021/acs.chemrev.6b00001.

114. Y. YANG, Q. ZHAO, W. FENG, F. LI, Luminescent chemodosimeters for bioimaging, Chem. Rev. 113 (2013) 192–270. https://doi.org/10.1021/cr2004103.

115. L. YOU, D. ZHA, E. V. ANSLYN, Recent Advances in Supramolecular Analytical Chemistry Using Optical Sensing, Chem. Rev. 115 (2015) 7840–7892. https://doi.org/10.1021/cr5005524.

116. J. YIN, Y. HU, J. YOON, Fluorescent probes and bioimaging: Alkali metals, alkaline earth metals and pH, Chem. Soc. Rev. 44 (2015) 4619–4644. https://doi.org/10.1039/c4cs00275j.

117. G.R.C. HAMILTON, S.K. SAHOO, S. KAMILA, N. SINGH, N. KAUR, B.W. HYLAND, J.F. CALLAN, Optical probes for the detection of protons, and alkali and alkaline earth metal cations, Chem. Soc. Rev. 44 (2015) 4415–4432. https://doi.org/10.1039/c4cs00365a.

118. V.G. MACHADO, R.I. STOCK, C. REICHARDT, Pyridinium *N*-phenolate betaine dyes, Chem. Rev. 114 (2014) 10429–10475. https://doi.org/10.1021/cr5001157.

119. K.P. CARTER, A.M. YOUNG, A.E. PALMER, Fluorescent sensors for measuring metal ions in living systems, Chem. Rev. 114 (2014) 4564–4601. https://doi.org/10.1021/cr400546e.

120. X. CHEN, T. PRADHAN, F. WANG, J.S. KIM, J. YOON, Fluorescent chemosensors based on spiroring-opening of xanthenes and related derivatives, Chem. Rev. 112 (2012) 1910–1956. https://doi.org/10.1021/cr200201z.

121. R.N. DSOUZA, U. PISCHEL, W.M. NAU, Fluorescent dyes and their supramolecular host/guest complexes with macrocycles in aqueous solution, Chem. Rev. 111 (2011) 7941–7980. https://doi.org/10.1021/cr200213s.

122. J. ARAÚJO, F.G. MENEZES, H.F.O. SILVA, D.S. VIEIRA, S.R.B. SILVA, A.J. BORTOLUZZI, C. SANT'ANNA, M. EUGENIO, J.M. NERI, L.H.S. GASPAROTTO, Functionalization of gold nanoparticles with two aminoalcohol-based quinoxaline derivatives for targeting phosphoinositide 3-kinases (PI3Kα), New J. Chem. 43 (2019) 1803–1811. https://doi.org/10.1039/c8nj04314k.

123. J.M. NERI, L.N. CAVALCANTI, R.M. ARAÚJO, F.G. MENEZES, 2,3-Dichloroquinoxaline as a versatile building block for heteroaromatic nucleophilic substitution: A review of the last decade, Arab. J. Chem. (2017). https://doi.org/10.1016/j.arabjc.2017.07.012.

124. J.M. NERI, A.H. DE OLIVEIRA, R.M. ARAUJO, L.N. CAVALCANTI, F.G. MENEZES, 2,3-Dichloroquinoxaline in Cross-coupling Reactions: A Single Substrate, Many Possibilities, Curr. Org. Chem. 22 (2018) 1573–1588. https://doi.org/10.2174/1385272822666180806104824.

125. J.A. PEREIRA, A.M. PESSOA, M.N.D.S. CORDEIRO, R. FERNANDES, C. PRUDÊNCIO, J.P. NORONHA, M. VIEIRA, Quinoxaline, its derivatives and applications: A State of the Art review, Eur. J. Med. Chem. 97 (2015) 664–672. https://doi.org/10.4172/2167-0501.1000e138.

126. G.R.S. DE FREITAS, S.E. COELHO, N.K.V. MONTEIRO, J.M. NERI, L.N. CAVALCANTI, J.B. DOMINGOS, D.S. VIEIRA, M.A.F. DE SOUZA, F.G. MENEZES, Theoretical and experimental investigation of acidity of the glutamate receptor antagonist 6,7-dinitro-1,4-dihydroquinoxaline-2,3-dione and Its Possible Implication in GluA2 Binding, J. Phys. Chem. A. 121 (2017) 7414–7423. https://doi.org/10.1021/acs.jpca.7b07775.

127. E.P. DA COSTA, S.E. COELHO, A.H. DE OLIVEIRA, R.M. ARAÚJO, L.N. CAVALCANTI, J.B. DOMINGOS, F.G. MENEZES, Multicomponent synthesis of substituted 3-styryl-1H-quinoxalin-2-ones in an aqueous medium, Tetrahedron Lett. 59 (2018) 3961–3964. https://doi.org/10.1016/j.tetlet.2018.09.048.

128. A.H. DE OLIVEIRA, W.P. SILVA, J.K. DA SILVA, J.C.O. FREITAS, M.A.F. DE SOUZA, R. CRISTIANO, F.G. MENEZES, Non-symmetrical three and two-core ring mesogens based on quinoxaline and benzimidazole derivatives: Supramolecular layers through amphoteric donating/accepting H-bonds, J. Mol. Struct. 1180 (2019) 399–405. https://doi.org/10.1016/j.molstruc.2018.12.007.

129. S. ACHELLE, C. BAUDEQUIN, N. PLÉ, Luminescent materials incorporating pyrazine or quinoxaline moieties, Dye. Pigment. 98 (2013) 575–600. https://doi.org/10.1016/j.dyepig.2013.03.030.

130. Q.N. GUO, C. ZHONG, Y.G. LU, C. SHI, Z.Y. LI, Dipyrrolylquinoxaline-bridged hydrazones: A new class of chemosensors for copper(II), J. Incl. Phenom. Macrocycl. Chem. 72 (2012) 79–88. https://doi.org/10.1007/s10847-011-9941-6.

131. A. KUMAR, V. KUMAR, U. DIWAN, K.K. UPADHYAY, Highly sensitive and selective naked-eye detection of Cu2+in aqueous medium by a ninhydrin-quinoxaline derivative, Sensors Actuators, B Chem. 176 (2013) 420–427. https://doi.org/10.1016/j.snb.2012.09.089.

132. L.C. DA SILVA, E.P. DA COSTA, G.R.S. FREITAS, M.A.F. DE SOUZA, R.M. ARAÚJO, V.G. MACHADO, F.G. MENEZES, Ascorbic acid-based quinoxaline derivative as a chromogenic chemosensor for Cu^{2+}, Inorg. Chem. Commun. 70 (2016) 71–74. https://doi.org/10.1016/j.inoche.2016.05.019.

133. L.C. DA SILVA, A. LINDNER, L.N. CAVALCANTI, E.P. DA COSTA, M.M. AZEVEDO, R.M. ARAÚJO, G.R.S. DE FREITAS, M.A.F. DE SOUZA, V.G. MACHADO, F.G. MENEZES, One-pot synthesis and structural elucidation of polyfunctionalized quinoxalines and their use as chromogenic chemosensors for ionic species, J. Mol. Struct. 1195 (2019) 936–943. https://doi.org/10.1016/j.molstruc.2019.06.025.

134. C.L.M. MORAIS, L.C. DA SILVA, N.A. PINHEIRO, F.G. MENEZES, K.M.G. LIMA, A low-cost video-based reflectometer for selective detection of Cu^{2+} using paper-based colorimetric sensors, J. Braz. Chem. Soc. 28 (2017) 2506–2513. https://doi.org/10.21577/0103-5053.20170087.

135. Q.X. LIU, Z.Q. YAO, X.J. ZHAO, Z.X. ZHAO, X.G. WANG, NHC metal (silver, mercury, and nickel) complexes based on quinoxaline-dibenzimidazolium salts: Synthesis, structural studies, and fluorescent chemosensors for Cu^{2+} by charge transfer, Organometallics. 32 (2013) 3493–3501. https://doi.org/10.1021/om400277z.

136. F. YU, W. ZHANG, P. LI, Y. XING, L. TONG, J. MA, B. TANG, Cu^{2+}-selective naked-eye and fluorescent probe: Its crystal structure and application in bioimaging, Analyst. 134 (2009) 1826–1833. https://doi.org/10.1039/b823360h.

137. E. KORIN, B. COHEN, C.C. ZENG, Y.S. XU, J.Y. BECKER, Phenylethylidene-3,4-dihydro-1H-quinoxalin-2-ones: Promising building blocks for Cu^{2+} recognition, Tetrahedron. 67 (2011) 6252–6258. https://doi.org/10.1016/j.tet.2011.06.047.

138. X.H. ZHANG, Q. ZHAO, X.M. LIU, T.L. HU, J. HAN, W.J. RUAN, X.H. BU, C2-symmetrical hexaazatriphenylene derivatives as colorimetric and ratiometric fluorescence chemsensors for Zn^{2+}, Talanta. 108 (2013) 150–156. https://doi.org/10.1016/j.talanta.2013.02.071.

139. H. HAN, Y.R. LIU, C. DONG, X. EN HAN, Novel ratio fluorescence probes for selectively detecting zinc ion based on Y-type quinoxaline framework, J. Lumin. 183 (2017) 513–518. https://doi.org/10.1016/j.jlumin.2016.11.065.

140. X. FANG, G. ZHAO, Y. XIAO, J. XU, W. YANG, A Europium-based luminescent chemosensor for Zn^{2+} with quinoxaline as the antenna, Tetrahedron Lett. 54 (2013) 806–810. https://doi.org/10.1016/j.tetlet.2012.11.108.

141. Y.P. LI, H.R. YANG, Q. ZHAO, W.C. SONG, J. HAN, X.H. BU, Ratiometric and selective fluorescent sensor for Zn^{2+} as an "off-on-off" switch and logic gate, Inorg. Chem. 51 (2012) 9642–9648. https://doi.org/10.1021/ic300738e.

142. K. OSTROWSKA, Ł. DUDEK, J. GROLIK, M. GRYL, K. STADNICKA, Pyrrolo[2,3-b]quinoxaline with 2-(2-aminoethyl)pyridine chain highly selective fluorescent receptor for Zn2+ exhibiting a dual fluorescence and AIEE in crystalline state, CrystEngComm. 17 (2015) 498–502. https://doi.org/10.1039/c4ce01612b.

143. S.W. RAGSDALE, Nickel-based enzyme systems, J. Biol. Chem. 284 (2009) 18571–18575. https://doi.org/10.1074/jbc.R900020200.

144. B. SHAHZAD, M. TANVEER, A. REHMAN, S.A. CHEEMA, S. FAHAD, S. REHMAN, A. SHARMA, Nickel; whether toxic or essential for plants and environment - A review, Plant Physiol. Biochem. 132 (2018) 641–651. https://doi.org/10.1016/j.plaphy.2018.10.014.

145. S. GOSWAMI, S. CHAKRABORTY, M.K. ADAK, S. HALDER, C.K. QUAH, H.K. FUN, B. PAKHIRA, S. SARKAR, A highly selective ratiometric chemosensor for Ni 2+ in a quinoxaline matrix, New J. Chem. 38 (2014) 6230–6235. https://doi.org/10.1039/c4nj01498g.

146. S. GOSWAMI, S. CHAKRABORTY, S. PAUL, S. HALDER, A.C. MAITY, A simple quinoxaline-based highly sensitive colorimetric and ratiometric sensor, selective for nickel and effective in very high dilution, Tetrahedron Lett. 54 (2013) 5075–5077. https://doi.org/10.1016/j.tetlet.2013.07.051.

147. S. GOSWAMI, S. CHAKRABORTY, A.K. DAS, A. MANNA, A. BHATTACHARYYA, C.K. QUAH, H.K. FUN, Selective colorimetric and ratiometric probe for Ni(II) in quinoxaline matrix with the single crystal X-ray structure, RSC Adv. 4 (2014) 20922–20926. https://doi.org/10.1039/c4ra00594e.

148. A. UPADHYAY, S. KARPAGAM, Synthesis and photo physical properties of carbazole based quinoxaline conjugated polymer for fluorescent detection of Ni^{2+}, Dye. Pigment. 139 (2017) 50–64. https://doi.org/10.1016/j.dyepig.2016.12.019.

149. M. MILEWSKA, A. SKWIERAWSKA, K. GUZOW, D. SZMIGIEL, W. WICZK, 3-[2-(2-Quinoxalinyl)benzoxazol-5-yl]alanine derivative - A specific fluoroionophore for Ni(II), Inorg. Chem. Commun. 8 (2005) 947–950. https://doi.org/10.1016/j.inoche.2005.07.008.

150. L. WANG, W. WONG, L. WU, Z. LI, A Highly Selective and Sensitive Fluorescent Chemosensor for Hg^{2+} in Aqueous Solution, J. Am. Chem. Soc. 34 (2004) 934–935. https://doi.org/10.1246/cl.2005.934.

151. F. ZAPATA, A. CABALLERO, P. MOLINA, A. TARRAGA, A ferrocene-quinoxaline derivative as a highly selective probe for colorimetric and redox sensing of toxic mercury(II) cations, Sensors. (2010). https://doi.org/10.3390/s101211311.

152. M. ALFONSO, A. TÁRRAGA, P. MOLINA, Ferrocene-based multichannel molecular chemosensors with high selectivity and sensitivity for Pb(II) and Hg(II) metal cations, Dalt. Trans. 39 (2010) 8637–8645. https://doi.org/10.1039/c0dt00450b.

153. L. FENG, W. SHI, J. MA, Y. CHEN, F. KUI, Y. HUI, Z. XIE, A novel thiosemicarbazone Schiff base derivative with aggregation-induced emission enhancement characteristics and its application in Hg^{2+} detection, Sensors Actuators, B Chem. 237 (2016) 563–569. https://doi.org/10.1016/j.snb.2016.06.129.

154. Q. ZHAO, R.F. LI, S.K. XING, X.M. LIU, T.L. HU, X.H. BU, A highly selective On/Off fluorescence sensor for cadmium(II), Inorg. Chem. 50 (2011) 10041–10046. https://doi.org/10.1021/ic2008182.

155. Q. ZHAO, X.M. LIU, H.R. LI, Y.H. ZHANG, X.H. BU, High-performance fluorescence sensing of lanthanum ions (La^{3+}) by a polydentate pyridyl-based quinoxaline derivative, Dalt. Trans. 45 (2016) 10836–10841. https://doi.org/10.1039/c6dt01161f.

156. X. ZHANG, Z.J. WANG, S.G. CHEN, Z.Z. SHI, J.X. CHEN, H.G. ZHENG, Cd-Based metal-organic frameworks from solvothermal reactions involving in situ aldimine condensation and the highly sensitive detection of Fe^{3+} ions, Dalt. Trans. 46 (2017) 2332–2338. https://doi.org/10.1039/c6dt04675d.

157. W. CUI, L. WANG, G. XIANG, L. ZHOU, X. AN, D. CAO, A colorimetric and fluorescence “turn-off” chemosensor for the detection of silver ion based on a conjugated polymer containing 2,3-di(pyridin-2-yl)quinoxaline, Sensors Actuators, B Chem. 207 (2015) 281–290. https://doi.org/10.1016/j.snb.2014.10.072.

158. Y.Y. ZHU, T.T. YIN, J. YIN, N. LIU, Z.P. YU, Y.W. ZHU, Y.S. DING, J. YIN, Z.Q. WU, Poly(3-hexylthiophene)-block-poly(5,8-di-p-tolylquinoxaline-2,3-diyl) conjugated rod-rod copolymers: One pot synthesis, self-assembly and highly selective sensing of cobalt, RSC Adv. 4 (2014) 40241–40250. https://doi.org/10.1039/c4ra06571a.

159. B.B. ARBA, A. KIVRAK, M. ZORA, A.M. ÖNAL, Synthesis of a novel fluorescent and ion sensitive monomer bearing quinoxaline moieties and its electropolymerization, React. Funct. Polym. 71 (2011) 579–587. https://doi.org/10.1016/j.reactfunctpolym.2011.02.008.

160. B.B. CARBAS, A. KIVRAK, M. ZORA, A.M. ÖNAL, Synthesis and electropolymerization of a new ion sensitive ethylenedioxy-substituted terthiophene monomer bearing a quinoxaline moiety, J. Electroanal. Chem. 677–680 (2012) 9–14. https://doi.org/10.1016/j.jelechem.2012.05.005.

161. D. PHLIP, Supramolecular chemistry: Concepts and perspectives. By J.-M. Lehn, VCH, Weinheim 1995, x, 271 pp., softcover, DM 58.00, ISBN 3-527-2931 1-6, Adv. Mater. 8 (1996) 866–868. https://doi.org/10.1002/adma.19960081029.

162. C. SUKSAI, T. TUNTULANI, Chromogenic anion sensors, Top. Curr. Chem. 255 (2005) 163–198. https://doi.org/10.1007/b101166.

163. P.D. BEER, P.A. GALE, Anion recognition and sensing: The state of the art and future perspectives, Angew. Chemie - Int. Ed. 40 (2001) 486–516. https://doi.org/10.1002/1521-3773(20010202)40:3<486::AID-ANIE486>3.0.CO;2-P.

164. R. MARTÍNEZ-MÁÑEZ, F. SANCENÓN, Fluorogenic and chromogenic chemosensors and reagents for anions, Chem. Rev. 103 (2003) 4419–4476. https://doi.org/10.1021/cr010421e.

165. T. GUNNLAUGSSON, M. GLYNN, G.M. TOCCI (NÉE HUSSEY), P.E. KRUGER, F.M. PFEFFER, Anion recognition and sensing in organic and aqueous media using luminescent and colorimetric sensors, Coord. Chem. Rev. 250 (2006) 3094–3117. https://doi.org/10.1016/j.ccr.2006.08.017.

166. L.M. ZIMMERMANN-DIMER, V.G. MACHADO, Quimiossensores cromogênicos e fluorogênicos para a detecção de analitos aniônicos, Quim. Nova. 31 (2008) 2134–2146. https://doi.org/10.1590/S0100-40422008000800038.

167. L. MUTIHAC, J.H. LEE, J.S. KIM, J. VICENS, Recognition of amino acids by functionalized calixarenes, Chem. Soc. Rev. 40 (2011) 2593–2643. https://doi.org/10.1039/c0cs00015a.

168. P.A. GALE, C. CALTAGIRONE, Anion sensing by small molecules and molecular ensembles, Chem. Soc. Rev. 44 (2015) 4212–4227. https://doi.org/10.1039/c4cs00179f.

169. V.G. MARINI, E. TORRI, L.M. ZIMMERMANN, V.G. MACHADO, An anionic chromogenic chemosensor based on 4-(4-nitrobenzylideneamine)-2, 6-diphenylphenol for selective detection of cyanide in acetonitrile-water mixtures, Arkivoc. 2010 (2010) 146–162. https://doi.org/10.3998/ark.5550190.0011.b13.

170. Y. JEONG, J. YOON, Recent progress on fluorescent chemosensors for metal ions, Inorganica Chim. Acta. 381 (2012) 2–14. https://doi.org/10.1016/j.ica.2011.09.011.

171. D. UDHAYAKUMARI, S. VELMATHI, Y.M. SUNG, S.P. WU, Highly fluorescent probe for copper (II) ion based on commercially available compounds and live cell imaging, Sensors Actuators, B Chem. 198 (2014) 285–293. https://doi.org/10.1016/j.snb.2014.03.063.

172. M. WANG, K.H. LEUNG, S. LIN, D.S.H. CHAN, D.W.J. KWONG, C.H. LEUNG, D.L. MA, A colorimetric chemosensor for Cu^{2+}ion detection based on an iridium(III) complex, Sci. Rep. 4 (2014). https://doi.org/10.1038/srep06794.

173. S. ELSAYED, A. AGOSTINI, L.E. SANTOS-FIGUEROA, R. MARTÍNEZ-MÁÑEZ, F. SANCENÓN, An instantaneous and highly selective chromofluorogenic chemodosimeter for fluoride anion detection in pure water, ChemistryOpen. 2 (2013) 58–62. https://doi.org/10.1002/open.201300010.

174. Y. ZHOU, J.F. ZHANG, J. YOON, Fluorescence and colorimetric chemosensors for fluoride-ion detection, Chem. Rev. 114 (2014) 5511–5571. https://doi.org/10.1021/cr400352m.

175. F.M. HINTERHOLZINGER, B. RÜHLE, S. WUTTKE, K. KARAGHIOSOFF, T. BEIN, Highly sensitive and selective fluoride detection in water through fluorophore

release from a metal-organic framework, Sci. Rep. 3 (2013). https://doi.org/10.1038/srep02562.

176. T. WANG, Y. BAI, L. MA, X.P. YAN, Synthesis and characterization of indolocarbazole-quinoxalines with flat rigid structure for sensing fluoride and acetate anions, Org. Biomol. Chem. 6 (2008) 1751–1755. https://doi.org/10.1039/b801447g.

177. R. SUNKE, P.V. BABU, S. YELLANKI, R. MEDISHETTI, P. KULKARNI, M. PAL, Ligand-free MCR for linking quinoxaline framework with a benzimidazole nucleus: A new strategy for the identification of novel hybrid molecules as potential inducers of apoptosis, Org. Biomol. Chem. 12 (2014) 6800–6805. https://doi.org/10.1039/c4ob01268b.

178. Y.S. CHEAH, S. SANTHANAKRISHNAN, M.B. SULLIVAN, K.G. NEOH, C.L.L. CHAI, The chemical reactivities of DOPA and dopamine derivatives and their regioselectivities upon oxidative nucleophilic trapping, Tetrahedron. 72 (2016) 6543–6550. https://doi.org/10.1016/j.tet.2016.08.068.

179. J. TIRADO-RIVES, W.L. JORGENSEN, Performance of B3LYP density functional methods for a large set of organic molecules, J. Chem. Theory Comput. 4 (2008) 297–306. https://doi.org/10.1021/ct700248k.

180. M.J.G. FRISCH, W. TRUCKS, H.B. SCHLEGEL, G.E. SCUSERIA, M.A. ROBB, J.R. CHEESEMAN, G. SCALMANI, V. BARONE, B. MENNUCCI, G.A. PETERSSON, H. NAKATSUJI, M. CARICATO, X. LI, H.P. HRATCHIAN, A.F. IZMAYLOV, J. BLOINO, G. ZHENG, J.L. SONNENBERG, Gaussian 16, 2016. https://doi.org/10.1111/j.1365-2486.2008.01751.x.

181. Y. TAKANO, K.N. HOUK, Benchmarking the conductor-like polarizable continuum model (CPCM) for aqueous solvation free energies of neutral and ionic organic molecules, J. Chem. Theory Comput. 1 (2005) 70–77. https://doi.org/10.1021/ct049977a.

182. J. HO, M.Z. ERTEM, Calculating Free Energy Changes in Continuum Solvation Models, J. Phys. Chem. B. 120 (2016) 1319–1329. https://doi.org/10.1021/acs.jpcb.6b00164.

183. S. SATHISH, G. NARAYAN, N. RAO, C. JANARDHANA, A self-organized ensemble of fluorescent 3-hydroxyflavone-Al (III) complex as sensor for fluoride and acetate ions, J. Fluoresc. 17 (2007) 1–5. https://doi.org/10.1007/s10895-006-0137-1.

184. S. PECKHAM, N. AWOFESO, Water fluoridation: A critical review of the physiological effects of ingested fluoride as a public health intervention, Sci. World J. 2014 (2014) 1–10. https://doi.org/10.1155/2014/293019.

185. L.M. ZIMMERMANN-DIMER, V.G. MACHADO, Chromogenic anionic chemosensors based on protonated merocyanine solvatochromic dyes: Influence of the medium on the quantitative and naked-eye selective detection of anionic species, Dye. Pigment. 82 (2009) 187–195. https://doi.org/10.1016/j.dyepig.2008.12.013.

186. C.R. NICOLETI, V.G. MARINI, L.M. ZIMMERMANN, V.G. MACHADO, Anionic chromogenic chemosensors highly selective for fluoride or cyanide based on 4-(4-

Nitrobenzylideneamine)phenol, J. Braz. Chem. Soc. 23 (2012) 1488–1500. https://doi.org/10.1590/S0103-50532012005000007.

187. Why interdisciplinary research matters, Nature. 525 (2015) 305. https://doi.org/10.1038/525305a.

188. H. LEDFORD, How to solve the world's biggest problems, Nature. 525 (2015) 308–311. https://doi.org/10.1038/525308a.

189. M.J. GOEDHART, A new perspective on the structure of chemistry as a basis for the undergraduate curriculum, J. Chem. Educ. 84 (2007) 971–976. https://doi.org/10.1021/ed084p971.

190. C.P. SCHALLER, K.J. GRAHAM, B.J. JOHNSON, M.A. FAZAL, T.N. JONES, E.J. MCINTEE, H. V. JAKUBOWSKI, Developing and implementing a reorganized undergraduate chemistry curriculum based on the foundational chemistry topics of structure, reactivity, and quantitation, J. Chem. Educ. 91 (2014) 321–328. https://doi.org/10.1021/ed400336d.

191. M.B. WIGGINS, E. HEATH, J. ALCÁNTARA-GARCÍA, Multidisciplinary Learning: Redox Chemistry and Pigment History, J. Chem. Educ. 96 (2019) 317–322. https://doi.org/10.1021/acs.jchemed.8b00358.

192. N. EMMANUEL, G. EMONDS-ALT, M. LISMONT, G. EPPE, J.C.M. MONBALIU, Exploring the Fundamentals of Microreactor Technology with Multidisciplinary Lab Experiments Combining the Synthesis and Characterization of Inorganic Nanoparticles, J. Chem. Educ. 94 (2017) 775–780. https://doi.org/10.1021/acs.jchemed.6b00899.

193. L.A. AL-SHATTI, S.A. ABDALLAH, A.F. ALHAJRAF, N.A. ALHAMMAD, B.M. ALAWADI, Chemistry , the Central Science : The Application of a Multidisciplinary Project based on the Centrality of Chemistry, J. Lab. Chem. Educ. 2 (2014) 79–84. https://doi.org/10.5923/j.jlce.20140205.01.

194. T. ABDINEJAD, M.R. ZAMANLOO, T. ALIZADEH, N.O. MAHMOODI, S.R. POURAN, Photochromic and Electrochromic Diimide Synthesized Simply from Inexpensive Compounds: A Multidisciplinary Experiment for Undergraduate Students, J. Chem. Educ. 95 (2018) 1642–1647. https://doi.org/10.1021/acs.jchemed.7b00540.

195. M. BARAK, Y.J. DORI, Enhancing undergraduate students' chemistry understanding through project-based learning in an IT environment, Sci. Educ. 89 (2005) 117–139. https://doi.org/10.1002/sce.20027.

196. G. SCHWARZ, W. FRENZEL, W.M. RICHTER, L. TÄUSCHER, G. KUBSCH, A Multidisciplinary Science Summer Camp for Students with Emphasis on Environmental and Analytical Chemistry, J. Chem. Educ. 93 (2016) 626–632. https://doi.org/10.1021/acs.jchemed.5b00211.

197. E. GHANEM, S.R. LONG, S.E. RODENBUSCH, R.I. SHEAR, J.T. BECKHAM, K. PROCKO, L. DEPUE, K.J. STEVENSON, J.D. ROBERTUS, S. MARTIN, B. HOLLIDAY, R.A. JONES, E. V. ANSLYN, S.L. SIMMONS, Teaching through Research: Alignment of Core Chemistry Competencies and Skills within a

Multidisciplinary Research Framework, J. Chem. Educ. 95 (2018) 248–258. https://doi.org/10.1021/acs.jchemed.7b00294.

198. G.L. CHEN, M.X. FAN, J.L. WU, N. LI, M.Q. GUO, Antioxidant and anti-inflammatory properties of flavonoids from lotus plumule, Food Chem. 277 (2019) 706–712. https://doi.org/10.1016/j.foodchem.2018.11.040.

199. R. K.R.R., K. H., G. S., L. R.J.L., M. F.M., K. Z., S. S., T. D., Z. G., H. S.T.S., P. S.K., The role of flavonoids in autoimmune diseases: Therapeutic updates, Pharmacol. Ther. 194 (2019) 107–131. https://doi.org/10.1016/j.pharmthera.2018.09.009

200. M. KHALID, SAEED-UR-RAHMAN, M. BILAL, D. FENG HUANG, Role of flavonoids in plant interactions with the environment and against human pathogens — A review, J. Integr. Agric. 18 (2019) 211–230. https://doi.org/10.1016/S2095-3119(19)62555-4.

201. M.J. FRUTOS, L. RINCÓN-FRUTOS, E. VALERO-CASES, Rutin, Nonvitamin Nonmineral Nutr. Suppl. (2019) 111–117. https://doi.org/10.1016/B978-0-12-812491-8.00015-1.

202. N.E.A. IKEDA, E.M. NOVAK, D.A. MARIA, A.S. VELOSA, R.M.S. PEREIRA, Synthesis, characterization and biological evaluation of Rutin–zinc(II) flavonoid -metal complex, Chem. Biol. Interact. 239 (2015) 184–191. https://doi.org/10.1016/J.CBI.2015.06.011.

203. W. WANG, C. SUN, L. MAO, P. MA, F. LIU, J. YANG, Y. GAO, The biological activities, chemical stability, metabolism and delivery systems of quercetin: A review, Trends Food Sci. Technol. 56 (2016) 21–38. https://doi.org/10.1016/j.tifs.2016.07.004.

204. F. DAJAS, Life or death: Neuroprotective and anticancer effects of quercetin, J. Ethnopharmacol. 143 (2012) 383–396. https://doi.org/10.1016/j.jep.2012.07.005.

205. F. PEREZ-VIZCAINO, J. DUARTE, R. JIMENEZ, C. SANTOS-BUELGA, A. OSUNA, Antihypertensive effects of the flavonoid quercetin, Pharmacol. Reports. 61 (2009) 67–75. https://doi.org/10.1016/S1734-1140(09)70008-8.

206. A.M. ENGIDA, N.S. KASIM, Y.A. TSIGIE, S. ISMADJI, L.H. HUYNH, Y.H. JU, Extraction, identification and quantitative HPLC analysis of flavonoids from sarang semut (Myrmecodia pendan), Ind. Crops Prod. 41 (2013) 392–396. https://doi.org/10.1016/j.indcrop.2012.04.043.

207. B.C. NUNES, M.M. MARTINS, R. CHANG, S.A.L. MORAIS, E.A. NASCIMENTO, A. DE OLIVEIRA, L.C.S. CUNHA, C. V. DA SILVA, T.L. TEIXEIRA, M.A.L.V. AMBRÓSIO, C.H.G. MARTINS, F.J.T. DE AQUINO, Antimicrobial activity, cytotoxicity and selectivity index of Banisteriopsis laevifolia (A. Juss.) B. Gates leaves, Ind. Crops Prod. 92 (2016) 277–289. https://doi.org/10.1016/j.indcrop.2016.08.016.

208. L. BARRIENTOS, C.L. HERRERA, G. MONTENEGRO, X. ORTEGA, J. VELOZ, M. ALVEAR, A. CUEVAS, N. SAAVEDRA, L.A. SALAZAR, Chemical and botanical characterization of chilean propolis and biological activity on cariogenic bacteria Streptococcus mutans and Streptococcus sobrinus, Brazilian J. Microbiol. 44 (2013) 577–585. https://doi.org/10.1590/S1517-83822013000200038.

209. G. DE V.L. CAVALCANTE, Estudo fitoquímico e análise biológica/farmacológica de Bredemeyera floribunda Willd, 2015. https://doi.org/10.1056/NEJMoa1311367.

210. E.R. KARIMOVA, L.A. BALTINA, M.I. ABDULLIN, Production of Quercetin by Acid Hydrolysis of Rutin, Vestn. Bashkirskogo Univ. 21 (2016) 78–80.

211. T.S. DE CASTILHO, T.B. MATIAS, K.P. NICOLINI, J. NICOLINI, Study of interaction between metal ions and quercetin, Food Sci. Hum. Wellness. 7 (2018) 215–219. https://doi.org/10.1016/J.FSHW.2018.08.001.

212. Y. FANG, Y. ZHANG, Q. HAN, M. JIA, M. ZHANG, L. WANG, Y. TAN, Z. CAO, Y. DENG, Complexation and solvent extraction behaviour towards lanthanide ions with quercetin, Inorg. Chem. Commun. 100 (2019) 70–74. https://doi.org/10.1016/J.INOCHE.2018.12.023.

213. N. GHOSH, T. CHAKRABORTY, S. MALLICK, S. MANA, D. SINGHA, B. GHOSH, S. ROY, Synthesis, characterization and study of antioxidant activity of quercetin-magnesium complex, Spectrochim. Acta - Part A Mol. Biomol. Spectrosc. 151 (2015) 807–813. https://doi.org/10.1016/j.saa.2015.07.050.

214. R. RAVICHANDRAN, M. RAJENDRAN, D. DEVAPIRIAM, Antioxidant study of quercetin and their metal complex and determination of stability constant by spectrophotometry method, Food Chem. 146 (2014) 472–478. https://doi.org/10.1016/j.foodchem.2013.09.080.

215. J.E.N. DOLATABADI, Molecular aspects on the interaction of quercetin and its metal complexes with DNA, Int. J. Biol. Macromol. 48 (2011) 227–233. https://doi.org/10.1016/j.ijbiomac.2010.11.012.

216. G. DEHGHAN, Z. KHOSHKAM, Tin(II)-quercetin complex: Synthesis, spectral characterisation and antioxidant activity, Food Chem. 131 (2012) 422–426. https://doi.org/10.1016/j.foodchem.2011.08.074.

217. S. BIRJEES BUKHARI, S. MEMON, M. MAHROOF TAHIR, M.I. BHANGER, Synthesis, characterization and investigation of antioxidant activity of cobalt–quercetin complex, J. Mol. Struct. 892 (2008) 39–46. https://doi.org/10.1016/J.MOLSTRUC.2008.04.050.

218. M.M. KASPRZAK, A. ERXLEBEN, J. OCHOCKI, Properties and applications of flavonoid metal complexes, RSC Adv. 5 (2015) 45853–45877. https://doi.org/10.1039/c5ra05069c.

219. F.A. CAREY, R.J. SUNDBERG, Advanced Organic Chemistry Part A: Structure and Mechanisms, 2007. https://doi.org/10.1021/ed065pA139.2.